# UNDERSTANDING THE TECTONIC EVOLUTION OF THE WEST ORPHAN BASIN, OFFSHORE CANADA, AND THE CONJUGATE ROCKALL BASIN, OFFSHORE IRELAND, USING A SEISMIC MEGATRANSECT

by © Heide M. MacMahon

A Thesis submitted

to the School of Graduate Studies in partial fulfilment of

the requirements for the degree of

**Master of Science/Earth Science/Geophysics**

Memorial University of Newfoundland

**May 2019**

St. John's Newfoundland and Labrador

## Abstract

The Orphan Basin, offshore Newfoundland, Canada, is approximately conjugate to the rifted margin basins on the Irish Atlantic margin. At the onset of seafloor spreading, plate reconstructions, based solely on oceanic magnetic anomalies, show the Rockall Basin, west of Ireland, forming a continuous Mesozoic basin with the West Orphan Basin. Here, the nature of this potentially continuous basin is examined through the development of a Newfoundland-Ireland conjugate basins model.

2D and 3D reconstructions of the West Orphan and Rockall basins yielded the thickness of the post-rift and syn-rift sedimentary packages, as well as the pre-rift crust. A discrepancy inspired additional analysis of the East Orphan Basin to aid in the reconstruction of the continuous Mesozoic basins. Based on the results of the reconstruction of the East Orphan Basin, it is possible that the Rockall Basin was originally conjugate to, and continuous with, the East Orphan Basin.

**Acknowledgments**

I would like to begin by thanking my supervisor Kim Welford for taking me on as a willing graduate student, for providing me this project and for facilitating the data access required for this project. I would also like to thank you for being the kind and welcoming supervisor that you are, I truly appreciate everything you have done for me. I would also like to thank Luke Beranek for his insightful comments as a committee member.

I would like to thank the Petroleum Affairs Division of the Department of Communications, Climate Action and Environment, of the Irish government for generously providing the Rockall Basin and Porcupine Basin 2D seismic data set. I would also like to thank TGS for providing the Orphan Basin 2D seismic data set. Thank you to the Canada-Newfoundland and Labrador Offshore Petroleum Board (C-NLOPB) for providing additional geological and geophysical well logs within the Orphan Basin. Additionally, thank you to Innovate NL for funding this project.

Another big thank you to Larry Sandoval for your help during this process, and indulging every question I had regarding Petrel. Thank you to Alex Peace for your structural knowledge and overall thesis advice. A big thank you to Stuart Smith, the senior support geologist at Move©, for his speedy and insightful help and without whom this project would have taken twice as long. I would also like to thank Mohamed Gouiza for his useful insights and numerous email correspondences.

A special thank you to my family for all their support, especially my mother, Susanne. Your constructive criticism and speedy edits pushed me forward every day. Your love and support has never gone unnoticed or unappreciated. Thank you for being a strong, independent female role

model in my life. Finally, to my boyfriend, Bill Clarke, thank you for your unwavering belief, never ending support and your unconditional love.

Dedication

This thesis is dedicated to my incredible mother,

Susanne MacMahon

You are strong and passionate,
You are smart and brave,
You are my inspiration.

I could not have done this without you.
I love you.

## Table of Contents

## List of Tables

## List of Figures (Abbreviated Titles)

## Chapter 1: Introduction

Several petroleum rich sedimentary basins (e.g., the Orphan Basin, the Flemish Pass Basin and the Jeanne D'Arc Basin) are located offshore Newfoundland and Labrador (Fig. 1.1a). These basins were formed during the opening of the North Atlantic Ocean (Chian *et al.*, 2001; Enachescu *et al.*, 2004; Lau *et al.*, 2015). On the conjugate Irish Atlantic margin, numerous basins were formed at approximately the same time (e.g., the Rockall Basin and the Porcupine Basin; Shannon 1991; O'Reilly *et al.*, 1996; Hopper *et al.*, 2006)(Fig. 1.1b). Whereas the Newfoundland-Iberia conjugate margin pair involves the world's most thoroughly studied rifted continental margins, less research has been conducted on the Newfoundland-Ireland conjugate basins immediately to the north. The aim of this M.Sc. project is to look specifically at the relationship between the West Orphan Basin, on the Newfoundland margin, and the Rockall Basin on the Irish margin. Using both modern and vintage geophysical data (Figs. 1.4 and 1.6), predominantly seismic reflection profiles, these rifted margins have been interpreted and restored back to their pre-rift state in order to determine if these basins formed a single large Mesozoic rift system prior to the opening of the modern North Atlantic Ocean.

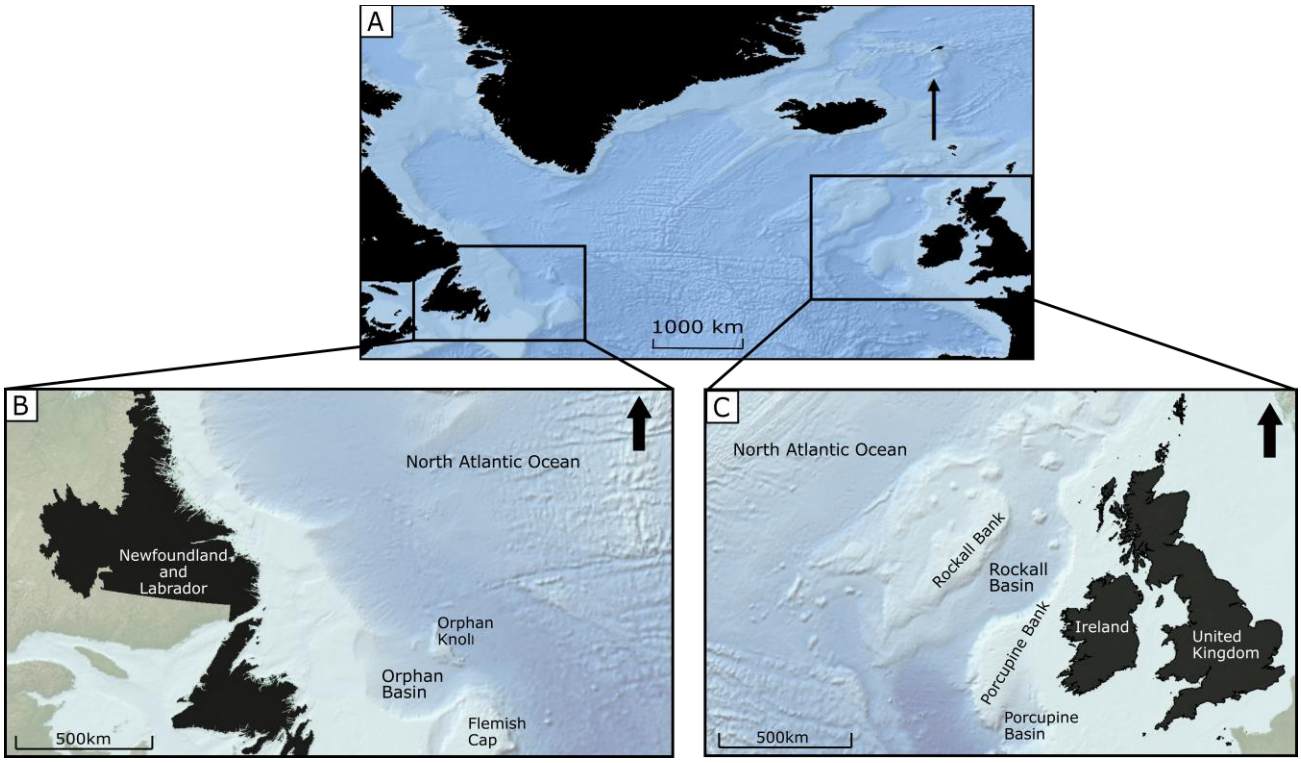


*Figure 1.1: (A) North Atlantic margins. (B) Enlarged view of the Orphan Basin, offshore Newfoundland, Canada. (C) Enlarged view of the Rockall Basin, offshore Ireland.*

## 1.1 Classification of Rifted Margins

Rifted margins are categorized into three "archetype" or "end member" groups: volcanic/magma rich, non-volcanic/magma poor, and sediment rich (Péron-Pinvidic *et al.*, 2013). These end-member margins are differentiated according to their overall basin geometry, sedimentary records, and magmatic history. Despite the differences observed over all three margin types, they appear to have a similar first-order geometry, with continental crust that thins toward the ocean from approximately 30 km to 0-5 km. All the margin types also exhibit a Moho that either rises rapidly over a short distance or gradually over a larger distance, while the top of the basement steadily deepens (Péron-Pinvidic *et al.*, 2013).

The Newfoundland-Ireland conjugate basins exhibit all of the common characteristics of a

typical non-volcanic/magma poor rifted margin (Reston, 2007a). These characteristics include: low to moderate sedimentary rock accumulation rates, extreme crustal thinning (increasing towards the ocean), rotated fault blocks, the presence of detachment faults, little evidence of syn-rift magmatism, and a broad region of partially serpentinized and exhumed mantle (Reston, 2007a).

Buck *et al*. (1999) linked the formation of rifted margins to both localizing and delocalizing processes. Localization processes are ones where deformation is concentrated on the original points of weakness in the lithosphere, whereas delocalization processes are ones that disperse the deformation. The important, localizing processes exhibited in a rifted margin include: thinning of the lithosphere resulting in weakening, which then propagates as faults, and rift-related melt generating dike intrusions that weaken the lithosphere mechanically and thermally (Buck, 2007). Conversely, the delocalizing processes include isostatic/gravitational forces working against lithospheric thinning by equilibrating lateral variations in layer thicknesses of different densities (Fleitout & Froidevaux, 1982). Finally, interactions between these processes are affected by the extension rate and far-field stresses, which ultimately result in wide or narrow (Buck *et al.*, 1999), symmetric or asymmetric (Buiter *et al.*, 2008), and failed or successful rifts (Brune *et al.*, 2017).

Reston (2007a) proposed a model of progressive extension leading to continental breakup at a cool, non-volcanic/magma poor rifted margin pair (Fig. 1.2). The evolution of the breakup allows for discrete differences between continental rifts, which generally undergo less extension, and continental rifted margins. The first stage of the proposed model shows extension of the lithosphere with faulting occurring in the upper crust, and boudinage of both the uppermost mantle and the lower crust. Depth-dependent stretching is likely to begin at this stage with the amount of symmetric stretching being controlled by the strain rate (Reston, 2007a). As

extension continues, the original normal faults stop propagating and new faults begin to form (Fig. 1.2a). During this time, the lower crust becomes coupled with the upper crust and lower crustal boudinage is replaced by faulting. Extension is focused towards the site of eventual break up, as the crust thins to approximately one-quarter of its original thickness (Fig. 1.2b) (Reston, 2007a). Simultaneously, the second generation of faults lock-up and a third phase of faults begin to propagate. Complete crustal embrittlement occurs during this time allowing faults to propagate through the entire crust, leading to serpentinization of the mantle (Fig. 1.2c). The serpentinization weakens the strong mantle lid and can lead to complete crustal separation (Pérez-Gussinyé & Reston 2001). Melt generation is typically expected at this stage, but is suppressed by a combination of mantle depth-dependent stretching and/or the presence of a cool subcontinental mantle (Reston, 2007a). Reston (2007a) goes on to postulate that sea-floor spreading is most likely controlled by the influx of warm asthenosphere and usually occurs after crustalseparation, as indicated by the presence of a broad zone of unroofed mantle within the ocean-continent transition. This is in agreement with the findings of Davis and Kusznir (2004) who conclude that the lack of basaltic material within exhumed mantle may be consistent with mantle exhumation occurring during early seafloor spreading such that the basaltic melt was focused into the ridge axis by the matrix pressure field associated with the divergent flow in the lithosphere and asthenosphere at the young ocean ridge (Spiegelman & Reynolds 1999).

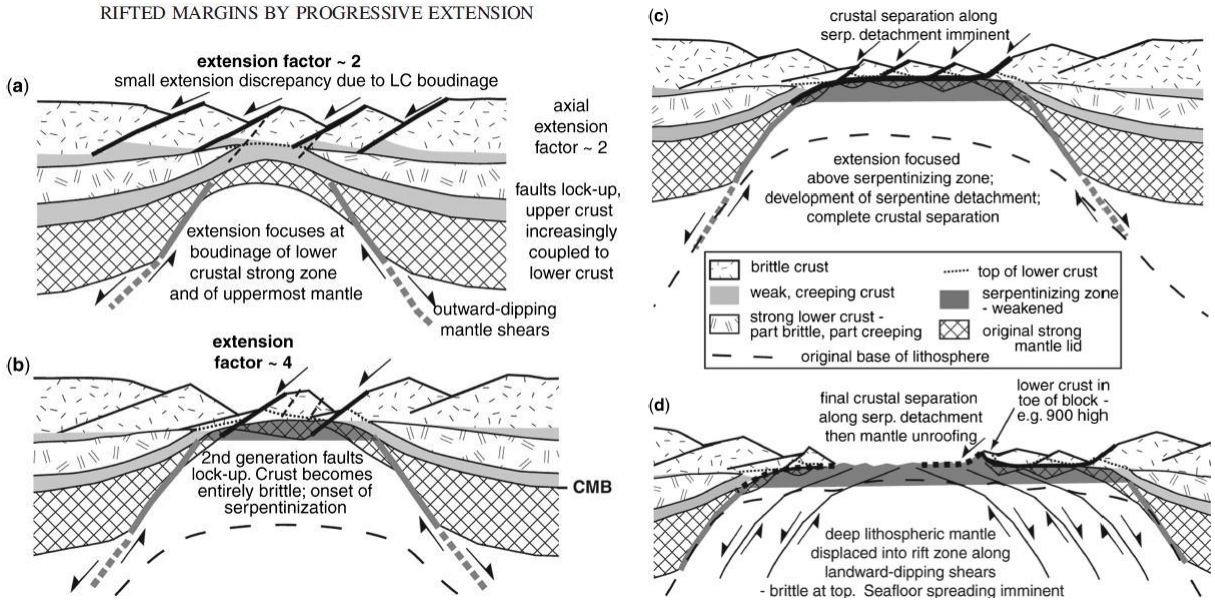


*Figure 1.2: Schematic illustration showing the important steps in the progressive extension of the lithosphere leading to continental break-up. (a) Early rift conditions up to the initiation of the second generation of faults (dashed lines). Initial decoupling zones at the base of the upper and mid crust (grey lines), and upper crust become increasingly coupled to the lower crust in the center of the rift. (b) The entire crust is now brittle mantle serpentinization (dark grey) has begun. A third generation of faults propagates down to the detachment surface (bold). (c) Crustal separation is imminent. (d) Post -crustal separation and continued unroofing of the lithospheric mantle may require displacement. Image from Reston (2007a).*

The above model (Fig. 1.2) captures the evolution of a symmetric non-volcanic/magma poor margin pair. However, as previously stated, the Newfoundland-Ireland conjugate margin system is asymmetric (Reston 2007a). Reston (2007a) also proposed a simplified model for asymmetric rift margin evolution. It is important to note that if extension occurred as a result of simple shear, along a low angle detachment fault, the failure to recognize this detachment could potentially result in a significant underestimation of the amount of extension accommodated by faulting (Fig. 1.3). To avoid this problem, it is important to accurately identify pre-rift units on both sides of the conjugate margin pair to differentiate between pre-faulting units deposited prior to development of the visible faults (Reston, 2007a). Eddy *et al.* (2017) suggest that large-scale detachment faulting continued until lithospheric breakup near the Aptian-Albian boundary. They go on to state that magmatism appears to have been focused at the point of mantle exhumation on

large-scale detachment faults and may have played a role in determining the location of breakup by weakening the overlying lithosphere (Eddy *et al.*, 2017).

When analyzing Reston's proposed asymmetric model with regards to the Newfoundland-Ireland conjugate margin pair, the lower plate is the Irish-Atlantic margin and the upper plate is the Newfoundland margin (Reston, 2007a). As a result of more extreme crustal thinning, the serpentinization and possible exhumation of the mantle is only observed on the Irish-Atlantic margin. Conversely, no serpentinization has been observed on the Newfoundland margin.

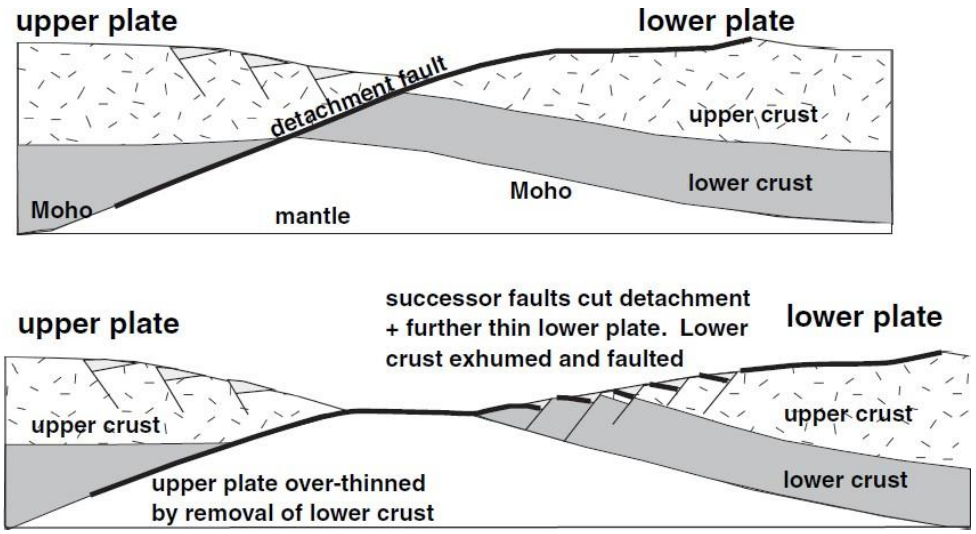


*Figure 1.3: Simplified schematic illustration of how movement along a crustal-scale shear zone can result in asymmetric conjugate margins (Reston, 2007a).*

The major detachment surface modelled at the crust-mantle boundary, commonly referred to as an "S" reflector on seismic data, is used to identify large scale asymmetry of entire rift systems (Davis & Kusznir 2004; Reston *et al.*, 1996). Hopper *et al.*, (2006) used seismic data to observe the asymmetries between the Newfoundland-Iberia conjugate margins. On the Newfoundland margin, notably beneath Flemish Cap, they observed that the crust thins from 30 to 3 km, where the Moho is well defined and dips locally by as much as 30 degrees. However,

on the Iberia margin, beneath Galicia Bank, extremely thin continental crust is observed only in a very narrow zone and evidence of the conjugate counterpart to the "S" reflector is lacking. Based on their interpretation of the geophysical data, it was concluded that beneath Galicia Bank, on the Iberia margin, thin continental crust either immediately bounds thin oceanic crust or is separated by less than 10 km of exhumed mantle. On the Newfoundland margin, off Flemish Cap, no broad zone of exhumed mantle is observed (Hopper *et al.*, 2006). However, Welford *et al.* (2010) interpreted a 25 km wide of zone of transitional crust along the northeastern margin of Flemish Cap, as exhumed serpentinized mantle. These observations are indicative of major asymmetry in the final development of continental rifting that led to seafloor spreading between the Flemish Cap-Goban Spur conjugate margins. The goal of this M.Sc. project is to determine whether similar structures are present on the Newfoundland-Ireland conjugate margins, which are located just north of the Flemish Cap-Goban spur conjugate margins.

## 1.2 The Newfoundland-Ireland Conjugate Margins

### 1.2.1 Introduction to the Rockall Basin

A number of deep-water sedimentary basins are located on the Atlantic continental margin west of Ireland. The two largest Irish basins are the Rockall and the Porcupine basins (Fig. 1.4), which have been the focus of intermittent exploration since the late 1970s (Shannon 1991; O'Reilly *et al.*, 1996; Mackenzie *et al.*, 2002; Morewood *et al.*, 2005). The Porcupine Basin is a large, deep-water sedimentary basin that lies within the continental shelf and is oriented parallel to the continental margin. The Rockall Basin is located to the north of the Porcupine Basin, and underlies a deep bathymetric depression, called the Rockall Trough. It is the largest sedimentary

basin on the Irish Atlantic continental margin measuring approximately 250 km by 1100 km (Morewood *et al.*, 2005). The Rockall Basin trends in a NE-SW direction with water depths ranging from 200 m on the margins to over 3000 m in the center. Shannon *et al.* (1999) were one of the first to suggest that both the Porcupine and the Rockall basins developed in response to three rift episodes in the Triassic, Late Jurassic and Early Cretaceous with periods of intermittent thermal subsidence.

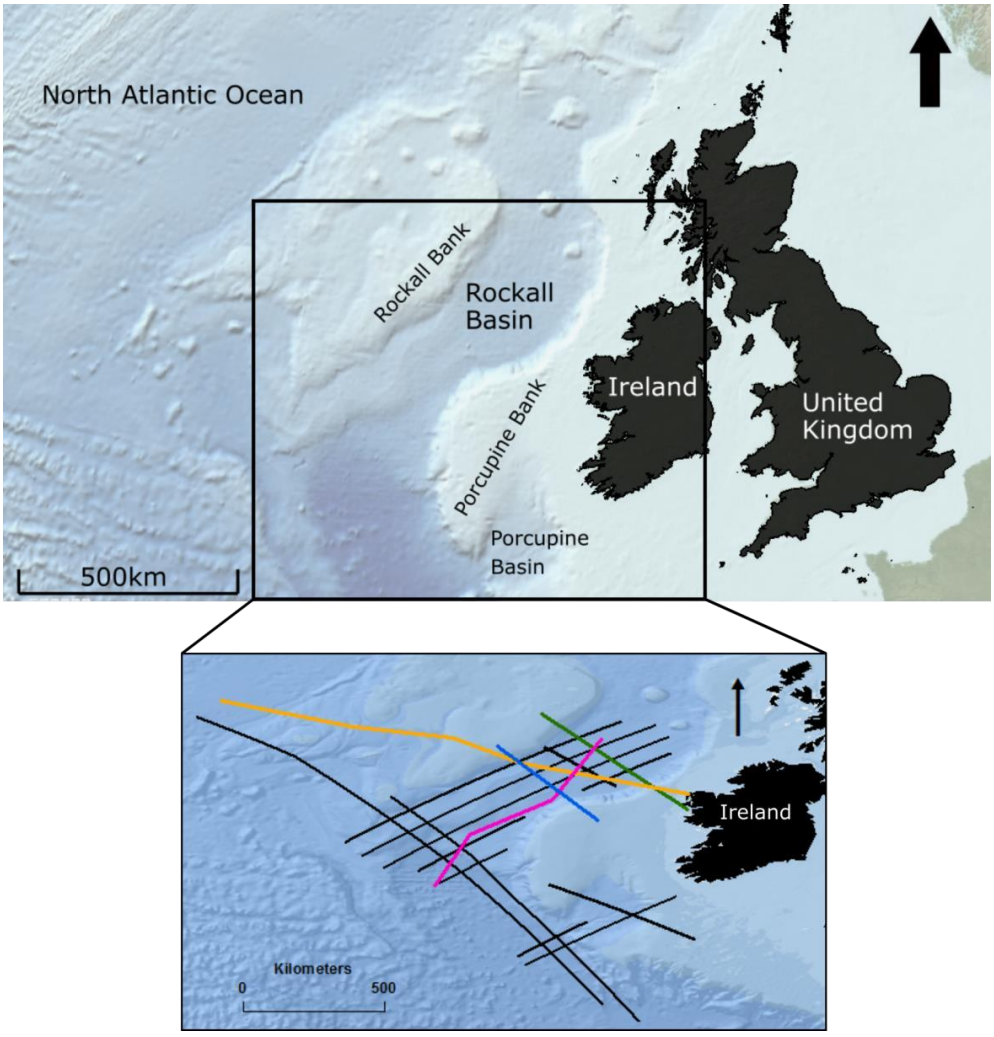


*Figure 1.4: (Top) Location of the Rockall Basin in the North Atlantic Ocean, offshore Ireland. The location of the Rockall Bank, Porcupine Bank and Porcupine Basin are also shown. Background shows bathymetry. (Bottom) Localized view of the Rockall Basin, showing the seismic lines used in this M.Sc. thesis. Black lines indicate the data provided to this project, the green line depicts the location of the seismic line from England & Hobbs (1997), the orange line shows the location of seismic line 2A and the pink line shows the location of seismic line 2B from Shannon et al. (1999). The blue line indicates the location of the seismic line from Kimbell et al. (2010). Background shows bathymetry.*

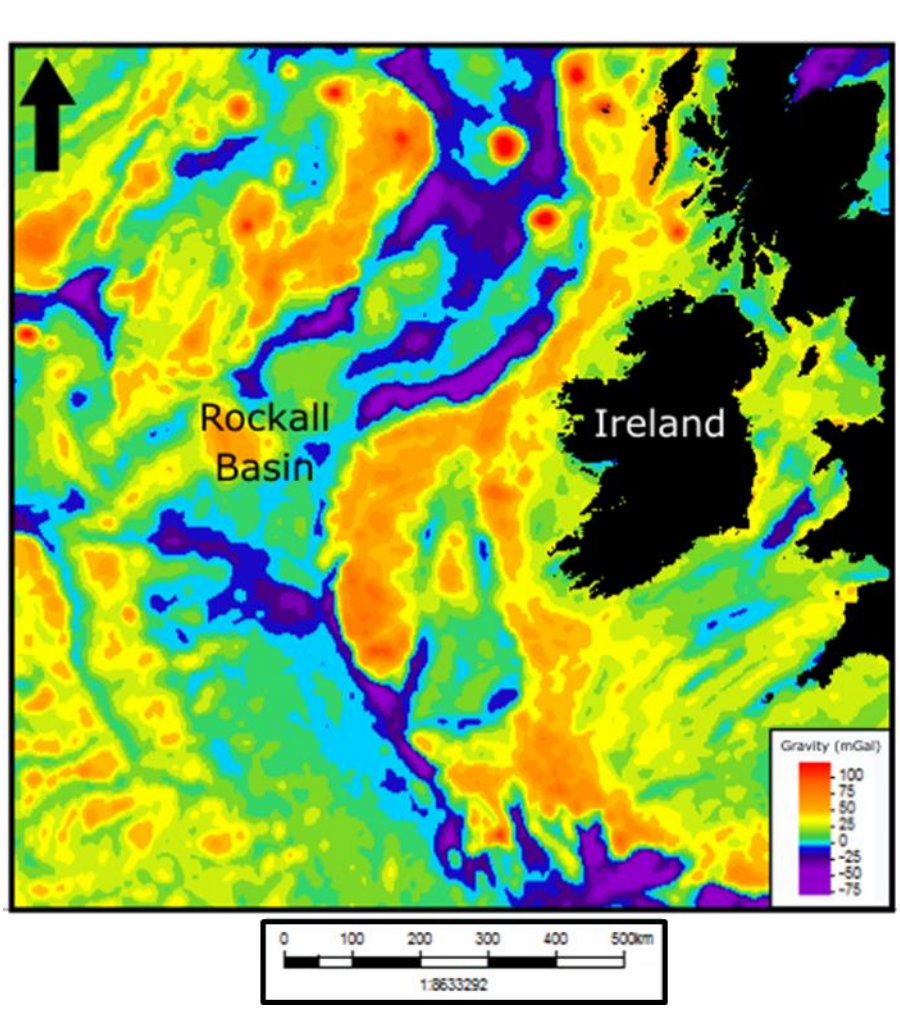


*Figure 1.5: Free air gravity anomaly map of the Rockall Basin, offshore Ireland. Source of data was the Technical University of Denmark, National Space Institute website, http://www.space.dtu.dk/english/Research/Scientific_data_and_models/Global_Marine_Gravity_Field.*

### 1.2.2 Introduction to the Orphan Basin

The Orphan Basin lies at the eastern limit of the North American continent, approximately 300 km seaward of the island of Newfoundland (Fig. 1.6). The Orphan Basin lies between the Orphan Knoll continental fragment and the continental shelf (Keen & Barrett, 1981). Rifting began around the Late Triassic to Early Jurassic based on age constraints from deep-water wells and seismic interpretation of Triassic strata (Chian *et al.,* 2001; Enachescu *et al.,* 2004; Welford *et al.,* 2012; Gouiza *et al.,* 2017). A system of NE–SW trending ridges and the White Sail Fault divide the Orphan Basin into a generally shallower eastern sub-basin and a deeper western sub-basin (Lau *et al.,* 2015). A plate reconstruction at the time of magnetic anomaly M0 (Srivastava & Verhoef 1992) shows that the East and the West Orphan basins and the Orphan Knoll, form a multi-basin rift system that is likely conjugate to the rift structures associated with the Porcupine Basin and the Rockall Basin on the Irish side of the Atlantic (Tucholke *et al.,* 1989; Hopper *et al.,* 2006; Lau *et al.,* 2015). Based on this plate reconstruction, it has been suggested that early rifting and basin development prior to crustal breakup were likely part of a complex, multi-stage process.

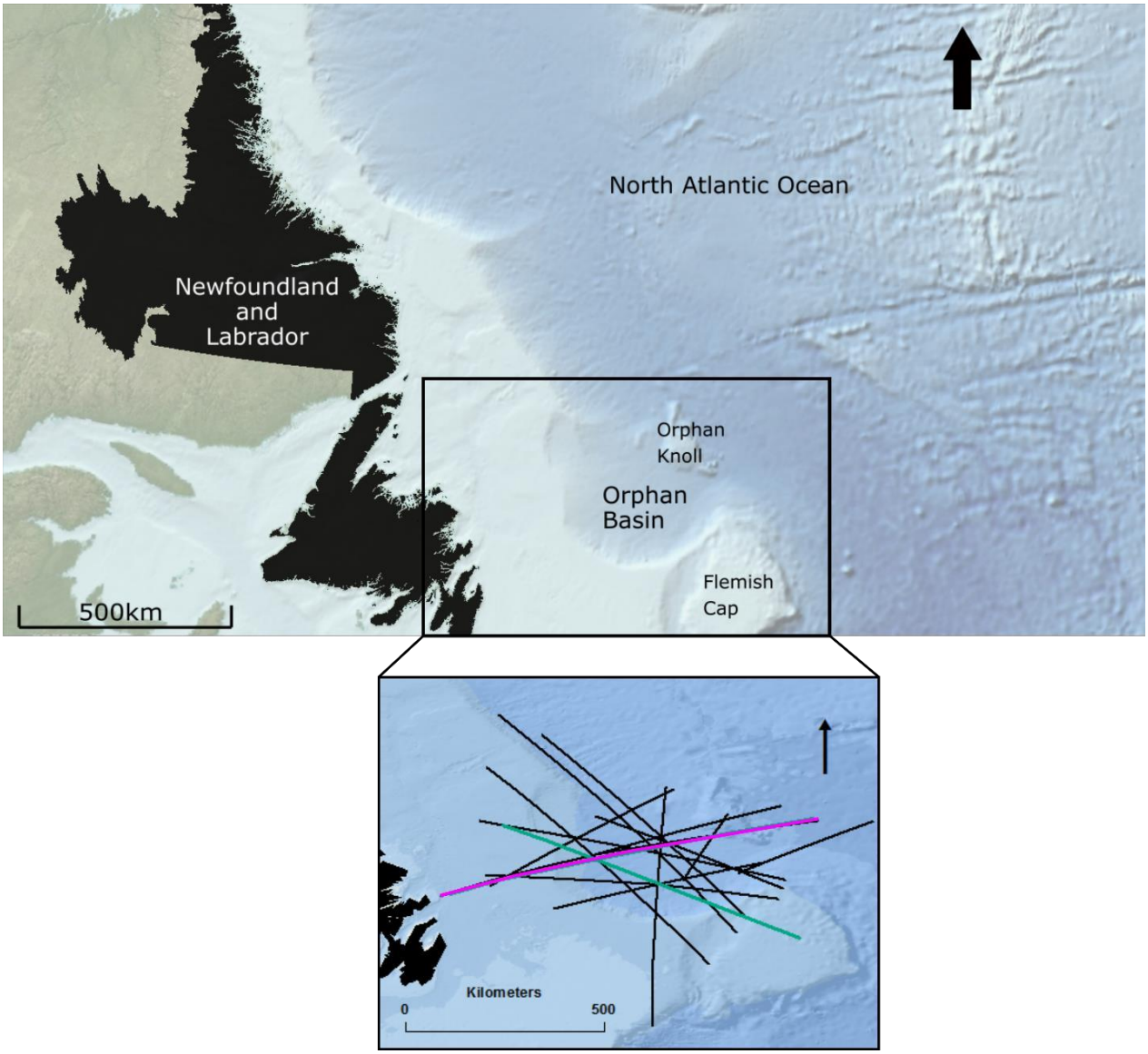


*Figure 1.6: (Top) Location of the Orphan Basin in the North Atlantic Ocean, offshore Newfoundland and Labrador. The location of Orphan Knoll and Flemish Cap are also shown. Background shows bathymetry. (Bottom) Localized view of the Orphan Basin and the locations of the seismic lines provided for this M.Sc. thesis (black lines). The pink line indicates the location of the seismic line from Chian et al. (2001) and the green line indicates the location of the seismic line from Lau et al. (2015).*

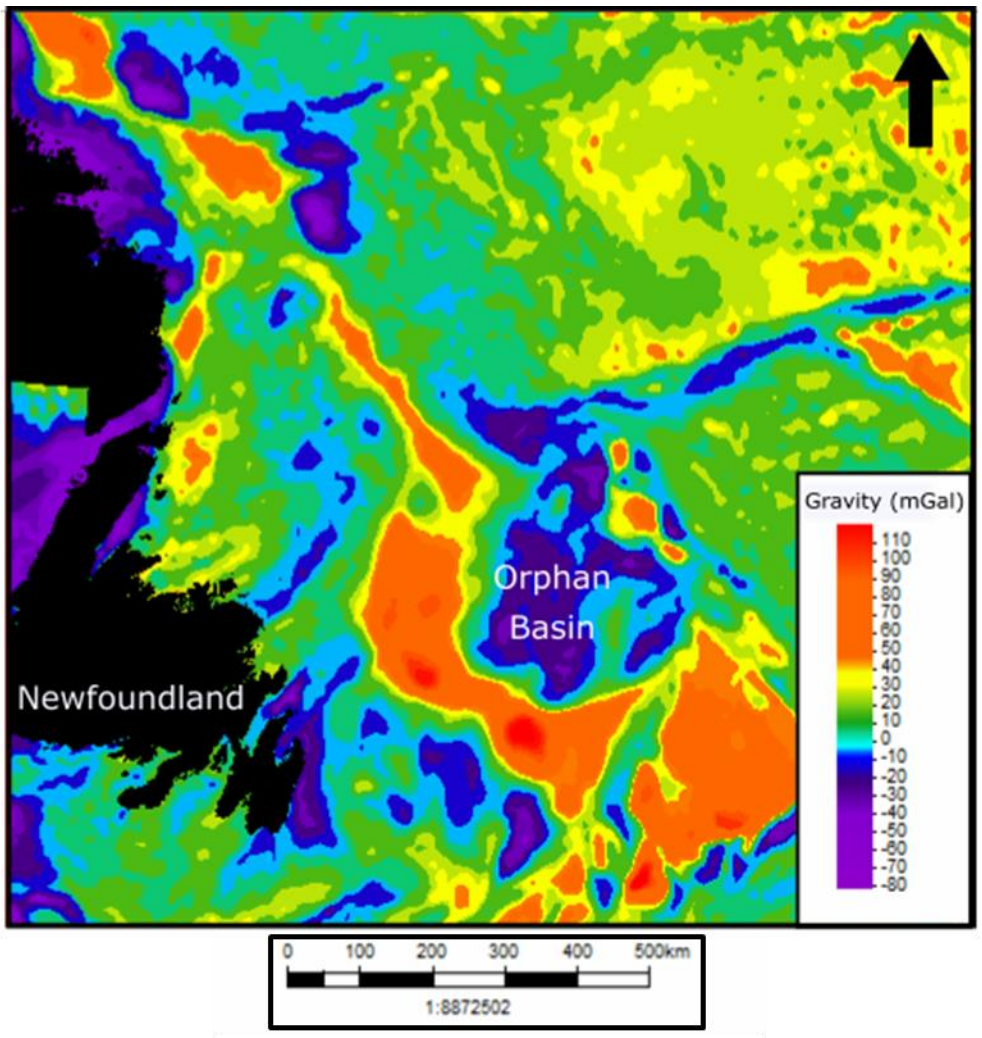


*Figure 1.7: Free air gravity anomaly map of the Orphan Basin, offshore Newfoundland and Labrador. Source of data was the Technical University of Denmark, National Space Institute website, http://www.space.dtu.dk/english/Research/Scientific_data_and_models/Global_Marine_Gravity_Field.*

## 1.3 Basin Evolution

### 1.3.1 Rockall Basin

The distribution of basement domains, established during the Caledonian orogeny (Shannon *et al.*, 1997), had considerable influence on the development of the entire Irish Atlantic margin (Naylor & Shannon 2005). Remnants of this orogeny are recorded in northern parts of Ireland, Britain, and parts of Scandinavia, encompassing events that occurred during the Ordovician to Devonian, 490–390 million years ago (O'Reilly *et al.*, 1996). By the late Carboniferous, an east-west trending oriented fabric was superimposed on the basement of the Irish continental margin due to northward migration of deformation from the Variscan orogeny to the south (Landes *et al.*, 2005). The Variscan orogeny was caused by the late Paleozoic continental collision between Euramerica and Gondwana, which formed the supercontinent of Pangaea (Schulmann *et al.*, 2014). Further deformation within the basin during the late Paleozoic was also controlled by Variscan tectonics. During the Permian, only local basin development occurred with minimal uplift due to late Variscan north-south compression in the Celtic Sea (Shannon 1991). Due to the reactivation of basement lineaments and the east-west extension from early Pangaea instability, the Rockall Basin began to develop (Shannon 1991).

On the Irish Atlantic margin, Mesozoic basin development took place due to the rifting of the Pangaea supercontinent (Shannon 1991). Triassic basin formation continued in a broadly similar setting as it did during the Permian. Along the margin of the Rockall Basin are a series of `perched' basins, which are suggested by Corfield *et al.* (1999) to be of Late-Triassic age and are bounded by numerous faults. During the Early Jurassic, there was a period of inactivity following the cessation of the Triassic rifting. Lower Jurassic strata are only known in the northern part of the Porcupine Basin and are thought to represent a series of deep marine shales

and limestones (Crocker & Shannon 1987). These Lower Jurassic strata are also assumed to be present in the Rockall Basin, however there is no geological evidence to confirm their presence. In the Mid- Jurassic, a period of major rifting occurred (Shannon 1991). Shannon (1991) states that the uppermost Jurassic strata show evidence of a rift phase, however it was locally developed and movement only took place along basin edges. The Upper-Jurassic strata reflect deposition of basin-edge sandy to conglomerate alluvial fans and deep-marine sandy fans in a series of syn-rift sub-basins (Crocker & Shannon 1987).

Thermal subsidence, marked by a regional unconformity, took place in the Cretaceous as basin rifting gave way to a phase of drift (Shannon 1991). This was followed by a minor rift episode that resulted in localized uplifting on the Rockall Basin margins producing a variety of deltaic fans (Shannon 1991). The Barra Volcanic Ridge System, located in the south of the Rockall Basin, has been interpreted as the product of extensive volcanism during this period (Shannon *et al.,* 2006).

Cenozoic tectonic activity is reflected in the interplay of post-rift thermal subsidence and compression from the formation of the Alpine Mountains (Shannon 1991). In the Rockall Basin, thermal subsidence continued through this period until it was interrupted by a major unconformity (Shannon 1991). This unconformity is likely due to sea-floor spreading in the North Atlantic, causing crustal heating and uplift from decompression melting (Shannon 1991). This era is marked by a period of intense igneous activity, which was interpreted by Naylor & Shannon (2005) to be associated with the British-Irish Thulean Province, a large igneous province in the North Atlantic. Accompanying this activity were large swarms of sills and flows, which were intruded into the Rockall region. The intrusion of these sills reactivated the volcanic systems in the basin (Shannon *et al.,* 2006).

### 1.3.2 Orphan Basin

While the Iapetus Ocean was closing during the Caledonian-Appalachian orogeny, the basement structures that ran NE-SW along the strike of the orogeny were established (Williams 1984, 1995). The formation of the Orphan Basin was largely controlled by these pre-existing basement structures (Shannon 1991). The initial phase of rifting affected mainly the East Orphan Basin and is thought to have occurred as early as the Triassic (Welford *et al.,* 2012*;* Enachescu *et al.,* 2004) or Early Jurassic (Gouiza *et al.,* 2017). Eastward dipping fault blocks and thick Jurassic sediment preserved in the hanging wall of half grabens provide proof that this initial rifting phase primarily affected the East Orphan Basin (Gouiza *et al.,* 2017). Rifting began in the East Orphan Basin and progressed westward, as evidenced by the change in orientation of faults and basement ridges from NE-SW to N-S. (Enachescu *et al.,* 2004). During the Late Triassic to Early Jurassic, continental break-up between Newfoundland and Western Iberia was initiated and the Orphan Basin began to develop.

The second phase of rifting occurred during the Late-Jurassic to Early Cretaceous (Enachescu *et al.,* 2004; Welford *et al.,* 2012), resulting in enlargement of the Orphan Basin. During this time, the Orphan Basin was divided into a younger West Orphan Basin and an older East Orphan Basin (Enachescu *et al.,* 2004). The West Orphan Basin is inferred to have only begun opening in the Late Jurassic (Enachescu *et al.,* 2004), but this conclusion may simply reflect a lack of deep well control (Welford *et al.,* 2012). The westward spread of deformation resulted in the formation of half grabens bounded by westward-dipping normal faults. The Late Jurassic-Early Cretaceous rift event also resulted in the formation of several conjugate Mesozoic rift basins, such as the Porcupine and Rockall basins in the Irish North Atlantic (Mackenzie *et al.,* 2002; Lau *et al.,* 2015).

The third phase of rifting occurred in the Aptian-Albian and was oriented NE-SW, overprinting the two previous rift phases (Welford *et al.,* 2012; Enachescu *et al.,* 2004). As a result of the change in extension direction, the faults in the East Orphan Basin were reactivated and widened. The faults in the West Orphan Basin were also reactivated during this phase of rifting. This fault reactivation of the West Orphan Basin was likely related to the northward propagation of extension and the opening of the Labrador Sea between Labrador and western Greenland (Chian *et al.,* 1995).

The mid-Late Cretaceous extension also separated the Newfoundland margin from the conjugate Irish margin (Welford *et al.,* 2012). Doré *et al.* (1997) interpreted this event as a reopening of the Caledonian-Appalachian basement structures. The East and West Orphan basins experienced extension and minor transtension from this Late Cretaceous rift episode (Enachescu *et al.,* 2004). During the Paleocene, the Orphan Basin evolved in a post-rift setting, with a long period of thermal subsidence resulting in the deposition of a thick Cenozoic succession (Gouiza *et al.,* 2017).

## 1.4 Past Work

### 1.4.1 Rockall Basin

The Rockall Basin is 250 km wide by 1100 km long, making it the largest basin located in the Irish offshore (England & Hobbs 1997, Kimbell *et al.,* 2010). Water depths range from 200 m on the eastern and western margins to over 3000 m in the center of the basin (Corfield *et al.,* 1999). Roberts *et al.* (1988) were the first to suggest that the Rockall Basin was floored by highly thinned continental crust. However, there was significant geological debate during the 1970s to 1990s (summarized by Smythe 1989) concerning the thickness of the underlying crust (Morewood *et al.,* 2004). Most recent work in this area indicates that the Rockall Basin contains up to 5 km of presumed late Paleozoic to recent sediments above thinned continental crust (Shannon *et al.,* 1999). Several smaller and older basins are present along the margins of the Rockall Basin, indicating a period of early lithospheric extension in the area (Shannon *et al.* 1999). There is a lack of deep well data for the entire Rockall Basin, which means that its underlying geology remains poorly constrained. Therefore the deep stratigraphy in the Irish Rockall Basin is principally constrained by regional correlation and jump-correlation to wells in the Porcupine Basin, which lies to the south (Crocker & Shannon 1987). Sills, intruded into the Cretaceous and Paleocene sediments, obscure the deep structure over large areas of the northern and southern parts of the basin (Corfield *et al.,* 1999). However, deep structures can still be seen where lateral gaps in the distribution of sills allow for improved deep seismic imaging. Several normal incidence reflection surveys in part of the southern Rockall Basin (e.g., England & Hobbs 1997 and Shannon *et al.,* 1999) provide good quality data, primarily above the complex of extensive sills.

The British Institutions Reflection Profiling Syndicate (BIRPS) presented the first

publicly available deep near-normal-incidence reflection profiles, shot across the entire width of the Rockall Basin (England & Hobbs 1997). The northwest slope of the Rockall Basin has an unreflective basement that is cut by a number of normal faults bounding a series of half-grabens (England & Hobbs 1997). Within the grabens, England & Hobbs (1997) observed fans of reflections that they interpreted as syn- or early post-rift sedimentary deposits (Fig. 1.8).

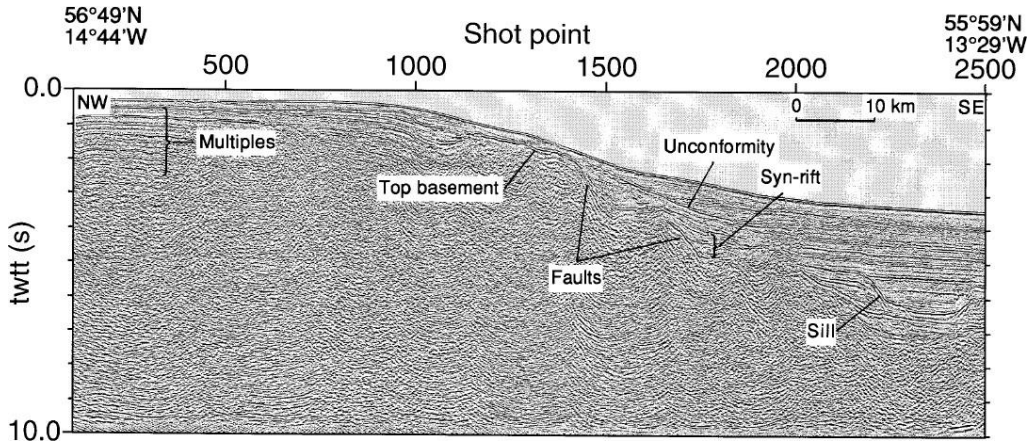


*Figure 1.8: Two way travel time profile of the Rockall slope and basin (England & Hobbs 1997). Location shown in Fig. 1.2.*

The joint Birmingham/Cambridge Universities experiment in the Rockall Basin acquired two expanding spread profiles (ESP) that provide a 1D velocity function at the mid-point of the profiles (England & Hobbs 1997). Since these data provide information about particular layers, they are useful for interpreting the reflection data. The ESP data confirmed that the observed high amplitude reflections were sills due to their coincidence with a sharp increase in velocity (England & Hobbs 1997). England & Hobbs (1997) also state that the top of the basement coincides with an increase in velocity and they suggest that the sediments described as syn-rift rest directly on basement rocks. Overall, England & Hobbs (1997) proved that there is no evidence of oceanic crust or a "reflective Moho" within the basin. They also conclude that the bulk of the sediment observed in the Rockall Basin accumulated during and following a major rifting event in the Early to mid-Cretaceous.

Shannon *et al.* (1999) present the results of a multi-disciplinary study using wide-angle and normal incidence seismic reflection data together with gravity information. As part of the Rockall and Porcupine Irish Deep Seismic (RAPIDS) project in 1988 and 1990, two wide-angle seismic profiles, with a combined length of 1600 km, were recorded in the Rockall Basin (Shannon *et al.*, 1999). Normal incidence seismic reflection data provided Shannon *et al.* (1999) with more information on the structure and sedimentary succession within the basin. The seismic model that Shannon *et al.* (1999) generated was constrained by the available gravity data (Fig. 1.9). The results indicated the presence of continental crust beneath all the basins in the Rockall region (Shannon *et al.*, 1999). For reference, the unstretched continental crust onshore in Ireland is approximately 30 km thick and consists of three distinct layers, underlain by a thin Moho transition (Lowe & Jacob 1989). Offshore, thinned continental crust extends along the entire length of the Rockall Basin (Shannon *et al.*, 1999). Shannon *et al.* (1999) suggest that the upper and middle crust within the basin experienced a stretching factor of 8-10, whereas the lower crust was stretched by a factor of 2-3. Overall, the bulk crustal stretching factor for the crust, as a whole is likely to range from 4-6 (Shannon *et al.*, 1999). Crustal rupture did not occur in the center of the Rockall Basin, likely due to the strength provided by the lower crust and the slightly thinned mantle lithosphere (Shannon *et al.*, 1999).

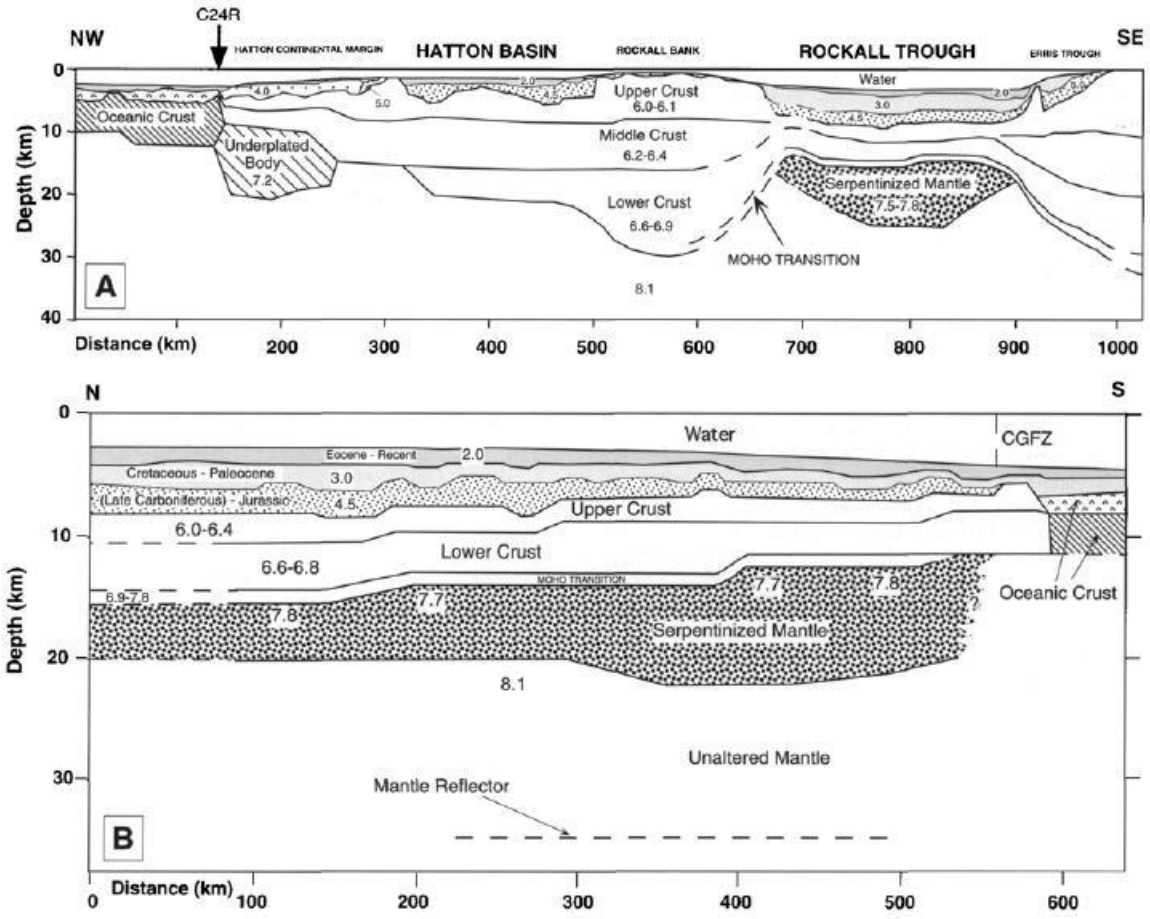


*Figure 1.9: (A) Model based on the RAPIDS wide-angle seismic transverse profile from Ireland to the Iceland Basin, 2A, from Shannon et al. 1999 (see Fig. 1.4 for location). Solid interfaces are regions where the model is well constrained by the seismic data. Numbers are seismic P-wave velocities (km/s). The location of magnetic anomaly 24 (C24R) of Early Eocene age is indicated. (B) Model based on RAPIDS wide-angle axial profile through the Rockall Trough, 2B (see Fig. 1.4 for location). The location of the Charlie Gibbs Fracture Zone (CGFZ) is indicated.*

The upper mantle low velocity zone beneath the Rockall Basin is interpreted to be the result of partial serpentinization of the upper mantle, with the underlying layer interpreted as normal mantle peridotite (Fig. 1.9; O'Reilly *et al.*, 1996). During the late Mesozoic, propagation of faults into the brittle mantle likely created conduits for the seawater circulation necessary to serpentinize the upper mantle (Shannon *et al.*, 1999). Overall, Shannon *et al.* (1999) suggested that the stretching factor of the entire basin was 4-6 and that the best fit of possible models suggests that the basin developed in response to rift episodes in the Triassic,

Late Jurassic and Early Cretaceous.

Morewood *et al.* (2005) present, review and discuss the results of their wide-angle seismic reflection/refraction experiments in the Irish sector of the northern Atlantic margin. They determined that the continental crust thins from 25 km to about 6 km in the center of the basin and has an overall stretching factor of approximately 4-6, in agreement with Shannon *et al.* (2006). The maximum thinning of the continental crust occurs at the margins of the Rockall Basin, resulting in an asymmetric Moho profile with a steeper gradient beneath the eastern margin. This asymmetry could reflect the presence of a deep-seated basement structural fabric that served as a focus for reactivation; however, no such fabric has ever been identified with confidence (Morewood *et al.,* 2005).

Using 3D gravity modelling of the lithospheric structure, Kimbell *et al.* (2010) defined the regional patterns of crustal thickness variations along the margin and geometries of the main sedimentary basins, including the Rockall Basin. A regional gravity map of the Rockall Basin is shown in Fig. 1.5. There are very few exploration wells in the Rockall region, but the constraints for the presented gravity model were sourced from previously acquired velocity data derived from wide-angle seismic experiments (e.g., Mackenzie *et al.,* 2002 and Shannon *et al.,* 1999). At a broad scale, the model confirms the well-known structural configuration of the continental part of the region, with highly stretched crystalline crust and shallow Moho beneath the Rockall Basin (Kimbell *et al.,* 2010). Across the Rockall Basin, there is asymmetrical crustal thinning, with steeper necking zones to the southeast than to the northwest (Fig. 1.10; Kimbell *et al.,* 2010).

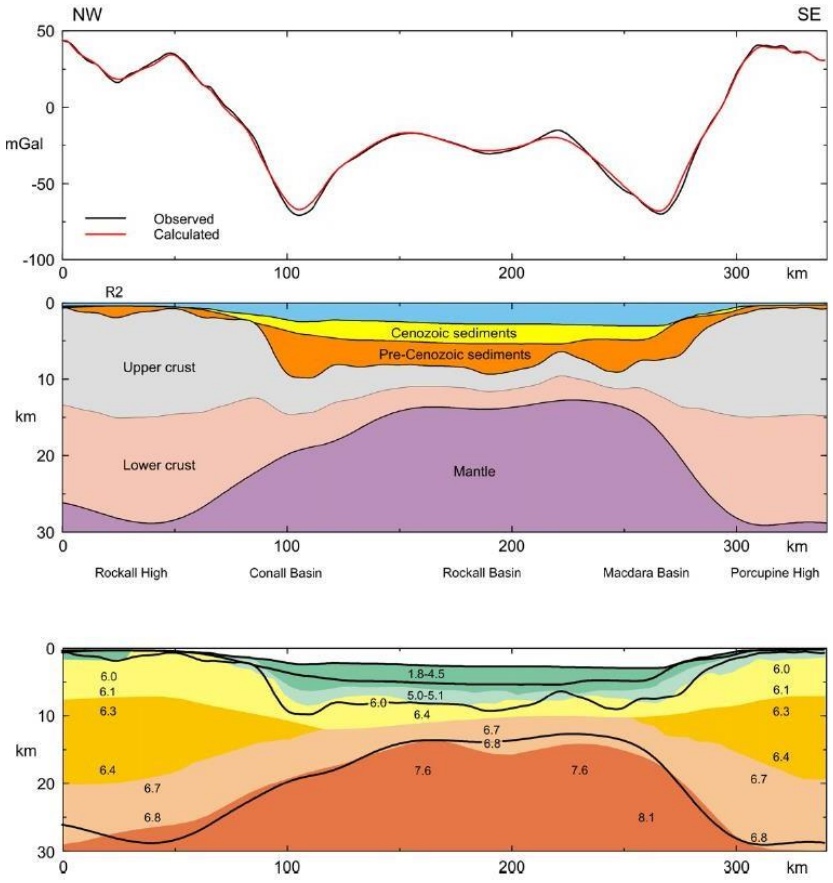


*Figure 1.10: Deep structure beneath a RAPIDS 3 seismic profile (location shown in Fig. 1.4), comparing a section through the 3D model (top two panels) with the seismic interpretation of Mackenzie et al. (2002) (bottom panel). 3D model interfaces are superimposed as heavy black lines on the seismic model. Numbers in the bottom panel are P -wave velocities in km/s (Kimbell et al., 2010).*

The agreement between the modelled Moho depths beneath the Rockall Basin is surprising, given the evidence for relatively low seismic velocities in the upper mantle beneath the basin, which has been interpreted as being a result of serpentinization (O'Reilly *et al.*, 1996 and Morewood *et al.*, 2005). The modelled average thickness of the crystalline crust beneath the Rockall Basin is 5-6 km, but there is a distinct increase in the north with values around 10 km (Kimbell *et al.*, 2010). This is in agreement with the previously acquired gravity and seismic data (e.g., Roberts *et al.*, 1988 and Kimbell *et al.*, 2005), suggesting that the crust beneath the northern part of the Rockall Basin is also somewhat thicker towards its flanks (Kimbell *et al.*,

2010). In the southern part of the Rockall Basin, Kimbell *et al.* (2010) observed that the magnetic field is dominated by the effects of the Barra Volcanic Ridge System. The Barra Volcanic Ridge System is comprised of a series of arcuate ridges that are considered to be extrusive volcanic edifices that were later draped by sedimentary rock (Kimbell *et al.,* 2010). Overall, Kimbell *et al.* (2010) conclude that the observed broad magnetic anomaly pattern can be explained in terms of variations in the thickness of the magnetic crystalline crust. It was also proposed that beneath the Rockall Basin is highly extended continental crust, which agrees with numerous other papers (e.g., O'Reilly *et al.,* 1996, Shannon *et al.,* 2001 and Morewood *et al.,* 2005).

### 1.4.2 Orphan Basin

Offshore Newfoundland has been broadly surveyed over several decades using geophysical methods including seismic profiling, gravity, and magnetic surveys (Keen & Barrett 1981, Keen & Dehler 1993, Chian *et al.,* 2001 and Welford *et al.,* 2012). Haworth (1977) presented the results of gravity and magnetic surveying across numerous offshore Newfoundland basins using magnetic trends. He suggested that the Orphan Basin is underlain by continental crust that has experienced significant subsidence.

Keen & Barrett (1981) carried out a seismic refraction survey using a series of ocean bottom seismometers (OBS) located at each end and in the centre of a N-S trending seismic line in the Orphan Basin. Their results suggest that the continental crust beneath the Orphan Basin underwent extensive stretching and they interpret the current overall crustal thickness to be 15-17 km, which is approximately 50% of its original thickness. A large positive gravity anomaly is

observed over the continental shelf and is interpreted to be the result of thinned continental crust beneath the outer shelf. Finally, Keen & Barrett (1981) proposed that the temperature distribution across the Orphan Basin reflects that rheology of the lithosphere may vary laterally across the basin and that it may also vary with time.

Keen & Dehler (1993) used high-quality maps of sedimentary thicknesses to obtain estimates of subsidence and therefore allow for estimates of stretching factors of the crust and mantle lithosphere to be computed across the Orphan Basin. They found that lithospheric deformation occurred by pure shear, whereas crustal deformation occurred by either pure or simple shear; a detachment between the upper and lower lithosphere may be present to explain the differences. Keen & Dehler (1993) also showed that crustal stretching was asymmetric across the basin and localized along the edges of the rift zone.

Chian *et al.* (2001) acquired a wide-angle seismic refraction profile and coupled it with previously acquired deep seismic reflection profiles as well as data from two local wells (Fig. 1.11). They found that the continental crust extends seaward for 410 km to the Orphan Knoll, where the ocean-continent transition begins. No high velocity lower crustal layer was presented in their model, indicating a non-volcanic rifting scenario (Fig. 1.11). This result was in contrast to work by Keen & Barrett (1981) who proposed a high velocity layer and interpreted it as a magmatic underplate. Chian *et al.* (2001) also observe a gravity high that is 110 km wide and accompanied by a shallow Moho boundary (approximately 17 km), which they attribute to a failed rift center.

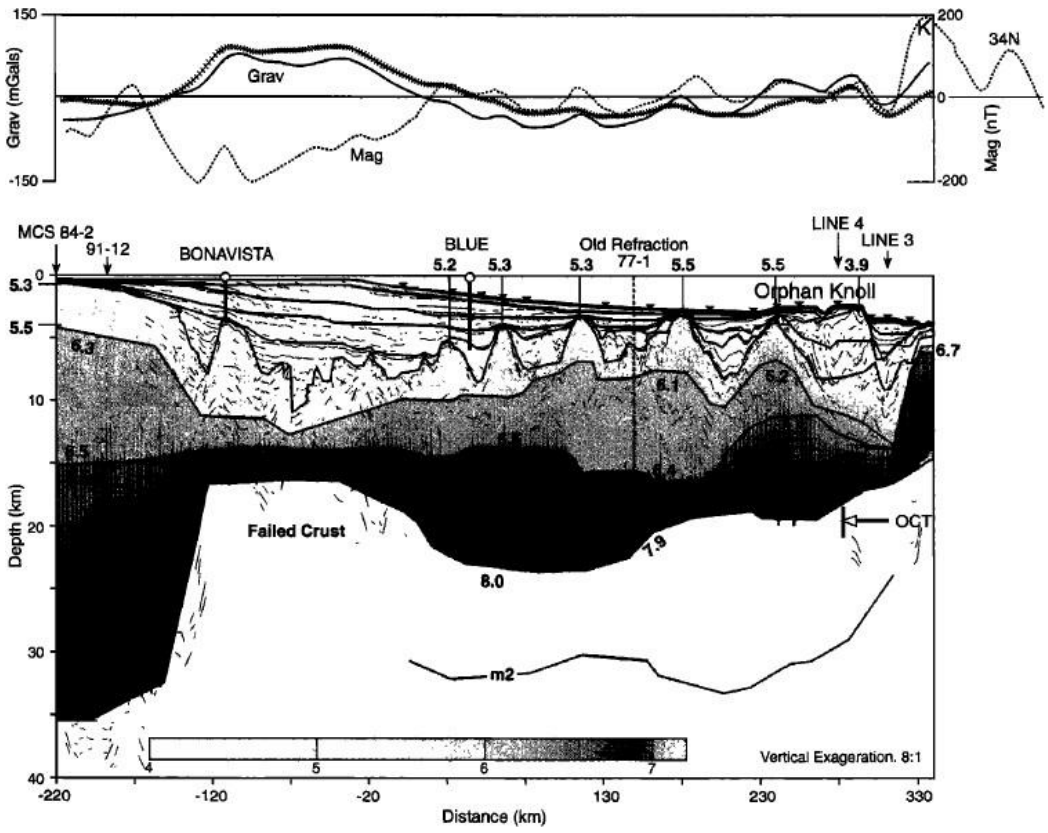


*Figure 1.11: Final velocity model from Chian et al. (2001), across the entire stretched continental crust, overlain with the multichannel seismic (MCS) interpretation. Observed (crosses) and computed (shaded line) gravity anomalies are shown on top along with the observed magnetic profile. OCT, ocean-continent transition zone. Location shown in Fig. 1.4.*

Welford *et al.* (2012) aimed to investigate early rifting history, crustal structure and geological evolution of the Orphan Basin-Flemish Pass and the Irish Atlantic conjugate margin. This was accomplished by using regionally constrained 3D gravity inversion. A regional free air gravity anomaly map of the Orphan Basin is shown in Fig. 1.7. From the observed data, they produced insightful images along and across these conjugate, continuous basins. When comparing the Irish margin to the Newfoundland margin, they found that the Irish margin experienced non-uniform rifting and localized extreme crustal thinning. In contrast, the Newfoundland margin underwent a more uniform thinning process. Serpentinization (and possible exhumation) of the mantle lithosphere has been proposed in the southern portion of the

Porcupine Basin and in select pockets within the Rockall Basin. However, no serpentinization of the mantle lithosphere has been observed beneath the Orphan Basin on the Newfoundland margin. Welford *et al.* (2012) suggest these differences may be due to a more rheologically strong crust-mantle lithosphere on the Irish margin and a weak crustal layer beneath the Orphan Basin. They also present several reconstruction maps of the Newfoundland and Irish Atlantic conjugate basins at the initiation of sea-floor spreading. These reconstruction maps show some of the inversion constraints and the results from both margins, including: bathymetry, depth to basement (Fig. 1.12), residual total magnetic anomaly, observed free air gravity anomaly, predicted free air gravity anomaly, Moho depth, and crustal thickness.

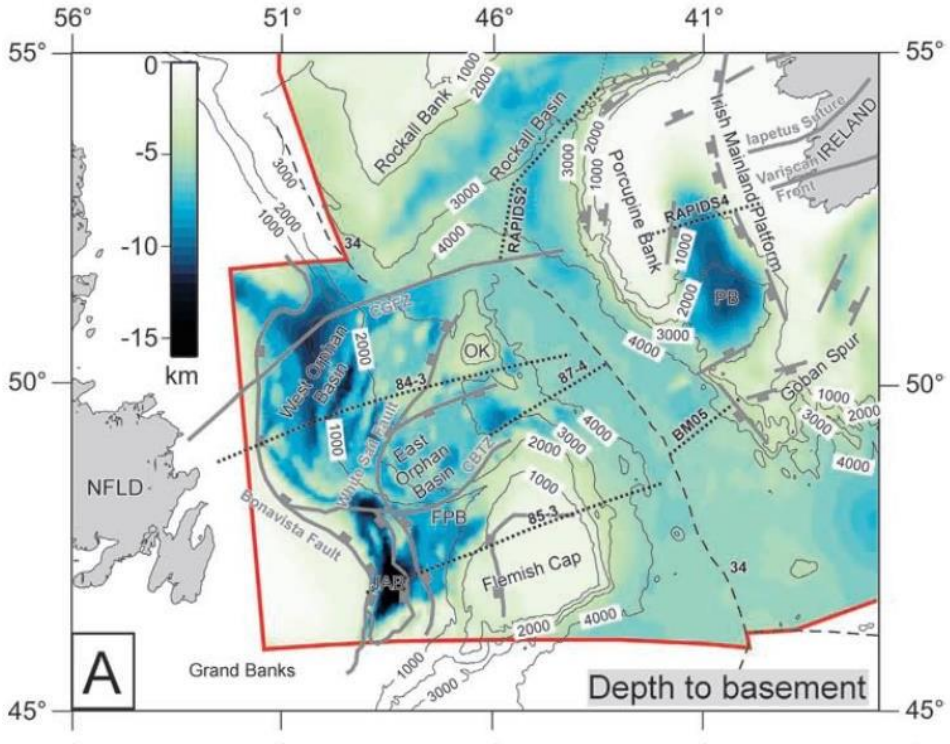


*Figure 1.12: Depth to basement reconstruction across both the Newfoundland and Irish Atlantic conjugate basins. The contours correspond to present-day bathymetry (1000 m contour interval). The red outlines define the limits of the regions used in the inversions (Welford et al., 2012).*

Lau *et al.* (2015) present a 2D P-wave velocity model, constructed using seismic refraction and wide-angle reflection data (Fig. 1.13). The model was constrained using gravity results and borehole logs from three local wells. From their model, they interpreted syn-rift Jurassic sedimentary rocks across the entire Orphan Basin, extending from the eastern sub-basin to the western sub-basin. Contrary to previous results, this new interpretation implies an earlier (Jurassic or earlier) rifting age.

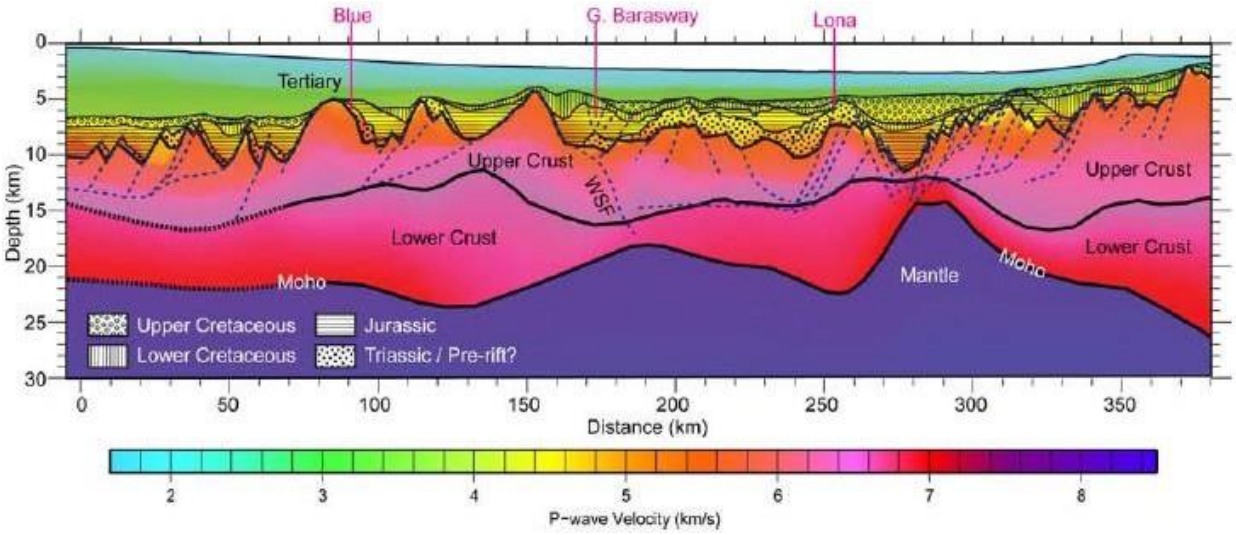


*Figure 1.13: Geological interpretation of depth section Or0–122 (Location in Fig. 1.4) from incorporating both the Multichannel Seismic (MCS) reflectivity and the wide -angle velocity model. Dashed blue lines are interpreted faults responsible for upper crustal thinning. Figure from Lau et al. (2015)*

Based on a reconstruction created by Lau *et al.* (2015), there is a complex connection between the West Orphan Basin and the Rockall Basin, the East Orphan Basin and the Porcupine Basin, and the Central Orphan High and the Porcupine Bank (Fig. 1.14). To further support this connection, there are similarities in the crustal structure between them. Beneath the East Orphan Basin, no serpentinization of the mantle is observed. This is contrary to what is observed in the Rockall and Porcupine basins, which agrees with the interpretation provided by Welford *et al.* (2012). However, Lau *et al.* (2015) suggest that the reasoning behind the lack of

serpentinization on the Newfoundland margin is due to a narrow zone (approximately 30 km wide) of potentially brittle crust being buried by syn-rift sedimentary rocks, which inhibited the flow of water down crustal-scale faults and therefore prevented serpentinization of the mantle.

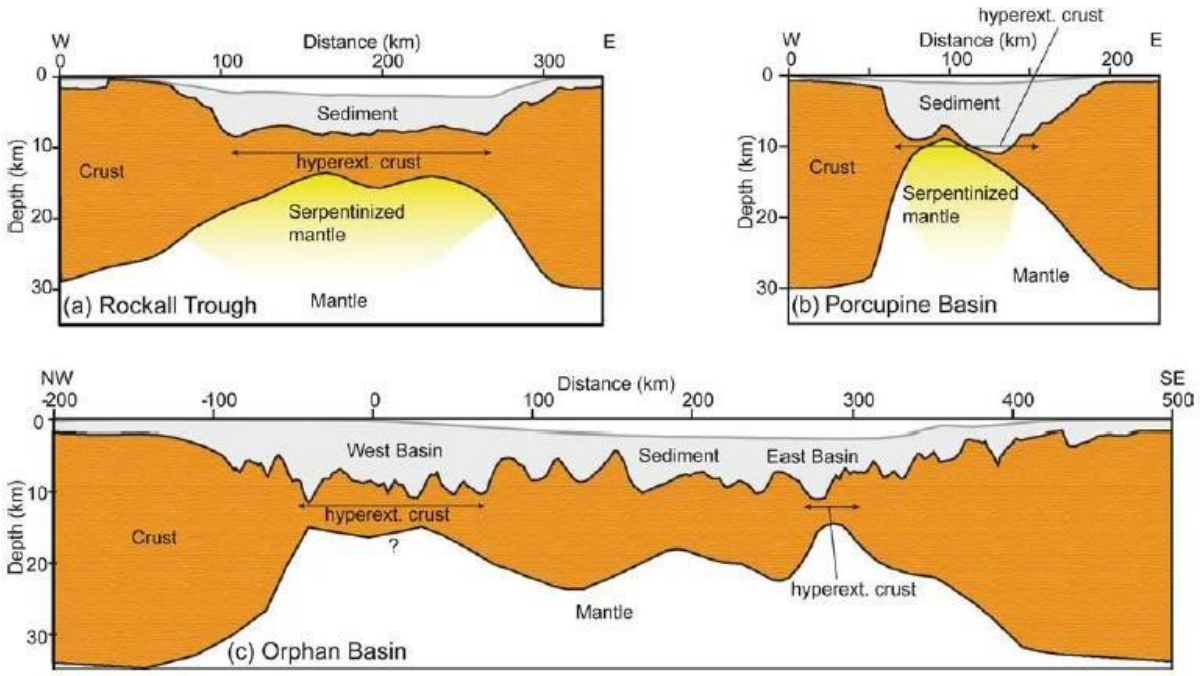


*Figure 1.14: Structural comparison between the Orphan Basin and its Irish counterparts from Lau et al. (2015). Structures are constrained by dense wide-angle data, except for the western end of Orphan Basin which is determined by gravity modelling (Lau et al., 2015). Zones with crustal thicknesses <10 km are marked as hyperextended crust. (a) Rockall Trough (Morewood et al., 2005). (b) Porcupine Basin (O'Reilly et al., 2006). (c) Orphan Basin (Lau et al., 2015). Question mark represents potential existence of serpentinized mantle.*

## 1.5 Purpose

The overall goal of this M.Sc. project is to create a Newfoundland-Ireland conjugate margin basin model from a single seismic megatransect that can be restored to a pre-rift state. This model will provide a more thorough understanding of the mechanisms involved in the rifting phases of the Newfoundland and Irish margins. One of the main scientific impacts of this research will be related to the petroleum exploration industry. The province of Newfoundland

and Labrador has significant petroleum deposits within its offshore basins and therefore this research will be locally relevant. This research will provide large-scale constraints that are necessary for explaining how a targeted basin developed, therefore aiding in major companies' knowledge of lesser explored basins. Due to the relatively high cost of exploration, these additional constraints will aid in mitigating inherent risks in targets of interest and hopefully attract new companies that can bring economic growth to the province of Newfoundland and Labrador.

## 1.6 Thesis Outline

In Chapter 2, seismic reflection lines and well data provided for this M.Sc. thesis in both the Rockall Basin and the Orphan Basin will be presented. The location of the wells and their proximity to the seismic lines in both basins will also be discussed, along with the research methodology for this thesis. In Chapter 3, the results of the seismic interpretations, carried out in Schlumberger's Petrel© software program, will be discussed in detail. Six seismic units will also be identified and described. In Chapter 4, the results of the Paleozoic basement reconstruction, along the primary and secondary seismic lines will be presented. The restoration process was carried out with Move© software and numerous 2D and 3D reconstructed figures are included to aid in the interpretation of the results. A discussion of the findings of this thesis will be presented in Chapter 5. Finally, the conclusions, based on the various reconstructions in the Rockall and Orphan basins, will be presented in Chapter 6, along with recommendations for future work.

# Chapter 2: Data and Methods

## 2.1 Data

The geophysical data used in this M.Sc. project were primarily seismic reflection data. The data for the Rockall Basin, offshore Ireland, were provided by the Petroleum Affairs Division of the Department of Communications, Climate Action and Environment, of the Irish government. The data for the Orphan Basin, offshore Newfoundland, were provided by TGS, a company specializing in geoscientific data acquisition.

The data were first imported into Schlumberger's Petrel© 2017 software program. Petrel© is primarily used in the exploration and production sectors of the petroleum industry, to interpret seismic data, create well correlations and build reservoir models. Regional scale seismic interpretation, in Petrel© along a primary and a secondary seismic line in each basin was performed. The seismic lines for each basin (for the Rockall Basin, IR1 and IR2, and for the Orphan Basin, NL1 and NL2) were subsequently used for depth analysis in Move©. An additional line on the Newfoundland margin, NL3, was used later in the thesis to compare the Rockall Basin with the East Orphan Basin and was reconstructed following the same methodology as NL1 and NL2 (detailed interpretations and reconstructions of NL3 not shown). Move©, a Midland Valley software product, is one of the most up to date structural modelling and analysis toolkits available. This software allows for fully integrated 2D and 3D model building, which forms a vital component to this M.Sc. project and will be discussed in detail in chapter 4.

### 2.1.1 Rockall Basin

The Rockall Basin seismic reflection data, acquired in 2013 and 2014, have been provided by the Petroleum Affairs Division of the Department of Communications, Climate Action and Environment, of the Irish government to Memorial University of Newfoundland. The Irish government also provided geological and geophysical well logs to accompany the seismic reflection data. Unfortunately, very few wells have been drilled in the center of the Rockall Basin, principally due to limited petroleum exploration and the depth of the water column.

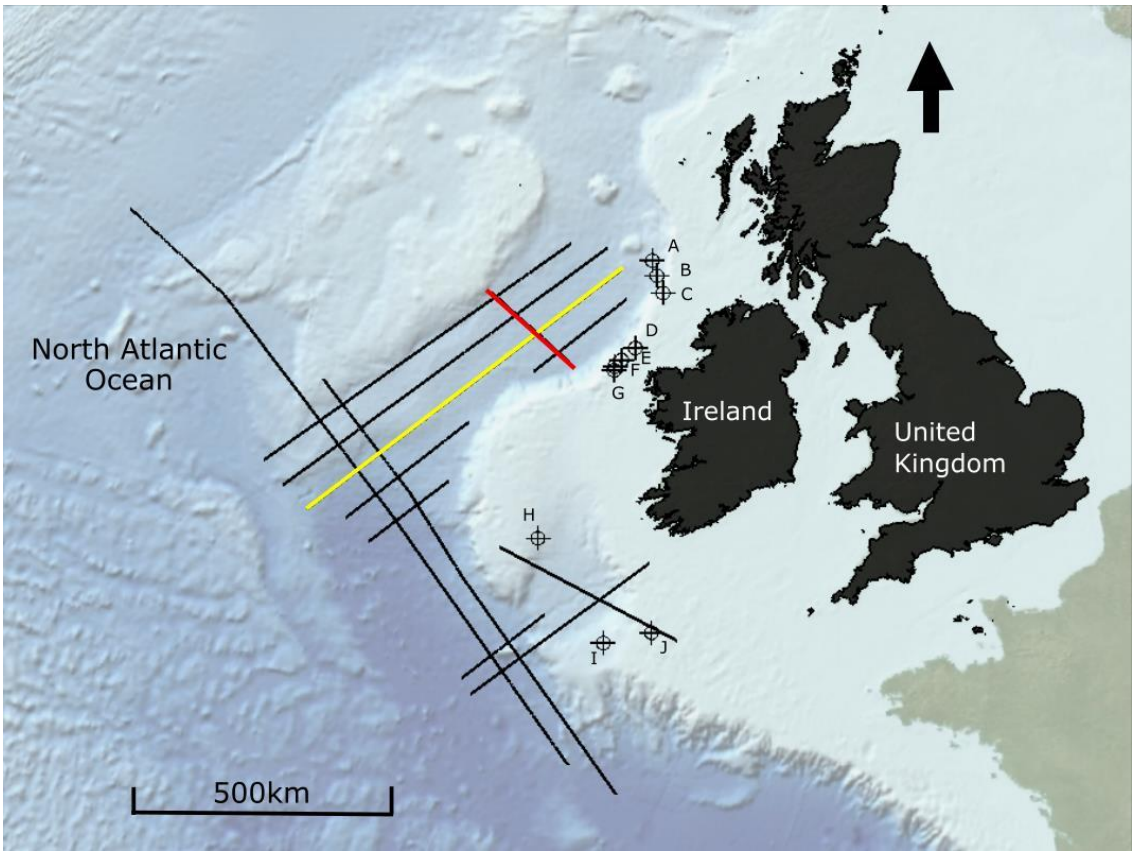


*Figure 2.1: All Irish Atlantic seismic and well data provided by the Irish Government. Well locations are marked by cross filled circles and labeled with letters. The primary seismic line for this M.Sc. project, IR1, is marked by the yellow line and the cross- sectional seismic line, IR2, is marked by the red line. The remainder of the seismic lines provided by the Irish Government are marked by black lines.*

The small number of wells drilled by various petroleum exploration companies are primarily located in a chain of Paleozoic-Early Mesozoic basins that are perched along the margins of and above the younger, Late Triassic, Rockall Basin (Figs. 2.1 and 2.2). The chain of perched basins extends from the Donegal Basin in the North to the South Brona Basin in the South (Fig. 2.3). These basins are thought to provide evidence of early lithospheric extension in the North Atlantic (Moorewood *et al.* 2004). Since these perched basins are of Paleozoic-Early Mesozoic age, much older than the Late Triassic Rockall Basin, and are approximately 50-100 km away from the nearest seismic line, the wells drilled in these basins provided minimal correlation to the seismic data within the center of the Rockall Basin.

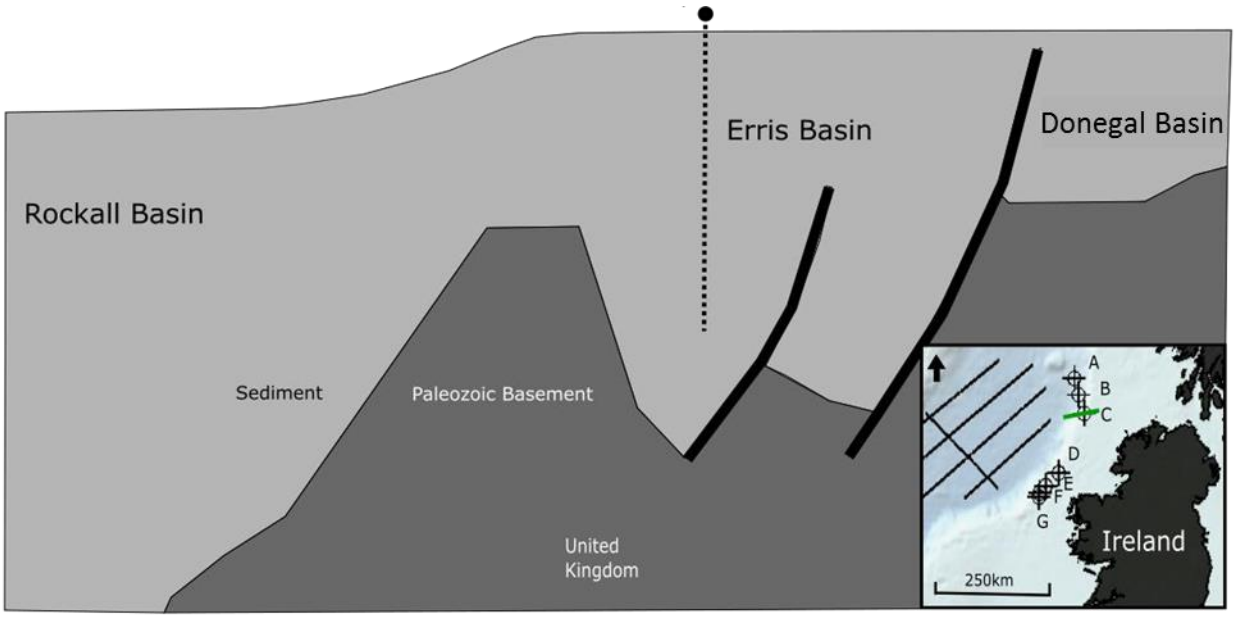


*Figure 2.2: A cross-section of the younger Rockall Basin and the older perched basins, the Erris Basin and the Donegal Basin. Well 12/13-1A, the dotted black line, was drilled into the Erris Basin, location shown here. The location of this figure is the green line in the inset box, the black lines represent the seismic lines in the Rockall Basin. This figure was adapted from Corfield et al. (1999).*

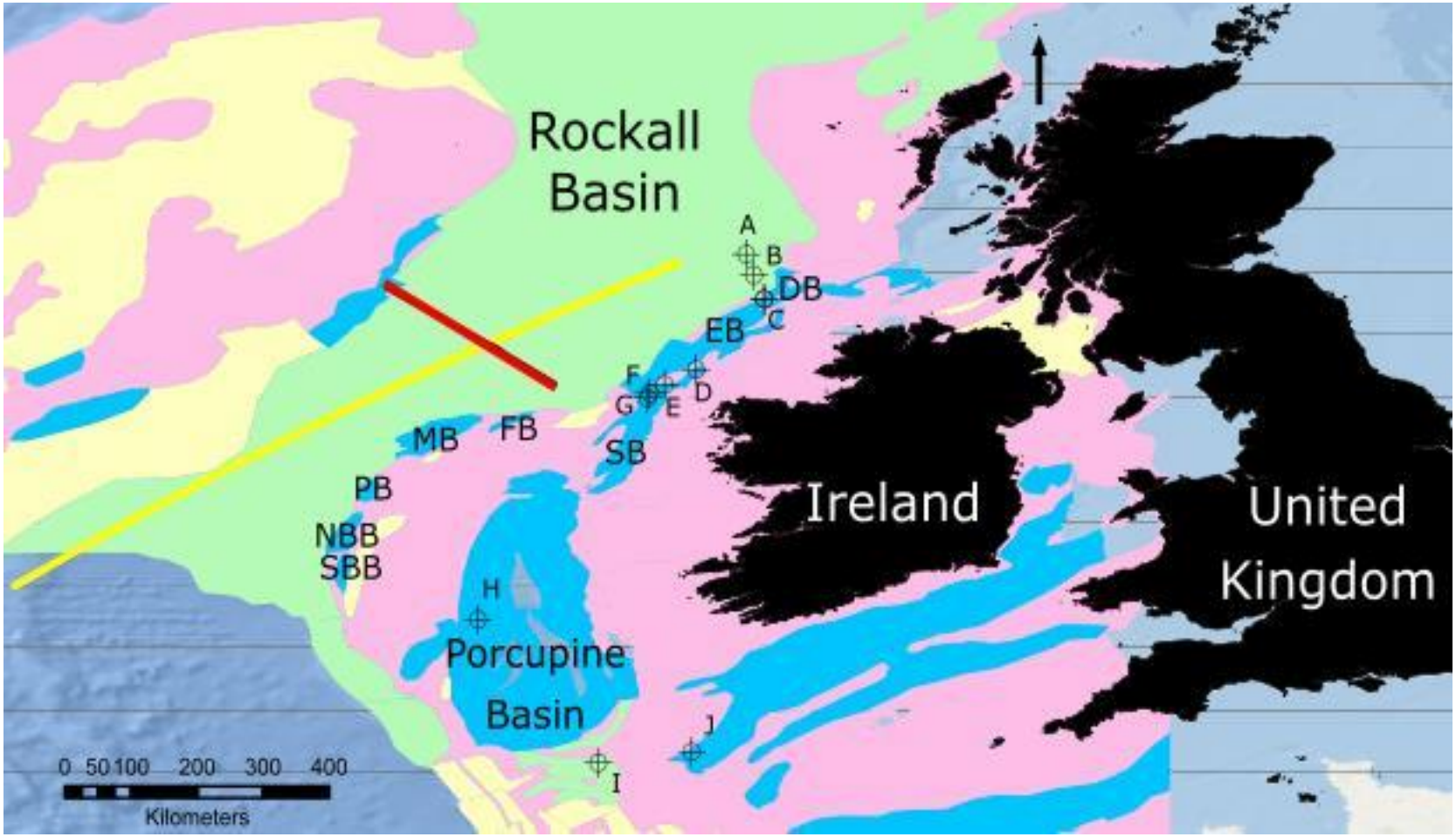


*Figure 2.3: Polygons showing the age of basins in the Irish North Atlantic. Pink polygons indicate Paleozoic Basement, blue polygons indicate Triassic basins, green polygons indicate Jurassic basins and yellow polygons indicate Cretaceous – Early Paleocene basins. Basin identifications are as follows: DB = Donegal Basin, EB = Erris Basin, SB = Slyne Basin, FB=Fursa Basin, MB = Macdara Basin, PB = Padraig Basin, NBB = North Brona Basin, SBB= South Brona Basin. The yellow line is the primary seismic line (IR1) in the Rockall Basin. The red line represents the secondary seismic line in the Rockall Basin (IR2). The cross-filled circles mark the well locations and are labeled with alphabetical letters. This image was adapted from: Ersi Delorme, NOAA NGDC and the Department of Communications, Climate Action and Environment of the Irish Government.*

### 2.1.2 Orphan Basin

The Orphan Basin seismic reflection data, acquired in 2001, have been provided by TGS© to Memorial University of Newfoundland. The C-NLOPB provided additional geological and geophysical well logs for numerous wells within the Orphan Basin (Fig. 2.4). Of these logs, only well H intersected seismic line NL1, which is the primary seismic line of focus for this thesis in the Orphan Basin. Unfortunately, well H was drilled into a basement high, characterized as an area of crustal uplift generated by faulting during episodes of rifting. Sediment accumulation was limited in these areas due to erosional events. As a result, all the sedimentary units that extend over these highs are much thinner and cannot be used as a direct representation of the sedimentary units as a whole in this location. This local basement high provides little constraint to the deeper seismic data where the units are much thicker, as interpreted from changes in the seismic character at depth. Well B was drilled into a basement high along seismic line NL2 (location shown in Fig. 2.4), an intersecting line with the primary seismic line NL1. This well was also drilled into a topographic basement high. As a result of the interpreted, limited sediment accumulation and erosional events over these highs, the sedimentary units only moderately aid in correlating the deeper, thicker seismic units within the West Orphan Basin.

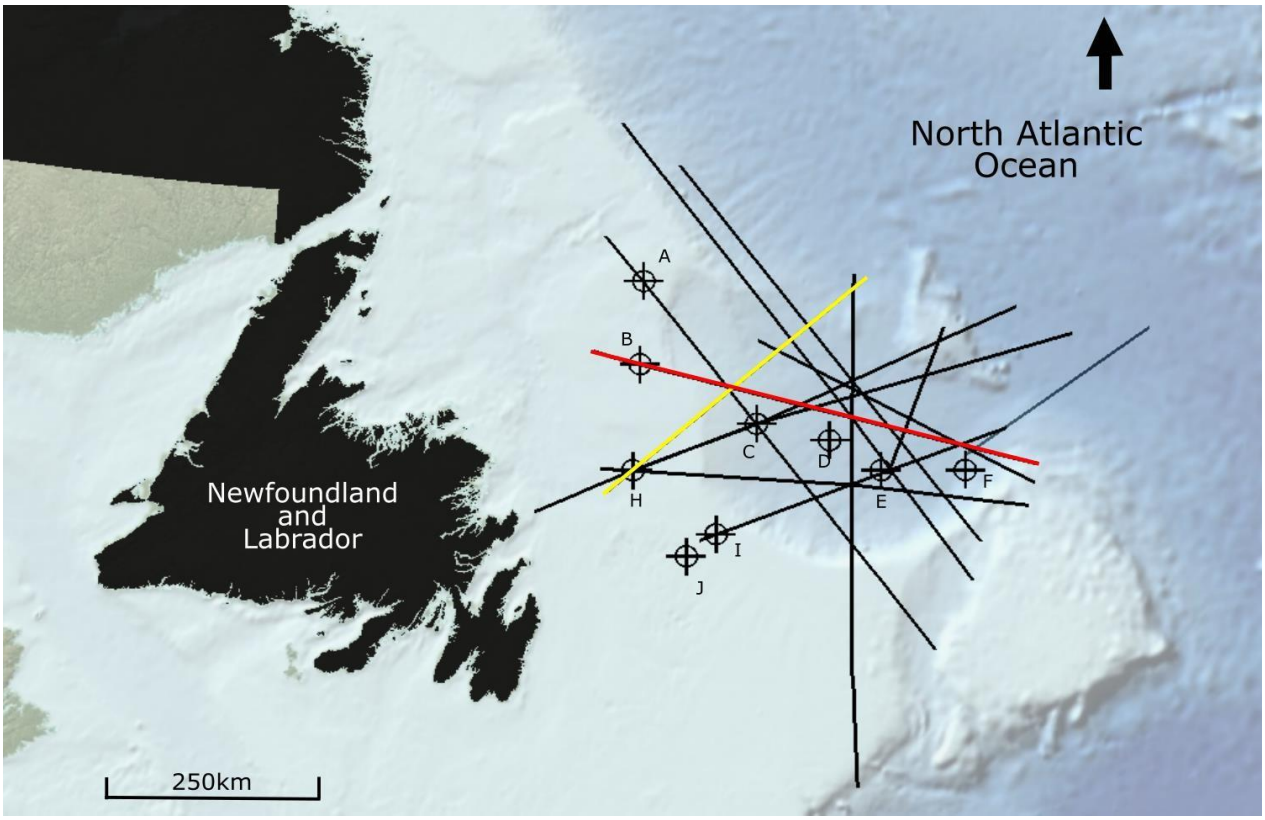


*Figure 2.4: Location of all the seismic lines provided by TGS. Location of some of the wells drilled in the Orphan Basin. Well logs were provided by the C-NLOPB. Yellow line indicates the location of NL1, the primary line of focus for the Orphan Basin. The red line indicates seismic line NL2, the cross-sectional line of focus for the Orphan Basin.*

## 2.2 Methods

### 2.2.1 Petrel© Seismic Analysis

Petrel© was the software package of choice for this thesis, allowing for detailed analysis and interpretation of all the seismic reflection data in the Rockall and West Orphan basins. Available well data, provided by the Irish Government and the C-NLOPB, were used to constrain key horizons within both the Rockall Basin and the West Orphan Basin.

Following the procedure of Gouiza *et al.* (2015), seismic units in both basins were defined and delineated based on syn-rift and post-rift characteristics. Syn-rift units are an accumulation of sediments that were deposited during rifting, consequently these units are generally heavily faulted and deformed. Post-rift units are sediments that accumulated after rifting had ceased, generally these sedimentary layers are laterally continuous.

### 2.2.2 Move© Model Restoration

#### 2.2.2.1 2D Depth Conversion

The 2D modelling algorithms in Move© for restoring basins remove the effect of deformation so that the un-deformed sections can be reassembled. The restoration preserves the line length and area balancing structural geology principles, taking into account the importance of geologic time and its impact on structure. Kinematic modelling in Move© requires each seismic line to be in the depth domain because the equations used to calculate the restorations have parameters that require the data to be in metres or kilometres. All four seismic lines, NL1, NL2, IR1 and IR2, were interpreted in Petrel© in the time domain (more commonly known as Two Way Travel Time (TWT)). Therefore each seismic line had to be converted from the time

domain into the depth domain before the restoration processes could begin.

The 2D Depth Conversion module in Move© provides a number of ways to carry out time to depth conversions. In this project, the Database method was used. This allows the velocity and rate of change of velocity values to be specified for each horizon in the model using the Stratigraphy and Rock Properties table (found in Appendix A). In Move©, the depth conversion is carried out using the equation:

$$Z = V_0 \frac{(e^{kt} - 1)}{k}$$

where Z represents the thickness of the layer in metres, $V_0$ represents the velocity at the top of the layer in metres per second, k represents the rate of change in velocity with increasing depth and t signifies the one way travel time for layer thickness, in seconds. The Horizon Velocity method was also used within the depth conversion. This velocity method assumes the velocity in the Rock Properties table is the velocity at the top of the horizon and k is the rate of change within the layer.

Parameters for the depth conversion within Move© were extracted for both the Rockall Basin and the Orphan Basin from previously published studies. The velocities for each sedimentary unit for seismic lines NL1 and NL2 in the Orphan Basin were interpreted from Lau *et al.* (2015) and Gouiza *et al.* (2017) (Table 2.1). The densities and thickness for each unit were taken from Gouiza *et al.* (2017) (Table 2.1). Gouiza *et al.* (2017) used well logs from the Orphan Basin to estimate thicknesses of units and gravity models to determine densities. The velocities for each sedimentary unit for seismic lines IR1 and IR2, in the Rockall Basin, were extracted from Morewood *et al.* (2005) and Mackenzie *et al.* (2002) (Table

2.1). Density and thickness values for each unit in the Rockall Basin were adapted from the values for the Orphan Basin from Gouiza *et al.* (2017), for consistency across the conjugate margins(Table 2.1). All the supplementary parameters used to calculate the 2D Depth Conversion in both the Rockall Basin and Orphan Basin can be found in Appendix A.

| | Density ($kg/m^3$) | Velocity for the Orphan Basin (m/s) | Velocity for the Rockall Basin (m/s) | Thickness of layers in the Orphan Basin (m) | Thickness of layers in the Rockall Basin (m) |
|---|---|---|---|---|---|
| Water Column | 1030 | 1450 | 1450 | 2000 | 3000 |
| Cenozoic | 2500 | 2500 | 2500 | 5000 | 2000 |
| Upper Cretaceous | 2500 | 4000 | 4500 | 750 | 1000 |
| Lower Cretaceous | 2700 | 4500 | 5100 | 1200 | 1500 |
| Jurassic | 2700 | 5000 | N/A | 2000 | N/A |
| Basement/ Continental Crust | 2870 | 6700 | 6700 | 7000 | 7000 |

*Table 2.1: Density parameters for each layer for both the Orphan and Rockall basins interpreted from Gouiza et al. (2017). Velocity parameters for each layer for the Orphan Basin interpreted from Lau et al. (2015) and Gouiza et al. (2017). Velocity parameters for each layer from the Rockall Basin interpreted from Mackenzie et al. (2002) and Morewood et al. (2005).*

The Mohorovicic Discontinuity or the "Moho", corresponds to an abrupt velocity increase at depth and is generally defined as the boundary between the Earth's crust and upper mantle (Prodehl & Mooney, 2012). This abrupt velocity increase generates wide-angle reflections on seismic refraction data, from which the depth to the Moho can be derived. Given that the abrupt velocity increase likely corresponds to an equivalent density increase, a proxy for the depth of the crust-mantle boundary can be defined based on this inferred density contrast. Welford *et al.* (2012) generated a Moho surface by running 3D gravity inversions on both the

Newfoundland and Irish margins using identical methodologies. Since the Moho is defined as a seismic discontinuity and is not normally defined in terms of a specific density contrast (as Welford *et al.* (2012) defined it), the generated surface represents more of a Moho proxy. To gauge the reliability of the 2D Depth Conversion performed by Move©, the Moho proxy was introduced to each model from Welford *et al.* (2012). The Moho proxy was created in the depth domain, therefore once it was imported into Move©, it provided a reasonable constraint on the depth-converted models.

#### 2.2.2.2 2D Decompaction

After all of the seismic lines (NL1, NL2, IR1, IR2, and later NL3) were converted from the time domain to the depth domain, kinematic modelling of each seismic line began in Move© with the end goal of restoring the two margins back to their pre-rift state. The first step in kinematic modelling is to account for sedimentary rock compaction over time. As sediment is accumulated within a basin, the weight of the overlying sedimentary rock compacts the underlying sedimentary rock through time. Therefore, to accurately restore the Rockall and Orphan basins through time, each layer must be decompacted as the overlying sedimentary rock is removed. This can be accomplished using the 2D Decompaction module in Move©. This module removes the top layer and adjusts the underlying layers by accounting for the compaction and porosity loss with burial. The 2D Decompaction module in Move© uses the following function:

$$f = f_0(e^{-cy})$$

where *f* represents the present-day porosity at depth, $f_0$ represents the initial porosity at the surface, *c* represents the porosity-depth coefficient ($km^{-1}$), and *y* represents the depth in metres.

The default compaction curve that Move© utilizes is based on the work by Sclater & Christie (1980), who used North Sea Basin data and assumed an exponential porosity decrease with increasing depth. Multiple iterations of the models were run to determine the impact of altering the decompaction parameters associated with each interval. These iterations revealed that by altering the porosity by ~10% and the decompaction coefficient by up to ~50%, the average resulting decompaction is only altered by ~50 m.

Isostasy is another important principle that must be accounted for during the kinematic modelling process. Isostasy describes vertical motion of the lithosphere due to buoyancy forces related to lateral variations in density (Watts 2001). These variations in density can be related to thermal effects or material compositions (Watts, 2001). It is important to account for isostasy as it affects the restored shapes of horizons and faults, paleo-topographies of restored seafloor surfaces, and the absolute height of the models during restoration.

Pratt's isostasy theory assumes that there are lateral changes in rock densities across the lithosphere (Lane, 1932; Lamb & Watts, 2010). The Pratt theory also assumes that the mantle is uniformly dense, with lower density crustal blocks floating higher to become mountains, and higher density blocks sinking to form basins and lowlands (Lane, 1932; Lamb & Watts, 2010). Airy isostasy theory assumes that across the lithosphere the rock density is approximately the same, but the crustal blocks have different thicknesses (Lane, 1932; Lamb & Watts, 2010). Therefore, mountains that have higher peaks also have roots that extend into the denser mantle below (Lane, 1932; Lamb & Watts, 2010).

The Pratt and the Airy theories both predict a relative deficiency of mass under high mountains, however Airy's theory is now known to provide a better and more plausible explanation of mountains within continental regions (Lamb & Watts, 2010). Additionally, Move© Help states that Airy isostasy modelling is more sensitive to massive thickness

variations. The sedimentary layers within the models generated for the Rockall Basin and the West Orphan Basin both have a variety of sedimentary layer thicknesses due to multiple phases of rifting. Therefore, local Airy isostasy is used in this thesis to account for the isostatic response to sedimentary unloading during decompaction.

#### 2.2.2.3 2D Thermal Subsidence

Thinning of the lithosphere during rift events results in large changes in elevation, mainly due to thermal subsidence. Sedimentary basins are produced by the stretching of continental lithosphere and the resulting thinning allows the hot asthenosphere to well up from below and elevate the thinned lithosphere. As the margin cools following rifting, the temperature decreases within the thinned lithosphere causing subsidence. Therefore, for each post-rift layer, thermal subsidence must be accounted for prior to decompaction, to accurately restore each basin. The 2D Thermal Subsidence module in Move© uses a thermal subsidence model generated by McKenzie (1978) to restore the shape and paleo-depth of the seafloor. This model produces a sedimentary basin by sudden stretching, followed by slow cooling of the lower part of the lithosphere, a process commonly observed at rifted margins (McKenzie, 1978).

The 2D Thermal Subsidence module in Move© requires numerous parameters for the calculation; these values were extracted from Shannon (1991) and Naylor & Shannon (2005). The parameters used in the Rockall Basin for age and syn-rift duration for seismic lines IR1 and IR2 were approximated from Shannon (1991) and Naylor & Shannon (2005) (Table 2.2). Shannon (1991) and Naylor & Shannon (2005) both identified three rift phases during the formation of the Rockall Basin, a Late-Triassic rift phase (228 Ma), a Mid-Late Jurassic rift phase (164 Ma), and a Mid Cretaceous rift phase (113 Ma). Since no Triassic or Jurassic sedimentary rocks were interpreted within the Rockall Basin (due to obscuring sills, discussed

in the next chapter), only the Mid Cretaceous rift phase was used for the thermal subsidence calculation. The syn-rift duration, the amount of time that the Rockall Basin experienced extension during the Mid Cretaceous rift episode, was set to 13 Ma (Shannon, 1991 and Naylor & Shannon, 2005). The thermal subsidence calculations in Move© require density and velocity values to be specified. The same parameters that were used in the 2D Depth Conversion (Table 2.1) were also used for the 2D Thermal Subsidence calculations (additional parameters provided in Table 3 of the Appendix).

The stretching factor (Beta) represents the ratio of final crustal thickness to the original crustal thickness and is a required parameter to calculate thermal subsidence. An original crustal thickness prior to rifting of 30 km was used (Lowe & Jacob 1989; Hauser *et al.,* 2008). The initial lithosphere thickness is also an important parameter when calculating thermal subsidence. A value of 125 km was used for the Rockall Basin (O'Reilly *et al.,* 1996). A uniform Beta value of 2.0 was used for the Rockall Basin (Gouiza *et al*., 2017).

The thermal subsidence parameters used in the West Orphan Basin for the age and syn- rift duration for seismic lines NL1, NL2, and later NL3, were interpreted from Enachescu *et al.* (2004), Welford *et al.* (2012), and Gouiza *et al.* (2017), and are listed in Table 2.2. Enachescu *et al.* (2004) and Welford *et al*. (2012) identified three rift phases in the Orphan Basin, a Late Triassic rift event (228 Ma), a Late Jurassic rifting event (164 Ma), and a Mid Cretaceous rift event (113 Ma). Due to the fact that no Triassic sedimentary rocks were interpreted in the West Orphan Basin, only the Late Jurassic and Mid Cretaceous rift events were used to calculate the thermal subsidence. The syn- rift duration of the Late Jurassic rift event was set to19 Ma, and the syn-rift duration of the Mid Cretaceous rift event was 13 Ma (Shannon, 1991 and Naylor & Shannon, 2005). The density and velocity values (from Gouiza *et al.,* 2017) that were used in the 2D Depth Conversion (Table 2.1) for the Orphan Basin

were also used for the 2D Thermal Subsidence calculations.

An original crustal thickness prior to rifting of 30 km was used for the West Orphan Basin (Gouiza *et al.*, 2017), to be consistent with the conjugate margin. The initial lithosphere thickness is also an important parameter when calculating thermal subsidence. A value of 125 km was used for the West Orphan Basin (Gouiza *et al.*, 2017). A uniform Beta value of 2.0 was used for the West Orphan Basin (Gouiza *et al.*, 2017). All of the additional parameters used to calculate the thermal subsidence for both the Rockall Basin and the Orphan Basin can be found in Appendix A.

| | Age of Rifting | Syn-rift Duration |
|---|---|---|
| Late Jurassic Rift Event | 164.0 Ma | 19.0 Ma |
| Mid Cretaceous Rift Event | 113.0 Ma | 13.0 Ma |

*Table 2.2: Rifting time-table for the West Orphan Basin used for 2D Thermal Subsidence calculations. Only the Mid Cretaceous rift event was used to calculate 2D Thermal Subsidence for the Rockall Basin.*

#### 2.2.2.4 2D Fault Restoration

After the 2D Decompaction and the 2D Thermal Subsidence calculations have restored each seismic line down to a horizon that has been heavily faulted due to rifting, fault modelling can begin. Move© offers several fault restoration modules, primarily the 2D Move-on-Fault and the 2D Block Restoration modules.

The 2D Move-on-Fault module can be used to create forward models and test new structural ideas, which allow different pre-rift and syn-rift tectonic successions and various displacements to be modelled. Based on fault geometries, different algorithms can be applied to the model: Simple Shear, Parallel Flow, or Trishear. The Simple Shear algorithm in Move© is

most applicable to extensional tectonic regimes with non-planar normal faults, because it maintains the area between beds. Furthermore, this algorithm can be applied to forward basin modelling where thicknesses of beds may vary. Since the Rockall Basin and the West Orphan Basin are both extensional tectonic regimes with normal faults, the Simple Shear algorithm was used. The "join beds" movement tool was used in the 2D Move-on-Fault module. The "join beds" movement tool allows for movement along the fault by realigning an interpreted hanging wall and footwall, thus restoring the horizon. A shear angle of ±60° was used depending on the dip direction of the fault (Fossen, 2016).

The 2D Block Restoration module in Move© is useful for quickly validating interpretations by piecing fault blocks back together. However, the 2D Block Restoration module can result in areas where the fault blocks overlap; this can be inferred to represent an excess rock volume. The 2D Block Restoration module can also result in gaps between the translated fault blocks; this represents deficiencies in the interpreted rock volume. According to Move© Help, these overlaps and gaps may be the result of using the wrong restoration algorithm. When the 2D Block Restoration module was applied to the models for this thesis, numerous gaps and overlaps were generated. Therefore, it was assumed that the 2D Block Restoration module was not the correct algorithm to be used, thus the 2D Move-on–Fault module was used to restore all of the models in the Rockall Basin and West Orphan Basin.

After the restorations of these faults were completed, all of the seismic lines were assumed to represent a pre-rift state and 3D model analysis could begin. Using the 3D viewer in Move©, the coordinates of the West Orphan Basin data, seismic lines NL1, NL2, and later NL3, were altered to create a seismic megatransect with the Irish margin lines within the same coordinate system. Finally, the results were compared to determine if the West Orphan Basin and the Rockall Basin formed a large continuous Mesozoic rift system prior to the opening of

the North Atlantic. These results will be presented in Chapter 4 and discussed in Chapter 5.

# Chapter 3: Seismic Interpretation

## 3.1 Introduction

Digital seismic data provided by the Petroleum Affairs Division of the Department of Communications, Climate Action and Environment, of the Irish government, and TGS, were uploaded into Schlumberger's Petrel software for seismic interpretation. Geophysical seismic interpretation is the science and the art of inferring geology, and associated geologic features and structures, from a processed seismic section. The two primary, conjugate lines that were chosen for this thesis are: seismic line IR1 (across the Rockall Basin, SW to NE) and seismic line NL1 (across the West Orphan Basin, SW to NE). A secondary line, which intersects the primary seismic line, was also chosen for each basin: seismic line IR2 in the Rockall Basin (intersecting IR1) and seismic line NL2 in the Orphan Basin (intersecting NL1). Within the Rockall and the West Orphan basins, five seismic units have been identified and interpreted. These units are: the acoustic basement, Jurassic sedimentary rocks, Lower Cretaceous sedimentary rocks, Upper Cretaceous sedimentary rocks, and Cenozoic sedimentary rocks. Each unit was identified and mapped in two-way travel time (TWT) along the interpreted seismic lines. This chapter contains a detailed analysis of each of these seismic units in both the Rockall and the Orphan basins.

## 3.2 Rockall Basin

The seismic reflection data, acquired in 2013 and 2014 within the Rockall Basin, are of very high quality, limited only in the resolution of the deep seismic data. Seismic interpretation of deep strata in the Rockall Basin was hindered by the presence of large Paleogene sills, intruded at approximately the top of the Cretaceous succession (Morewood *et al.*, 2005). For this study, seismic interpretations were focused on intermittent localized zones, where these

igneous intrusions were less prevalent. Fig. 3.1 depicts the units and geologic structures interpreted along IR1, the primary seismic line within the Rockall Basin.

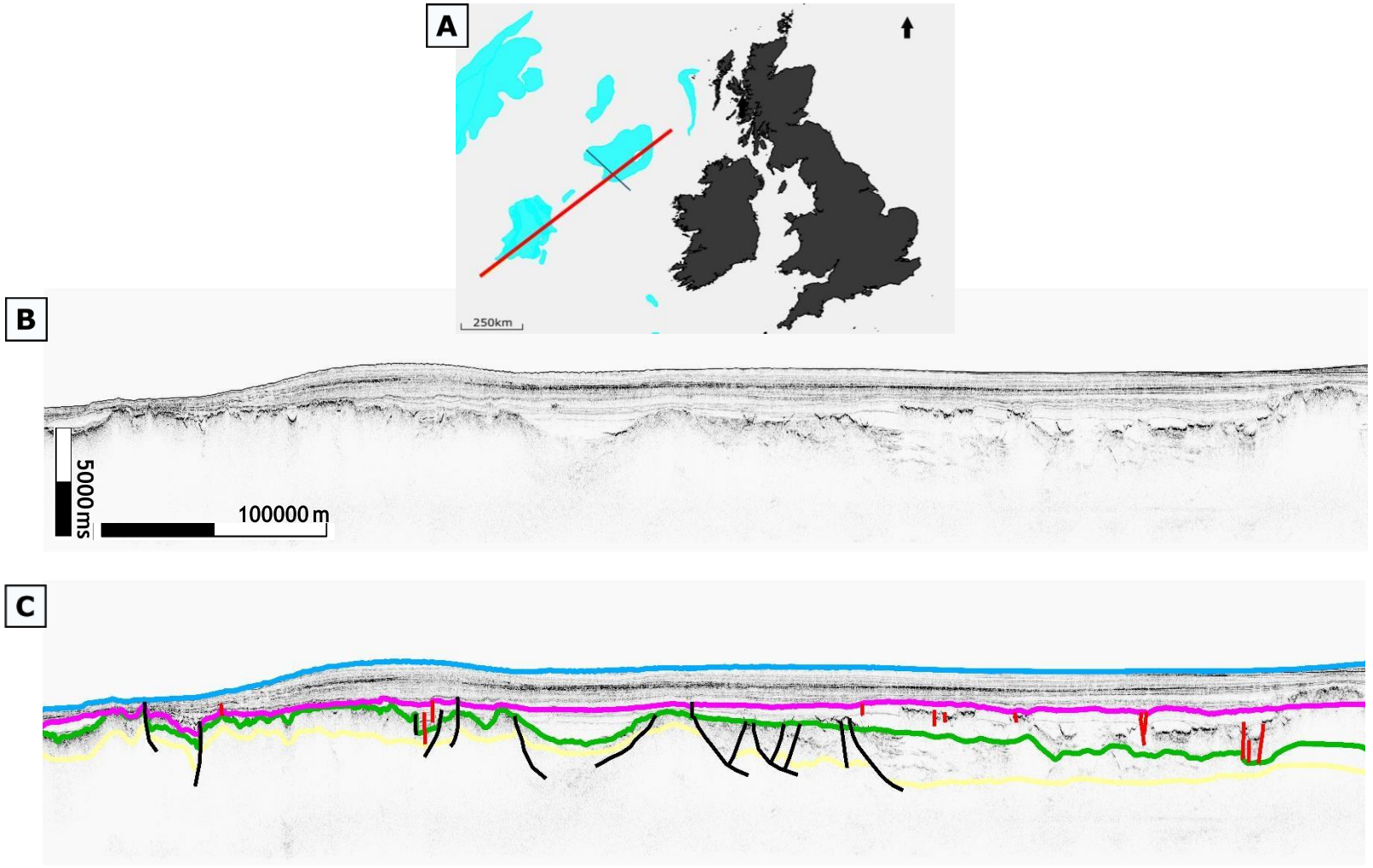


*Figure 3.1: (A) Map of offshore Ireland, showing the location of seismic lines IR1 and IR2 in the Rockall Basin. Blue polygons show the location of the igneous intrusions within the basin. (B) Uninterpreted seismic line IR1 in the Rockall Basin. (C) Interpreted seismic line IR1. Seismic horizons are: Basement, yellow; top of Lower Cretaceous, green; top of Upper Cretaceous, pink; top of Cenozoic, light blue. The black lines indicate primary faults, red lines indicate secondary faults. The location of seismic line IR1 is shown in the top image as the red line. IR2, the cross-sectional line to IR1, is shown in (A) as the thin black line.*

### 3.2.1 Seismic Stratigraphy

#### 3.2.1.1 Cenozoic Stratigraphic Unit

The Cenozoic unit along IR1 in the Rockall Basin is bounded at depth by an unconformity resulting from deposition of post-rift sedimentary rocks during a phase of thermal subsidence. The top of the Cenozoic unit maps the boundary between the water column and the seafloor along IR1. The thickness of the Cenozoic unit along IR1 is laterally continuous until the transition from continental to oceanic crust, located towards the southwestern end of the seismic line, where the package thins dramatically. The overall bathymetry of the basin is featureless with no obvious seamounts or volcanic structures on the seafloor, indicating that if there was volcanic activity in the immediate area, it occurred before the Cenozoic.

The top of the Cenozoic unit is the first positive, high amplitude event observed and therefore allows for excellent seismic correlation and a high level of confidence in the pick. Since the focus of this study is on the Paleozoic basement continental crust and the associated syn-rift and post-rift depositional sedimentary rocks, the Cenozoic unit was not subdivided into multiple sub-units. Without this further division, there are numerous seismic characteristics observed within this unit. In Fig. 3.3, the top of the Cenozoic unit is marked in the figure by the light blue horizon.

IR1 runs from the SW to the NE along the Rockall Basin, parallel to a Caledonian orogenic trend, rather than a Variscan trend (Shannon, 1991). IR1 directly intersects two of the large sill complexes in the basin (Fig. 3.1a). IR1 also appears to include a zone of transitional crust, from continental to oceanic, at the southwestern end of the line. The transition from continental to oceanic crust is interpreted on the seismic data as a change in the character of the basement horizon and a general thinning of all overriding sedimentary rocks. The primary focus

of this study is on restoring the continental crust across the Newfoundland-Ireland conjugate margins and therefore the transitional crustal zone was not interpreted in detail.

Magnetic anomaly A34, as interpreted by Srivastava *et al.* (1988), was used to position the boundary between the transitional zone and the continental crust. It was necessary to extrapolate the A34 anomaly northward to intersect with IR1. This was in part due to more prominent magnetic anomalies in the area (likely from the Barra Volcanic Ridge System; Keen *et al.*, 2014) that may have interfered with the original structure. The extent of anomaly A34, as well as the change in the character of basement and overlying strata, are depicted in Fig. 3.2.

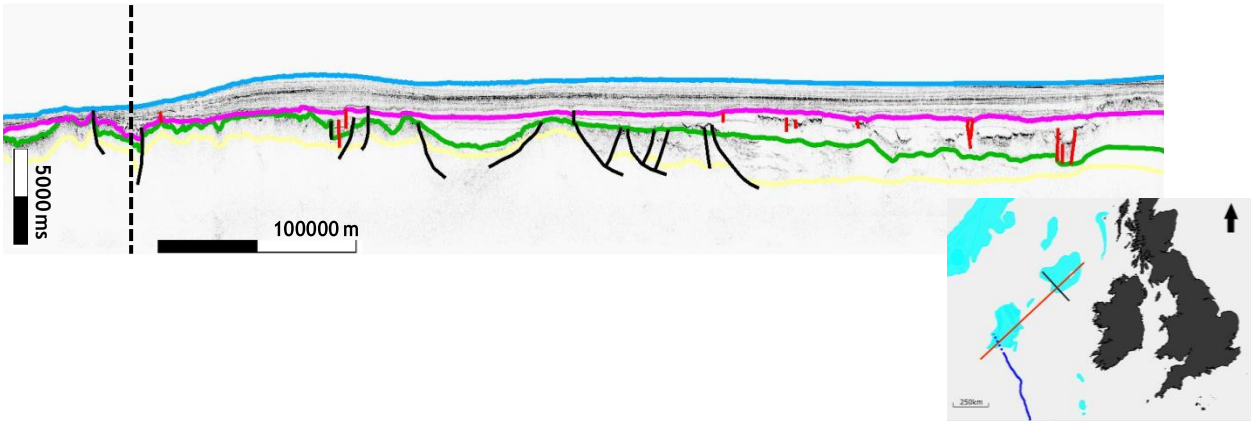


*Figure 3.2: The inset image depicts magnetic anomaly A34 from Srivastava et al. (1988), shown as the blue line. The dashed black line depicts the extrapolation of anomaly A34 to intersect IR1 (highlighted in red). The dashed black line on the main image depicts the intersection of anomaly A34 with seismic line IR1. Black lines indicate primary faults and red lines indicate secondary faults.*

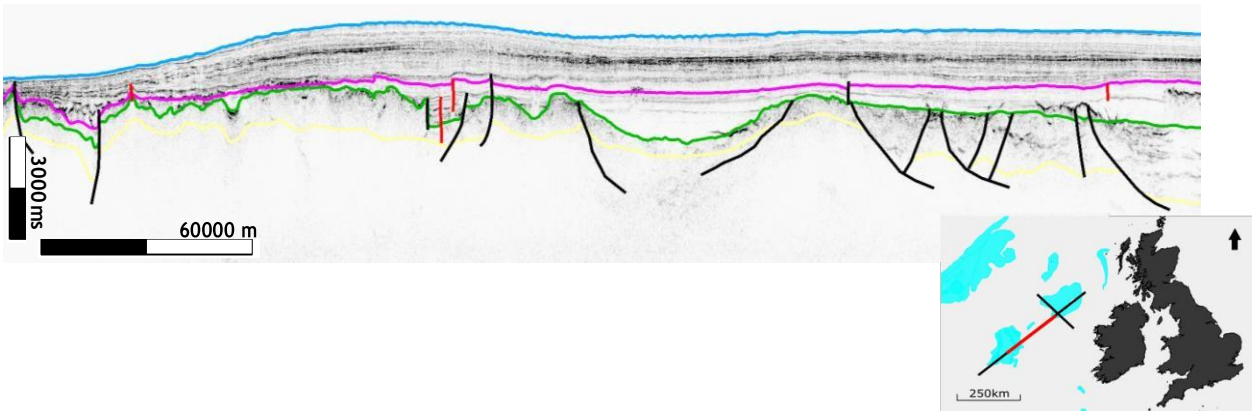


*Figure 3.3: A large central section of seismic line IR1 in the Rockall Basin. The Cenozoic (light blue) horizon is shown here to be smooth with no large bathymetric features. The unit can also be seen thinning toward the SW (left hand portion of the line) as the transitional zone is approached. The basement (yellow), top of the Lower Cretaceous (green) and the top of the Upper Cretaceous (pink) horizons are also observed, as well as numerous faults (black lines). The location of the section is shown in the inset map as the red highlighted line. Black lines indicate primary faults and red lines indicate secondary faults.*

#### 3.2.1.2 Upper Cretaceous Stratigraphic Unit

The large igneous sill complexes that are observed in the Rockall Basin were intruded into the Upper and Lower Cretaceous units during the Paleogene (O'Reilly *et al.*, 1996; Naylor & Shannon 2005). The Lower Cretaceous and basal structures of the Upper Cretaceous units are comprised of mechanically strong rocks (Magee *et al.*, 2014). Consequently, the regional tectonic stresses (continental rifting) and compression events due to basin subsidence, have rendered the lower units susceptible to lateral/planar brittle fractures (Magee *et al.*, 2014). As a result of a rheological change, from a brittle to a non-brittle state towards the top of the Upper Cretaceous, the intrusion of the sills did not progress upward (Magee *et al.*, 2014). This change in the host rock behavior is likely due to a reduction in porosity and pore fluid volume, whereby the mechanically stronger rocks at depth could sustain brittle fracture (Magee *et al.*, 2014). The top of the Lower Cretaceous boundary marks the change from syn-rift sedimentation to post-rift sedimentation, therefore the Upper Cretaceous unit is a post-rift unit.

The Upper Cretaceous unit thins toward the SW and thickens toward the NE. This post-rift unit is not heavily faulted. The lack of observed faulting is likely due to the fact that the majority of the faulting within the Rockall Basin occurred during pre-rift and syn-rift episodes. Due to the post-rift nature of this unit, the horizon is continuous across the top of the structural features and maintains a relatively constant thickness. The secondary faults observed in this unit (shown in Fig. 3.4 in red) are most likely associated with volume accommodations required by the non-coaxial component of strain and likely do not account for very much of the extension observed in the region.

The continuously high amplitude reflection associated with the top of the Upper Cretaceous horizon allowed it to be picked with a high degree of confidence. The Upper Cretaceous unit contains numerous parallel, laterally continuous reflectors across line IR1. These high amplitude events are only observed in the shallower portions of this unit. The reflections exhibit lower amplitudes in the localized basins along IR1. Lateral continuity is maintained within these faint reflections, indicating that signal attenuation is likely the cause of the perceived amplitude changes (Fig. 3.4). On the interpreted seismic line IR1, in the Rockall Basin, the top of the Upper Cretaceous unit is highlighted on the figure by the pink horizon.

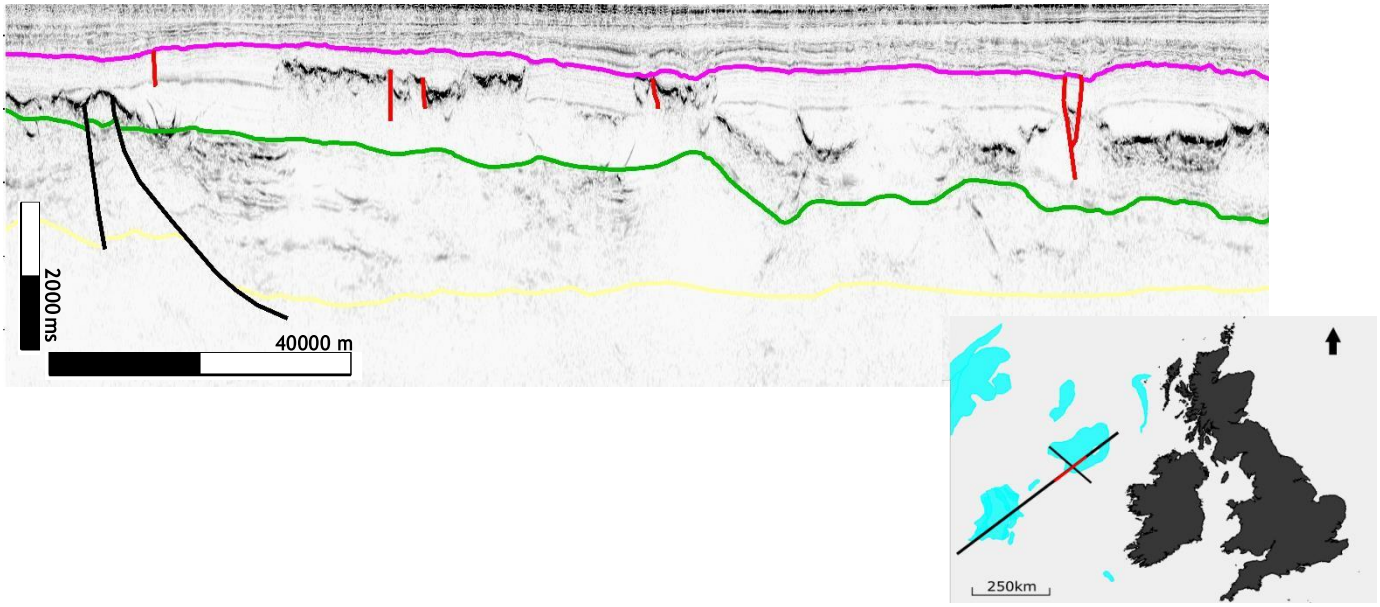


*Figure 3.4: A NE section of seismic line IR1 showing that the top of the Upper Cretaceous (pink) horizon lies above the majority of the Paleogene sills. The basement (yellow) horizon and the top of the Lower Cretaceous (green) horizon are also observed in this section, as well as numerous faults (black lines). The location of the section is shown in the inset image as the highlighted red line. Black lines indicate primary faults and red lines indicate secondary faults.*

#### 3.2.1.3 Lower Cretaceous Stratigraphic Unit

Due to the prevalence of the large igneous sills within the Rockall Basin and lack of deep distinct reflections in the seismic data, no Jurassic or Triassic strata were interpreted. The lack of reflections observed deep in the seismic section is likely the result of signal attenuation; the reduction of signal strength during transmission that is experienced during most seismic surveys, caused by numerous energy loss mechanisms, such as geometric spreading (Bugeja, 2011). Therefore, it is likely that Triassic and/or Jurassic strata are present in the basin, but have not been adequately imaged or interpreted on the seismic sections due to the presence of the sills. The uninterpreted Triassic and Jurassic strata are nonetheless included in the results of this study because they are assumed to make up part of the Lower Cretaceous unit.

Above the basement, the next distinct seismic reflection unit corresponds to the Lower Cretaceous unit. The Lower Cretaceous unit contains syn-rift sedimentary rocks that were

deposited into depocenters during rifting. This unit is continuous across the entirety of IR1 and is only interrupted by the intrusion of the younger Paleogene sills. These sills drastically decrease the amplitude of the reflections recorded from the deeper strata and therefore the top of the Lower Cretaceous boundary was laterally interpolated and inferred (Fig. 3.5). The top of the Lower Cretaceous boundary does not display typical syn-rift characteristics, as the sedimentary rocks are not solely deposited into local depressions of the basement and do not pinch-out along faults or horizons. Instead the Lower Cretaceous unit maintains a relatively constant thickness across numerous faults.

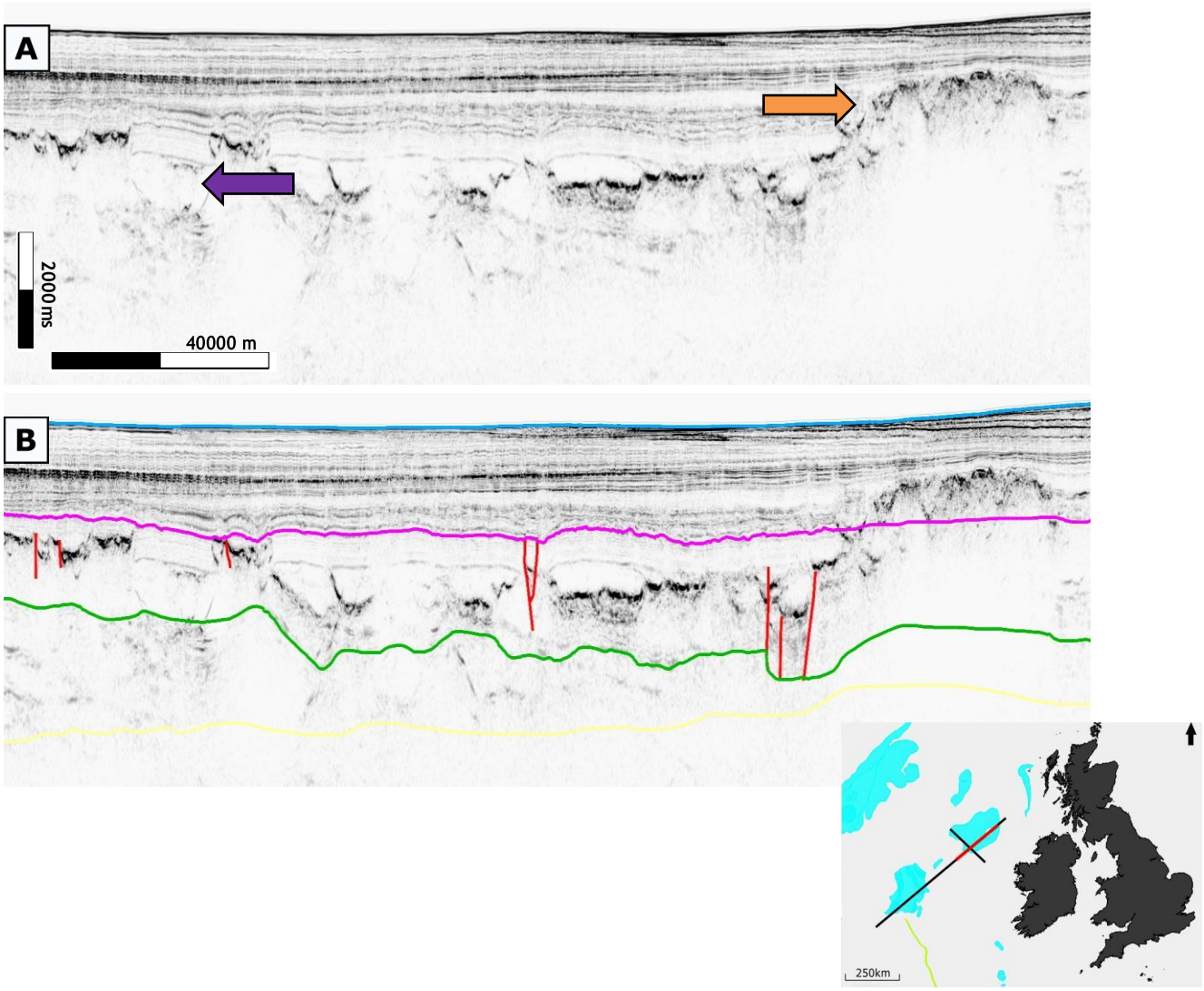


*Figure 3.5: (A) An uninterpreted section of IR1 in the northeastern portion of the Rockall Basin that depicts how the sills obscure the deeper strata. (B) The interpretation of the same section observed above, showing how the top of the Lower Cretaceous (green) horizon was laterally extended under the sills. The top of the Upper Cretaceous unit is shown in pink. The black lines represent primary faults and the red lines indicate secondary faults. The red highlighted section on the inset image indicates the location of the seismic section. The orange arrow indicates an example of the saucer shaped sills on the seismic section. The purple arrow indicates a gap in the sills where deeper structures are visible.*

The Lower Cretaceous unit is characterized by relatively high amplitude continuous to discontinuous reflections. The amplitudes of the reflections decrease as the unit thickens in large depocenters. On the interpreted seismic line, IR1, the top of the Lower Cretaceous syn-rift sedimentary unit is defined in the image by the green horizon (Fig. 3.6).

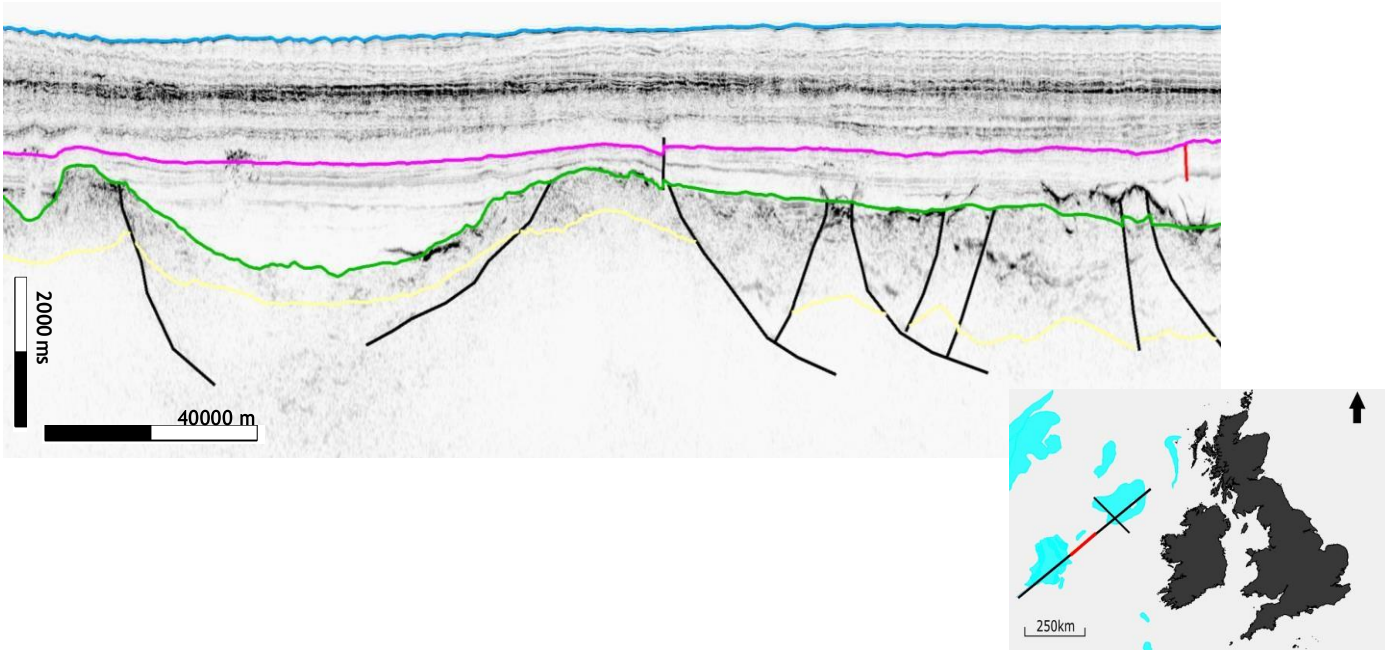


*Figure 3.6: A central section of seismic line IR1 in the Rockall Basin. The top of the Lower Cretaceous horizon (green) is shown here with a relatively uniform thickness, thickening slightly over large fault blocks/depocenters. The basement horizon (yellow) and the top of the Upper Cretaceous horizon (pink) are also shown here, as well as numerous faults (black lines: primary faults; red lines: secondary faults). The location of the seismic section is shown in the inset image as the red highlighted line.*

#### 3.2.1.4 Acoustic Basement

For this project, the top of the Paleozoic acoustic basement structure was interpreted as the base of laterally coherent seismic energy. The basement horizon is interpreted across the entirety of the Rockall Basin and is dissected by numerous listric faults and multiple horst and graben structures. This horizon separates the pre-rift sedimentary rocks and the Paleozoic basement from the syn-rift sedimentary rocks that were deposited during the time of rifting (100-200 Ma) (Shannon, 1991; O'Reilly *et al.*, 1996).

Due to the lack of additional constraints, such as wells or prominent crustal features, the interpretation of the basement horizon is poorly constrained in the Rockall Basin. To increase the overall confidence in the location of the horizons, constraints at numerous line intersections within the Rockall Basin were utilized. Jump-correlation of seismic line analysis from the

Porcupine Basin, to the south, also provided additional point controls for the overall basement horizon model. In Fig. 3.7, the top of the basement in the Rockall Basin, along line IR1, is denoted by the yellow horizon.

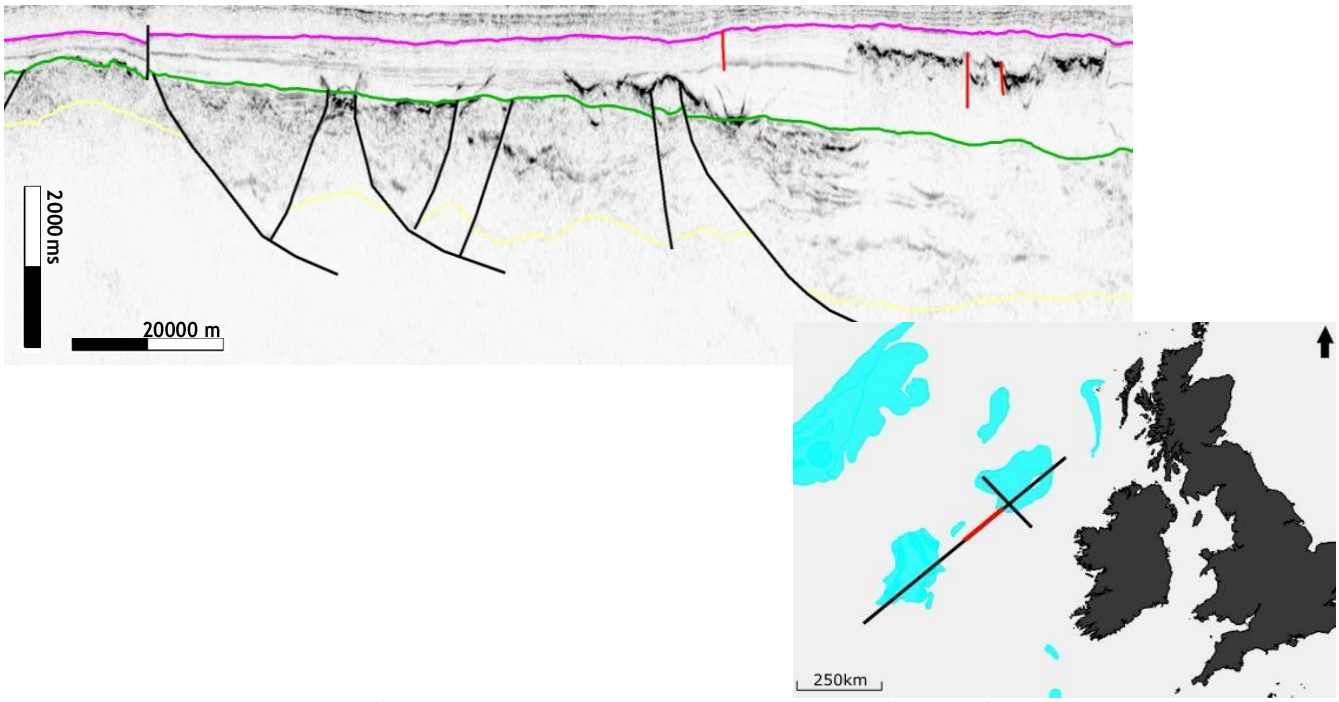


*Figure 3.7: A central section of seismic line IR1 depicting the interpreted listric faulting of the basement horizon (yellow). The top of the Lower Cretaceous (green) and the top of the upper Cretaceous (pink) horizons are also present, as well as numerous faults (black lines: primary faults; red lines: secondary faults). Location of this section is shown in the inset image as the red highlighted section.*

## 3.3 Orphan Basin

### 3.3.1 Seismic Stratigraphy

Within the Orphan Basin, multiple wells have been drilled by various petroleum exploration companies, however the western-most sections of the West Orphan Basin have remained relatively un-drilled. Well H intersects seismic line NL1, which is the primary focus line for this thesis, within the Orphan Basin. Unfortunately, well H was drilled into a basement high, characterized as an area of crustal uplift generated by faulting during episodes of rifting (location shown in Figs. 3.8 and 3.9). Sediment accumulations are limited in these areas due to erosional events. As a result, all the sedimentary units that extend over these highs are much thinner and do not provide an accurate representation of the units as a whole. This local basement high provides minimal constraints for the deeper seismic section where the units are much thicker. Well B was drilled in the northwestern section of the West Orphan Basin along seismic line NL2, an intersecting line with NL1. This well was drilled into a separate basement high within the continental shelf and as a result it offers minimal help in correlating the seismic data within the West Orphan Basin.

Due to the lack of deep well data in proximity to the primary seismic line, NL1, other methods of seismic correlation were utilized. NL2, the intersecting line to NL1, was provided to this project by TGS and has been previously interpreted in a published paper by Gouiza *et al.* (2017) (Fig. 3.8). Interpretations of NL2 from Gouiza *et al.* (2017) were utilized in this thesis to aid in the correlations of the seismic horizons from the cross-sectional seismic line, NL2 to the primary seismic line, NL1.

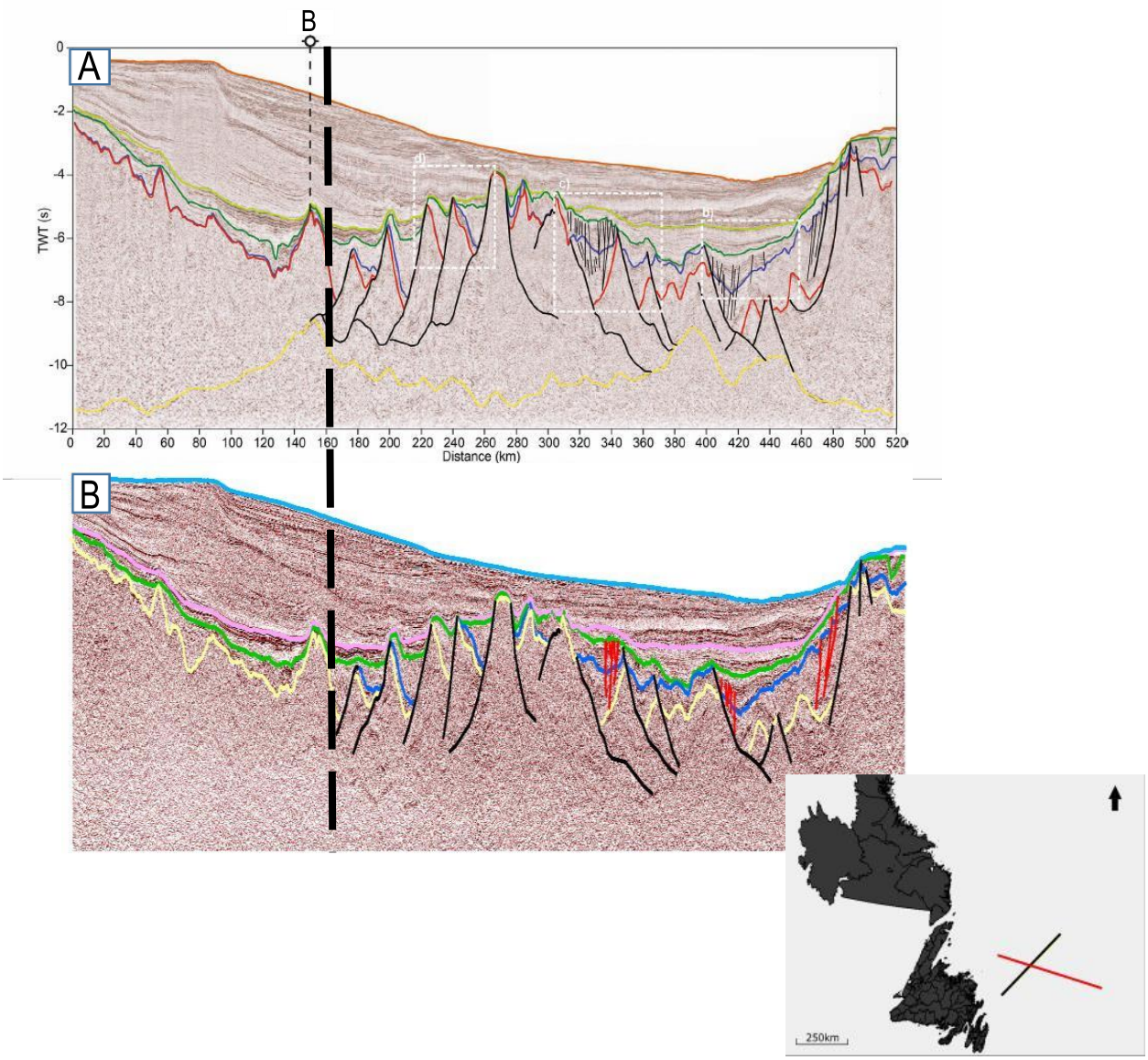


*Figure 3.8: (A) Interpreted seismic line NL2 adapted from Gouiza et al. (2017). Seismic horizons: mantle, yellow; basement, red; top of the Jurassic, blue; top of the Lower Cretaceous, dark green; top of the Upper Cretaceous, light green; top of the Cenozoic, light orange. Black lines indicate faults. The location of well B is shown here as the thin, black dashed line. (B) The interpretation of seismic line NL2 for this thesis. Seismic horizons: basement, yellow; top of the Jurassic, dark blue; top of the Lower Cretaceous, green; top of the Upper Cretaceous, pink; top of the Cenozoic, light blue. Solid black lines indicate faults and multi-coloured X's mark cross-sectional ties with other interpreted seismic lines in the Orphan Basin. The thick black dashed line indicates the location of intersection of NL2 with the primary line NL1. The location of NL2 is shown in the inset image as the highlighted red line, the black line is the primary seismic line, NL1.*

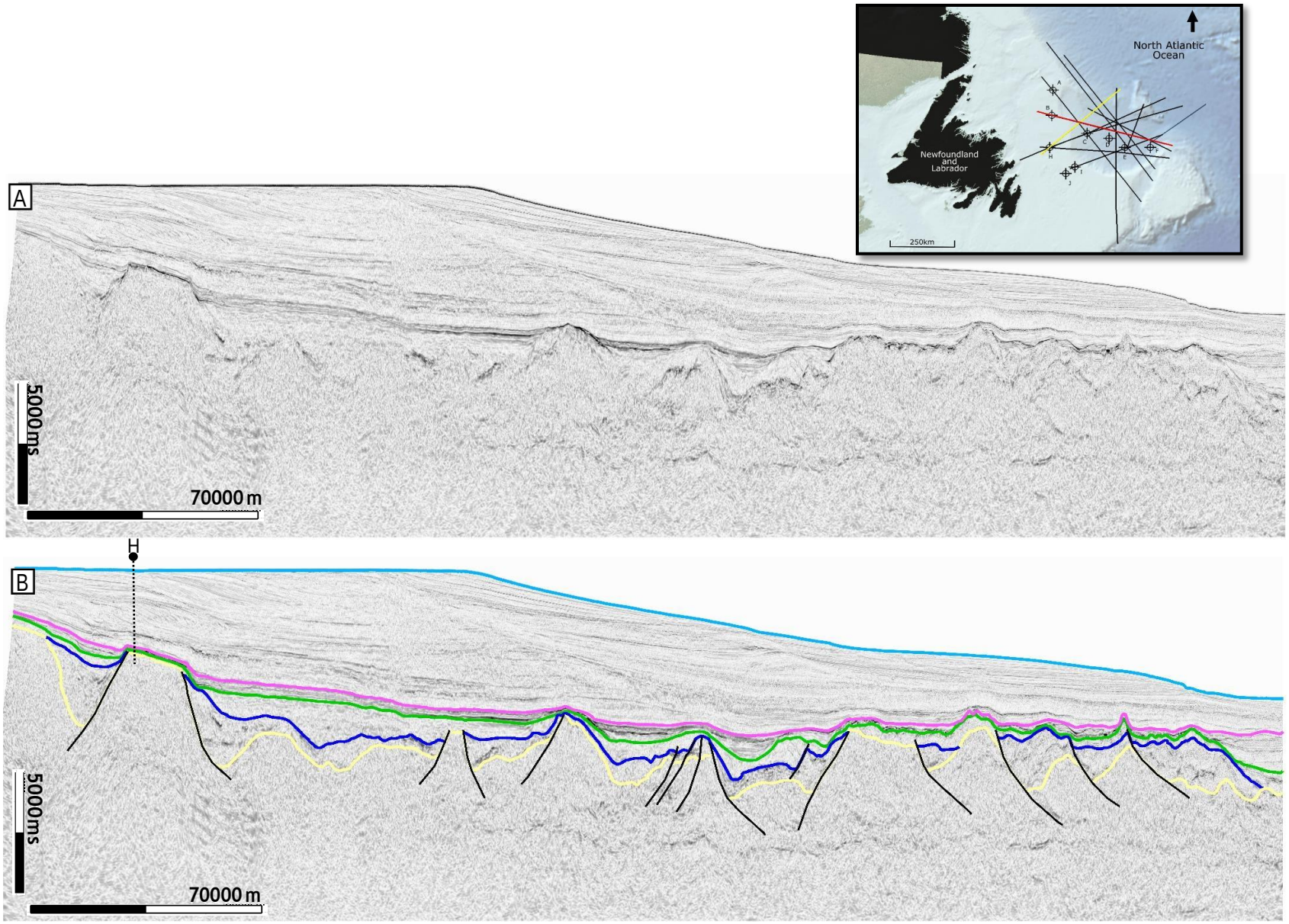


*Figure 3.9: (A) Uninterpreted seismic line NL1 in the Orphan Basin. (B) Interpreted seismic line NL1. Seismic horizons: basement, yellow; top of the Jurassic, dark blue; top of the Lower Cretaceous, green; top of the Upper Cretaceous, pink; top of the Cenozoic, light blue. Black lines indicate faults. The location of NL1 is shown in the inset image as the highlighted yellow line, the red line indicates the location of NL2. Location of well H is shown by black dashed line in (B).*

#### 3.3.1.1 Cenozoic Stratigraphic Unit

The top of the Cenozoic unit in the Orphan Basin along NL1 is bounded at depth by an unconformity resulting from deposition of post-rift sedimentary rocks during a phase of thermal subsidence (Gouiza *et al.*, 2017). The top of the Cenozoic unit maps the boundary between the water column and the seafloor along line NL1. This horizon is the shallowest positive reflection observed along the line and therefore allows for a high degree of seismic correlation, as well as a high level of confidence in the interpretation. The regional focus of this study precluded the necessity of further subdividing the Cenozoic unit. The seismic character of the Cenozoic unit is highly variable due to this lack of further division.

The Cenozoic unit is thickest to the SW, over the continental slope, and thins gradually towards the NE. The bathymetry along seismic line NL1 captures the entire continental slope, however the transition zone from continental to oceanic crust is not observed. On the interpreted seismic line NL1, in the West Orphan Basin, in Fig. 3.10, the top of the Cenozoic unit is denoted by the light blue horizon.

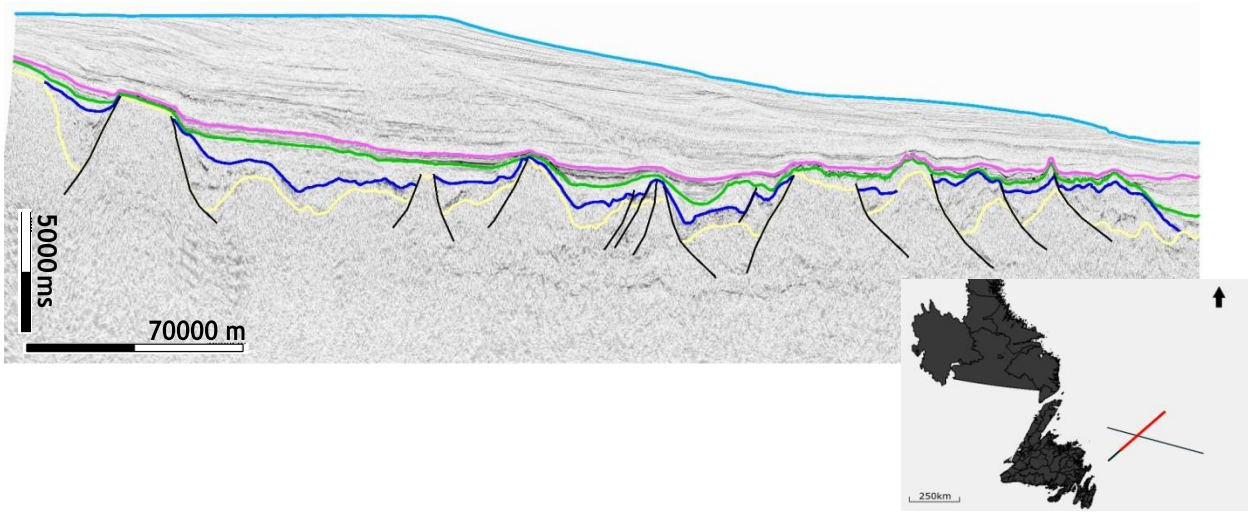


*Figure 3.10: Line NL1 in the West Orphan Basin. This image shows the extent of the continental slope, as well as the lack of seamounts and volcanic features. Seismic horizons present: Basement, yellow; the top of the Jurassic, dark blue; the top of the Lower Cretaceous, green; the top of the Upper Cretaceous, pink; top of the Cenozoic, light blue. The location of this section is shown in the inset image, denoted by the red highlighted line.*

#### 3.3.1.2 Upper Cretaceous Stratigraphic Unit

The Upper Cretaceous unit marks a change from syn-rift sedimentation to post-rift sedimentation, as the Orphan Basin transitioned from a period of rifting to a period of thermal subsidence (Gouiza *et al.*, 2017). The confidence in the interpretation of the Upper Cretaceous unit is adequate, due to consistent reflections from the horizon and constraints provided by intersecting seismic lines within the West Orphan Basin.

This post-rift unit is continuous across all of line NL1 and does not extend down into depocenters, but is laterally continuous across all the structural features. The Upper Cretaceous unit is thickest over local depressions of the basement and thins slightly over local basement highs, a typical post-rift characteristic. Towards the SW, over the continental shelf, this unit thins marginally. The thinning of the southwestern portion of the Upper Cretaceous unit is likely due to the thickening of the continental crust along the continental slope. Most of the faulting in the West Orphan Basin occurred during the time of rifting, therefore this post-rift

unit is only moderately faulted.

The top of the Upper Cretaceous unit is marked by a high amplitude positive reflection that can be traced throughout the entirety of seismic line NL1. Numerous parallel, high amplitude reflectors are observed throughout the entire unit. Due to the post-rift depositional environment of this unit, the sedimentary rock was deposited in laterally continuous layers with little to no disruption, thus generating the parallel, high amplitude reflectors. In Fig. 3.11, the top of the Upper Cretaceous unit is denoted by the pink horizon.

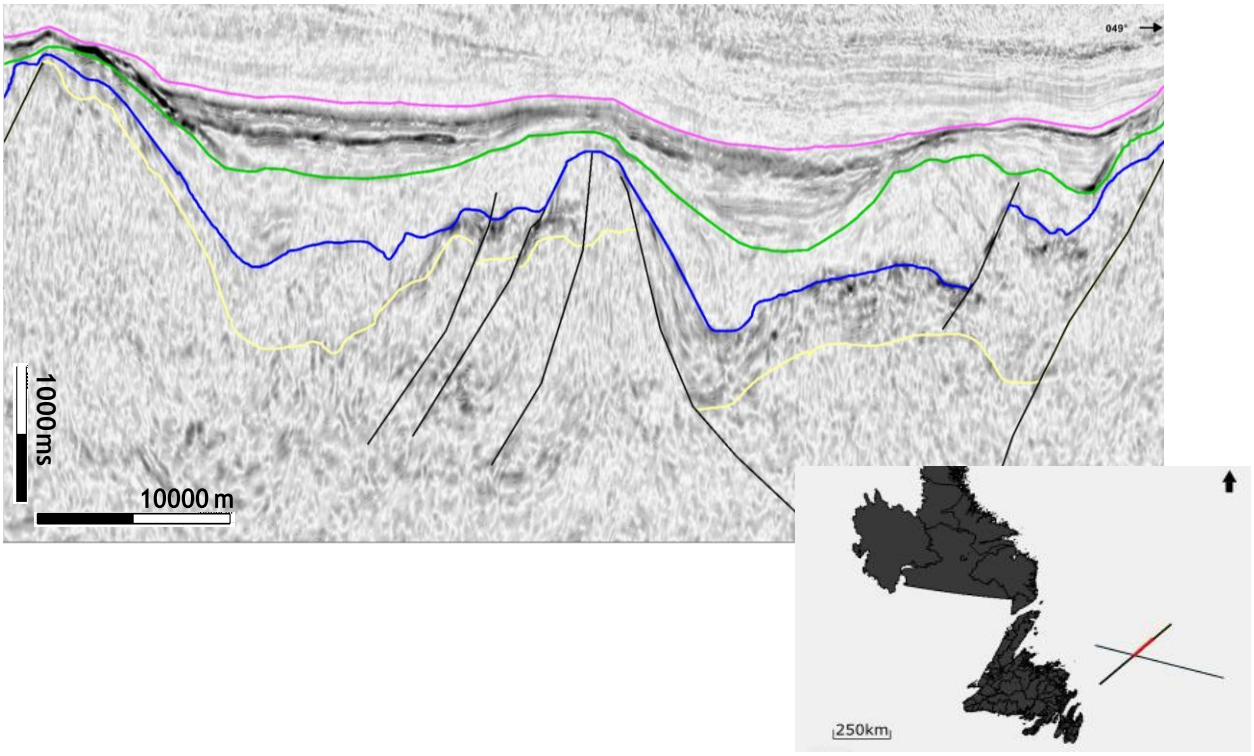


*Figure 3.11: A central section of seismic line NL1 in the West Orphan Basin depicting the post-rift characteristics of the top of the Upper Cretaceous (pink) horizon. This unit is relative uniform in thickness, but thins over local basement highs. Other seismic horizons present: Basement, yellow; the top of the Jurassic, dark blue and the top of the Lower Cretaceous, green. Faults are indicated by the black lines. The location of this section is shown in the inset image, denoted by the red highlighted section.*

#### 3.3.1.3 Lower Cretaceous Stratigraphic Unit

The Lower Cretaceous unit is a syn-rift sedimentary unit within the Orphan Basin. This unit is laterally continuous across the entirety of NL1 with a variable thickness. Due to its syn-rift depositional environment, the Lower Cretaceous unit is thicker in localized basins and depocenters and thinner over local basement highs. The thickest portion of the Lower Cretaceous unit is observed along the southwestern half of NL1, approaching the continental shelf. A syn-rift unit would typically be moderately faulted because the sedimentary rock is being deposited while rifting is occurring. However, in the West Orphan Basin, along NL1, the Lower Cretaceous unit displays a post-rift characteristic, in that the unit is not heavily faulted.

The top of the Lower Cretaceous unit is marked by a high amplitude reflector that can be traced across the entire seismic line. The seismic character of the unit is chaotic with minimal internal coherency. In Fig. 3.12, the top of the Lower Cretaceous unit within the West Orphan Basin is marked by the green horizon.

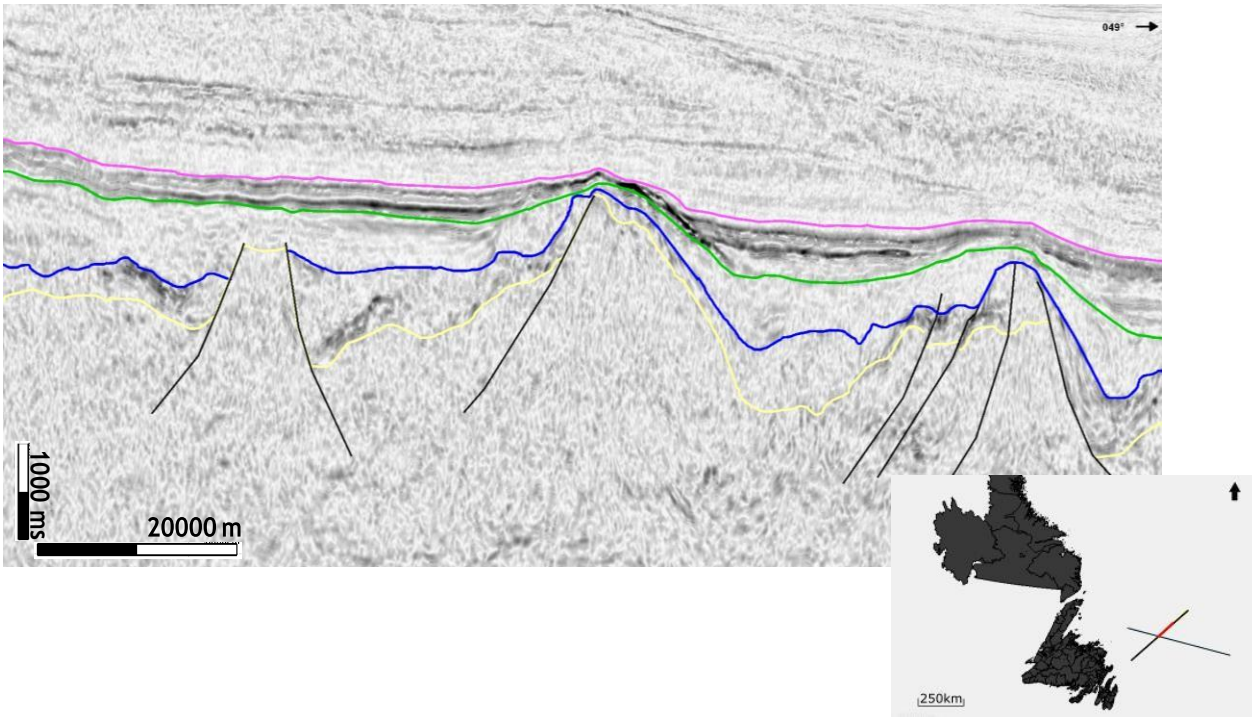


*Figure 3.12: A northeastern section of seismic line NL1 in the West Orphan Basin showing the abnormal syn-rift characteristics of the top of the Lower Cretaceous (green) horizon. The horizon does not abut or pinch out along faults or the basement horizon in the depocenters, as would be expected by a syn-rift unit. Other seismic horizons present: Basement, yellow; the top of the Jurassic, dark blue and the top of the Upper Cretaceous, pink. The location of this section is shown in the inset image, denoted by the red highlighted line.*

#### 3.3.1.4 Jurassic Stratigraphic Unit

The Jurassic unit directly overlies the Paleozoic basement and is moderately continuous across the basement, absent only over local basement highs. The Jurassic unit is the first syn-rift unit indicating that it was deposited during a rifting event. The confidence in choosing the top of the Jurassic unit is low, due to the lack of well control and the poorly defined reflectors likely caused by the attenuation of signal at depth and the lower resolution of the data.

The thickness of the unit of Jurassic sedimentary rocks is moderately laterally continuous (approximately 1.3 km), with some depocenters exhibiting thicker amounts of deposition (up to approximately 5 km). The amount and location of Jurassic sedimentary formations in the West

Orphan Basin has recently been debated (Lau *et al.,* 2015; Gouiza *et al.,* 2017). McCallum (personal communication, Nalcor Energy Ltd., 2018) and the prospect team at Nalcor Energy Ltd. have interpreted NL1 to have units of Jurassic sedimentary rocks across the entire extent of the seismic line, absent only over the basement high where well H was drilled (location shown in Fig. 3.9). The interpretation of Jurassic sedimentary rocks for this thesis is in relative agreement with the interpretation performed by the team at Nalcor. However, no wells have been drilled that capture the units of Jurassic sedimentary rocks in the deepest extents of the West Orphan Basin.

The seismic character of this unit is highly variable. A package of high amplitude, chaotic reflectors are typically associated with this sedimentary unit. These reflectors are not parallel and have minimal lateral continuity. Furthermore, this syn-rift unit, which was deposited during the time of rifting, is heavily faulted due to the fact that the majority of faulting occurred during this time (Enachescu *et al.,* 2004; Gouiza *et al.,* 2017). Each deposit of Jurassic sedimentary features abuts and/or pinches out along a listric fault or the basement horizon. This is due to the syn-rift environment that the unit was deposited throughout. On the interpreted seismic line NL1, in the West Orphan Basin (Fig. 3.13), the top of the Jurassic unit is denoted by the dark blue horizon.

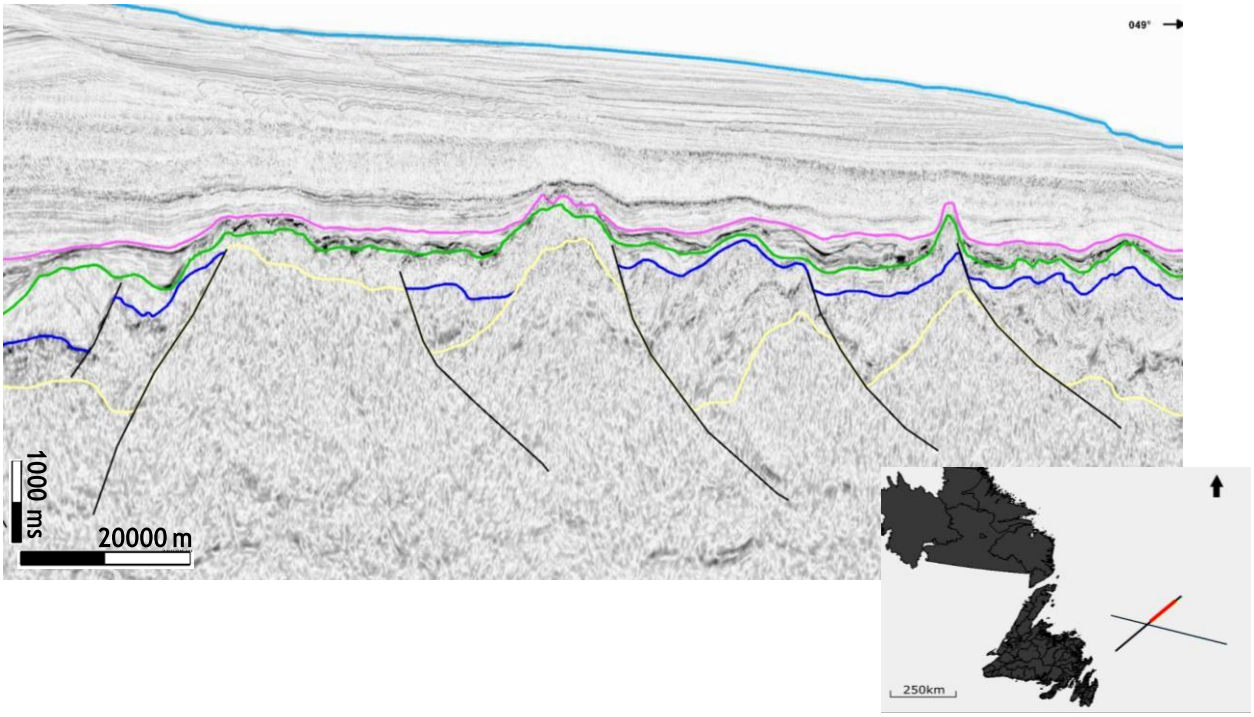


*Figure 3.13: A northeastern section of seismic line NL1 in the West Orphan Basin depicting the pinch -out characteristic of the Jurassic (dark blue) horizon, along faults (black lines) and the basement (yellow) horizon. Other seismic horizons present: the top of the Lower Cretaceous, green and the top of the Upper Cretaceous, pink. The location of this section is shown in the inset image, denoted by the red highlighted line.*

#### 3.3.1.5 Acoustic Basement

The top of the Paleozoic basement structure was interpreted beneath the last laterally coherent seismic event observed. This horizon separates the pre-rift sedimentary rocks and basement from the syn-rift sedimentary rocks that were deposited during rift episodes (100-200 Ma; Shannon, 1991; O'Reilly *et al.,* 1996). In the Orphan Basin, NL1 is the primary focus of this study. Cross- sectional ties from the published work of Gouiza *et al.* (2017) along NL2 were used to aid in correlating the location of the basement horizon.

NL1 runs SW to NE across the West Orphan Basin and the entire seismic line includes only continental crust. The line does not extend past the Orphan Knoll, beyond which the crust is thought to be oceanic (Srivastava *et al.,* 1990). The structure of the basement shows multiple

tilted fault blocks, primarily dipping NE. These tilted fault blocks are characteristic of an extended rifted margin, which align with the known evolution of the Orphan Basin (Shannon 1991, Enachescu *et al.*, 2004, Welford *et al.*, 2012, Gouiza *et al.*, 2017).

Confidence in the basement horizon was achieved by verifying the horizon at intersections with other lines and by comparing its character across the conjugate pair. On the interpreted seismic line NL1, in the West Orphan Basin, (Fig. 3.14), the top of the basement is denoted by the yellow horizon.

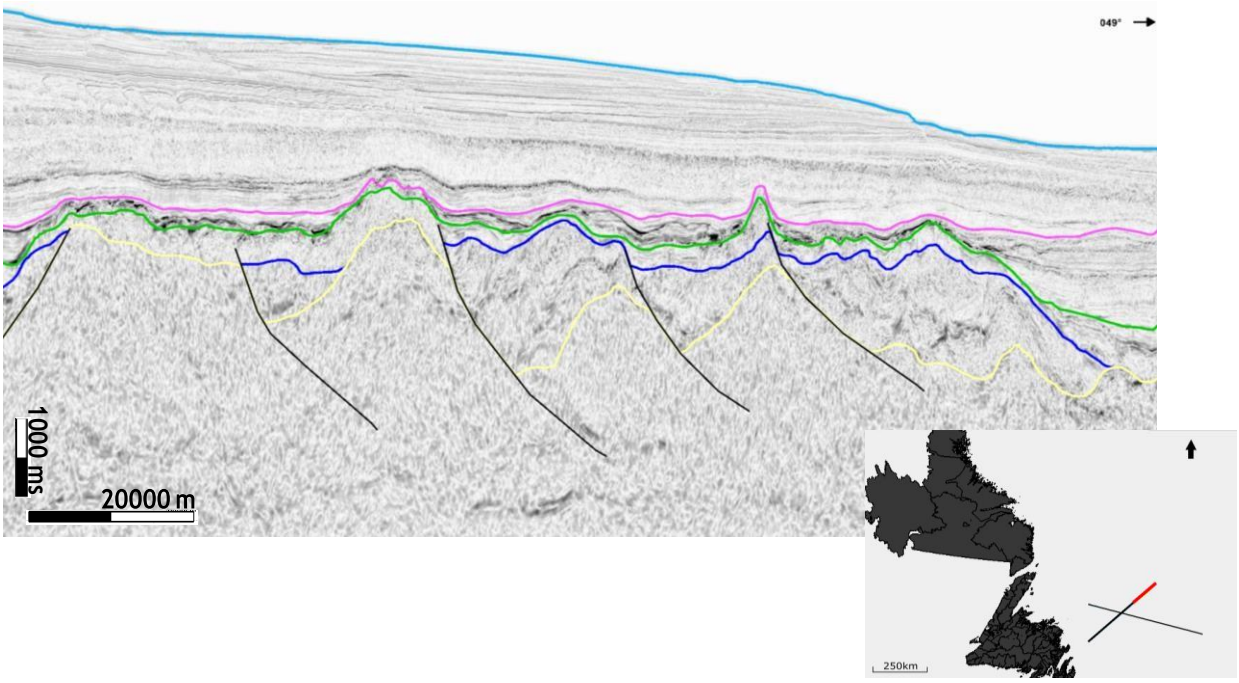


*Figure 3.14: A northeastern section of seismic line NL1 in the West Orphan Basin showing the tilted fault blocks of the Paleozoic basement (yellow). Faults are indicated by black lines. Other seismic horizons: top of the Jurassic, dark blue; top of the Lower Cretaceous, green and top of the Upper Cretaceous, pink. The location of this section is shown in the inset image as the red highlighted line.*

### 3.4 From Seismic Interpretation to Modelling

Following the seismic interpretations in Petrel©, all of the seismic lines, NL1, NL2, IR1, IR2, and later NL3, and their associated faults and horizons were loaded into Move© for 2D and 3D reconstructions and analysis. The process and results of these reconstructions across the Newfoundland-Ireland conjugate, continuous basins will be discussed in Chapter 4.

# Chapter 4: Basin Modelling in Move©

## 4.1 Introduction

Move© was created by Midland Valley and it is the most up to date structural modelling and analysis toolkit available. This software allows for fully integrated 2D and 3D model building, which is an integral portion of this M.Sc. project. Following the interpretation of all of the seismic lines. The primary and secondary seismic lines in the Rockall Basin, IR1 and IR2, and the primary and secondary lines in the West Orphan Basin, NL1 and NL2, were then transferred into Move© along with their corresponding interpreted features.

Move© is used to decompact underlying strata and restore thermal subsidence while back stripping/removing successive layers of strata. When the back stripping process has generated a model with an uppermost unit that exhibits faulting due to rifting, the fault restoration process can begin. The process of decompacting, restoring thermal subsidence, and restoring the faults continues until the upper and lower continental crust are fully restored along all of the seismic lines.

## 4.2 2D Modelling

### 4.2.1 Time to Depth Conversion

The 2D modelling algorithms for restoring basins in Move© remove deformation in order to reassemble them back to their un-deformed state, adhering to the line length and area balancing structural geology principles, as well as taking into account the importance of geologic time and its impact on the structure. Kinematic modelling in Move© requires that each seismic line is in the depth domain, as the equations used to calculate the restorations have parameters

that require the data to be in metres or kilometres. All four seismic lines, NL1, NL2, IR1, and IR2, were interpreted in Petrel© in the time domain (more commonly known as Two Way Travel-time (TWT)). Thus, each seismic line had to be converted from the time domain into the depth domain before the restoration process could begin. The 2D Depth Conversion module, in Move©, provides different possible methodologies to carry out time to depth conversions. The Database method was used, as it allows the velocity and rate of change of velocity values to be specified for each horizon in the model using the Stratigraphy and Rock Properties table (properties found in Appendix A).

To assess the results of the 2D Depth Conversion, a Moho proxy was introduced to each model as derived by Welford *et al.* (2012using 3D gravity inversion. The Moho proxy was created in depth, and once it was imported into Move© it provided an additional boundary within the depth converted models.

The conversion from the time domain (Figs. 4.2a and 4.3a) to the depth domain (Figs. 4.2b and 4.3b) does not significantly change the geometry of the faults or the relative thickness of the sedimentary units. Additionally, there were no significant irregularities related to the Moho proxy or any irregular fault geometries involving faults crossing the Moho proxy. As such, the Moho proxy, as provided by Welford *et al.* (2012), helped to show that the depth calculation performed by Move© was reasonable.

For the purpose of this thesis, each seismic stratigraphic unit was assigned a coloured polygon; light pink represents the water column, light blue represents the Cenozoic unit, dark pink represents the Upper Cretaceous unit, green represents the Lower Cretaceous unit, dark blue represents the Jurassic unit, and yellow represents the basement/crust. Based on the Moho proxy provided by Welford *et al.* (2012), a purple mantle polygon was also generated (seen in Figs.

4.2b and 4.3b). However, this polygon is not included in the Move© restorations for the remainder of this M.Sc. project. The lower extent of the mantle polygon represents the depth of the seismic data collected, and not a geological boundary. Additionally, the influence of the mantle does not contribute to the restoration of the continental crust across the conjugate margins, in Move©. Therefore, the mantle horizon (or Moho) is only used as a surface throughout the remainder of this project.

The magnetic anomaly A34, as interpreted by Srivastava *et al.* (1988), was used to position the boundary between transitional crust and continental crust. On the Irish margin, it was necessary to extrapolate the A34 anomaly northward to intersect with IR1 (Fig. 4.1). This extrapolation was necessary due to the interpreted termination of the A34 magnetic anomaly from Srivastava *et al.* (1988), likely due to more prominent magnetic anomalies in the area (likely from the Barra Volcanic Ridge System) that may have interfered with the original interpretation of the anomaly.

As the focus of this study is on the Paleozoic basement continental crust and the associated syn-rift and post-rift depositional sedimentary rocks, the transition zone from continental to oceanic crust is beyond the scope of this thesis. Thus, the seismic units and faults that are located on the oceanward side of anomaly A34 along IR1 are henceforth excluded. The extent of anomaly A34, as well as the change in the character of basement and overlying strata, are depicted in Figs. 4.1 and 4.2.

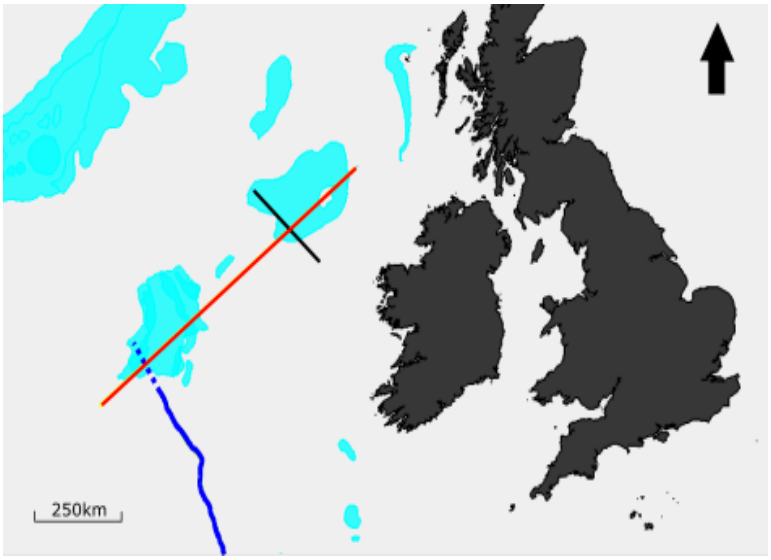


*Figure 4.1: The extent of magnetic anomaly A34 from Srivastava et al. (1988), shown as the blue line. The dashed blue line depicts the extrapolation of anomaly A34 to intersect IR1 (highlighted in red). IR2 is shown as the solid black line. The turquoise bodies represent the extent of the igneous intrusions within the Rockall Basin.*

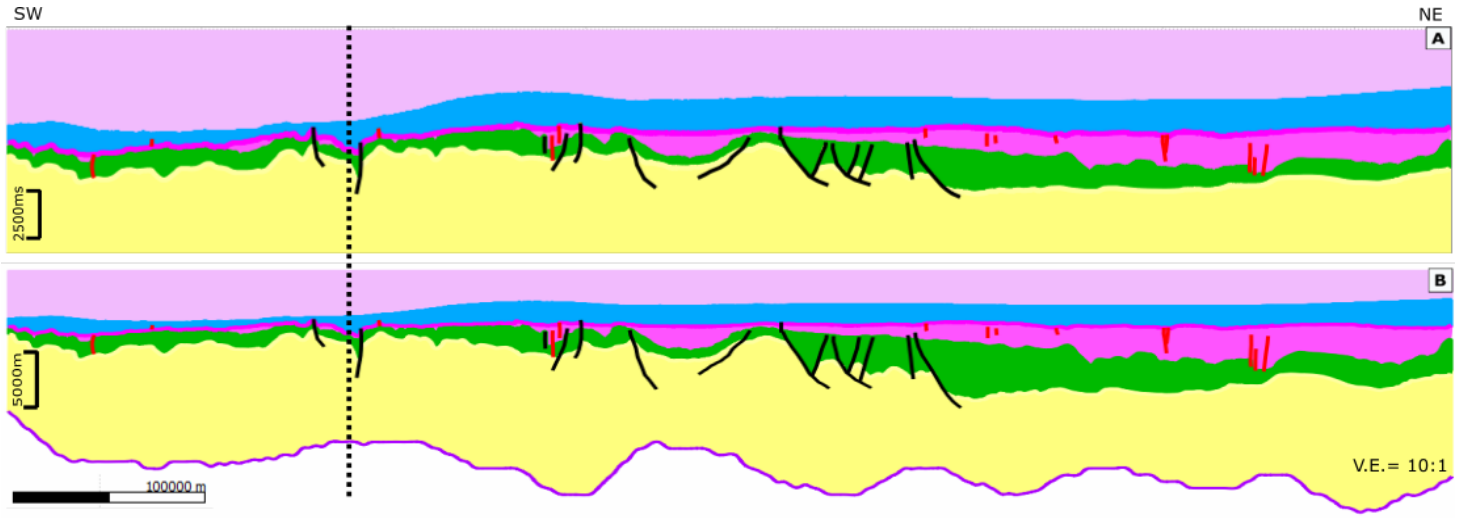


*Figure 4.2: (A) The entirety of line IR1 in the time domain (TWT). The solid black lines depict major faults and solid red lines depict minor faults. The black dashed line indicates the location of magnetic anomaly A34. All data to the left of this line are excluded for the remainder of this thesis. (B) The entirety of line IR1 converted to the depth domain. The purple line represents the Moho proxy from Welford et al. (2012).*

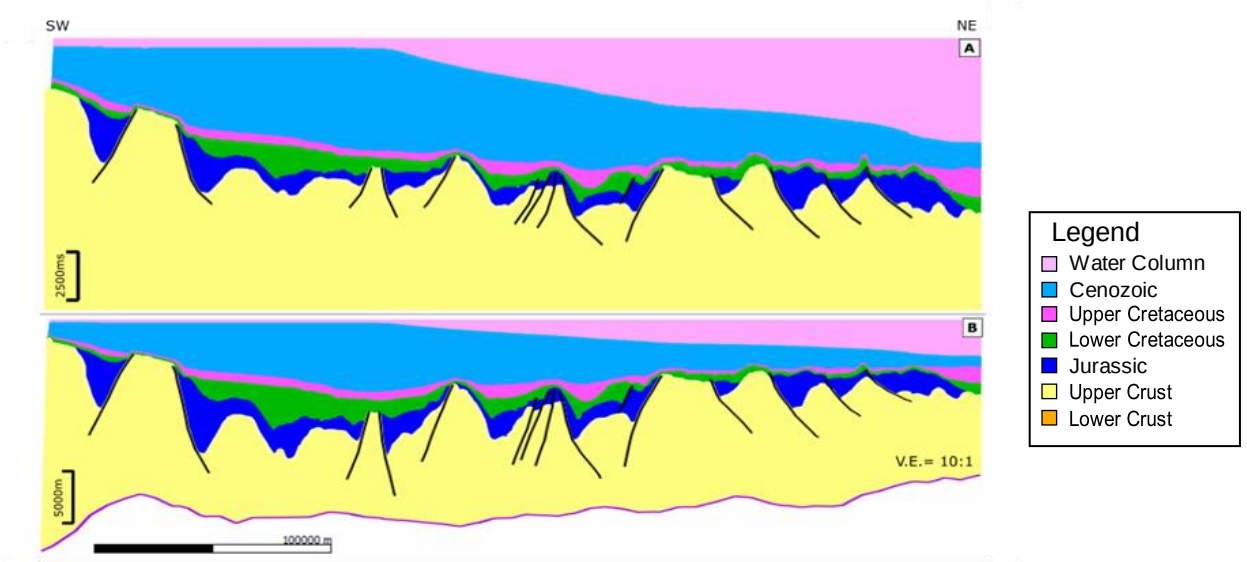


*Figure 4.3: (A) The entirety of line NL1 in the time domain (TWT). The solid black lines depict major faults. (B) The entirety of line NL1 converted to the depth domain. The purple line represents the Moho proxy from Welford et al. (2012).*

### 4.2.2 Cenozoic Sedimentary Rock Decompaction

The next step in the restoration process, after converting all of the seismic lines (IR1, IR2, NL1, NL2, and later NL3) from the time domain to the depth domain is to systematically decompact each unit. As sediment accumulates within a basin, the weight of the overlying sedimentary rock compresses the underlying sedimentary rock through time. This process is known as compaction. In order to accurately restore the Rockall and West Orphan basins to a pre-rift state, each unit must be decompacted by removing the overlying sedimentary rock. This is accomplished using the 2D Decompaction module in Move©.

The first unit to be decompacted in Move© is the Cenozoic unit. This decompaction is accomplished by removing the overlying water column. This step is necessary to restore the conjugate basins because, during the Mesozoic, when these basins are hypothesized to have been connected, there was no water column present. The results of removing the water column and the corresponding decompaction of the Cenozoic sedimentary unit can be seen in Fig. 4.4. The decompacted seismic line IR1, has been restored to a time before the Cenozoic unit was compressed by the water column and therefore the Cenozoic unit has increased in thickness slightly. The decompaction process also appears to have moderately flattened topographic changes that were previously observed along the Cenozoic horizon. The decompacted seismic line, NL1, appears to have been most affected by the decompaction in the southwest-central portion of the seismic line compared to the NE. The Cenozoic strata eventually thin toward the SW along NL1, toward the continental shelf, where decompaction has a minor effect. Where the sediment layer thins towards the NE, where the crust transitions from continental to oceanic, the decompaction process only moderately increased the thickness of the Cenozoic unit.

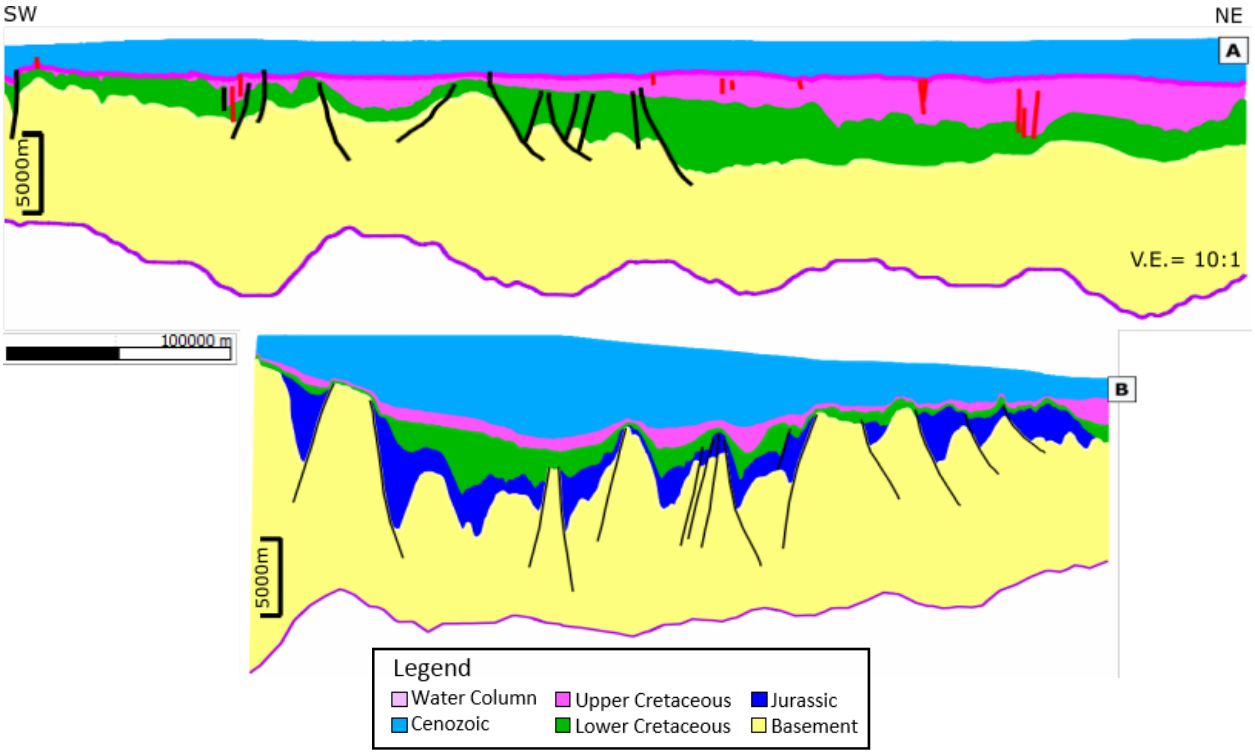


*Figure 4.4: (A) Cenozoic decompaction of seismic line IRI, offshore Ireland, only showing continental crust. (B) Cenozoic decompaction of seismic line NL1, offshore Newfoundland and Labrador. The black lines represent the primary faults and the red lines indicate the secondary faults. The purple line represents the Moho proxy from Welford et al. (2012).*

### 4.2.3 Cenozoic Thermal Subsidence Restoration

Thinning of the lithosphere during rift events results in large changes in elevation, mainly due to thermal subsidence (Keen & Dehler 1993). As a sedimentary basin is created, by the stretching of continental lithosphere, the thinning of the lithosphere allows the asthenosphere to well up beneath it. The resulting increase in temperature, generated by the upwelling asthenosphere, eventually decreases, causing subsidence. Therefore, thermal subsidence must be accounted for at each post-rift layer, prior to decompaction, to accurately restore each basin. The 2D Thermal Subsidence module in Move© uses a thermal subsidence model generated by McKenzie (1978) to restore the shape and paleo-depth of the seafloor.

The 2D Thermal Subsidence module in Move© requires numerous prescribed parameters

for the calculation: the number of rifting events, age of the rifting events, the duration of syn-rift, the upper and lower stratigraphic limits of the unit that is to be restored, the beta/stretching value, the thickness of the lithosphere, the thickness of the continental crust, and the densities of the mantle, the continental crust, the sedimentary rock, and the seawater. Although three rift events have been identified in the Rockall Basin, a Late-Triassic rift phase, a Mid-Late Jurassic rift phase and a Late Cretaceous rift phase, only the Late Cretaceous event was used in the thermal subsidence calculation for this thesis. This is in part due to no Triassic or Jurassic sedimentary rocks being interpreted within the Rockall Basin (see section 3.2.1.2). The parameters used in the Rockall Basin for the Late Cretaceous rift age, 113 Ma, and syn-rift duration, 13 Ma, for seismic lines IR1 and IR2, were approximated from Shannon (1991) and Naylor & Shannon (2005) (Table 1.2). The upper and lower stratigraphic limits of the Cenozoic unit are 0 and 66 Ma respectively. The stretching factor (β) represents the ratio of final crustal thickness to the original crustal thickness and is a required parameter to calculate thermal subsidence. A β value map of the North Atlantic, provided by Welford *et al.* (2012), was used to determine that a uniform β value of 2.0 was appropriate for the Rockall Basin.

The thermal subsidence parameters used in the West Orphan Basin for seismic lines NL1, NL2, and later NL3, were interpreted from Enachescu *et al.* (2004), Welford *et al.* (2012), and Gouiza *et al.* (2017) and are listed in Table 1.2. Three rift events have also been identified in the Orphan Basin, a Late Triassic rift event, a Late Jurassic rifting event and a Late Cretaceous rift event. As in the Rockall Basin, there are no Triassic sedimentary rocks interpreted in the West Orphan Basin, so only the Late Jurassic rift event (164 Ma) and the Late Cretaceous rift event (113 Ma) were used to calculate the thermal subsidence. The Late Jurassic rift event had a syn-rift duration of 19 Ma and the Late Cretaceous rift event had a syn-rift duration of 13 Ma (Shannon, 1991 and Naylor & Shannon, 2005). The upper and lower stratigraphic limits of the

Cenozoic unit are 0 and 66 Ma, respectively. The β value map of the North Atlantic, provided by Welford *et al.* (2012), was used to determine that a uniform β value of 2.0 was appropriate for the West Orphan Basin. All of the additional parameters used to calculate the thermal subsidence for both the Rockall Basin and the Orphan Basin can be found in Appendix A.

Based on the assigned parameters, the continental crust subsided uniformly by approximately 770 m in both the Rockall Basin and the West Orphan Basin during the Cenozoic period. Move© uses the equation from Mckenzie (1978) to calculate thermal subsidence. This equation uses only crustal and lithospheric properties, as well as the age and duration of rifting and does not take into account individual thicknesses of sedimentary layers. It is important to note that the same crustal, lithospheric and rifting properties were used across the Newfoundland-Ireland conjugate basins for the purpose of consistency for this M.Sc. project. Therefore, it is not surprising that both basins required the same amount of crustal rebound even though the thermal subsidence in the Rockall Basin is only accounting for one rift event, whereas in the Orphan Basin it is accounting for two rift events. The results of the Cenozoic 2D Thermal Subsidence calculations for both the Rockall Basin and the West Orphan Basin are shown in Fig. 4.5.

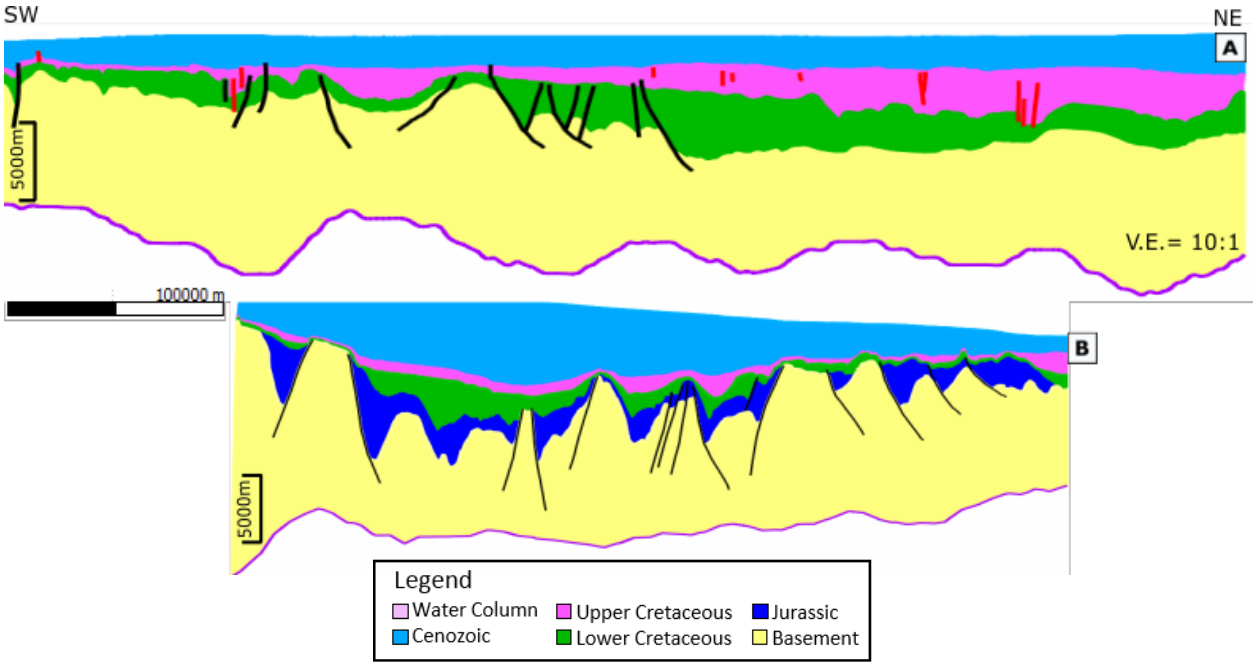


*Figure 4.5: (A) Seismic line IR1 corrected for Cenozoic thermal subsidence, offshore Ireland. (B) Seismic line NL1 corrected for Cenozoic thermal subsidence, offshore Newfoundland and Labrador. The black lines represent the primary faults and the red lines indicate the secondary faults. The purple line represents the Moho proxy from Welford et al. (2012).*

### 4.2.4 Upper Cretaceous Sedimentary Rock Decompaction

Following the correction for the Cenozoic thermal subsidence, the post-rift Upper Cretaceous sedimentary unit was decompacted via the removal of the Cenozoic unit. Using the 2D decompaction tool in Move©, the Cenozoic unit was removed and the underlying units were adjusted according to the compaction curve and the porosity loss with burial as defined by Sclater & Christie (1980). Additionally, the isostatic response to unloading during the decompaction process was also accounted for at this stage.

The decompaction process did not significantly alter fault geometries in either basin. In the Rockall Basin, along seismic line IR1, the decompaction process had a stronger effect towards the NE, where more Upper Cretaceous sedimentary rocks were interpreted. This is likely because the 2D Decompaction module in Move© uses porosity loss with increased burial depth to model the rock volume change. An area of thicker sedimentary cover implies that the

area has a greater overall porosity and could therefore become more compacted over time, than an area with a lesser amount of sedimentary cover.

Towards the SW, where only a thin veneer of sedimentary rocks were interpreted, the decompaction process had a more minimal effect. In the West Orphan Basin, the decompaction process resulted in a relatively uniform lateral decompaction. The decompaction process also smoothed any topographic features of the unrestored Upper Cretaceous horizon. The results of the decompaction process of the Upper Cretaceous sedimentary unit in both the Rockall Basin and the West Orphan Basin can be seen in Fig. 4.6.

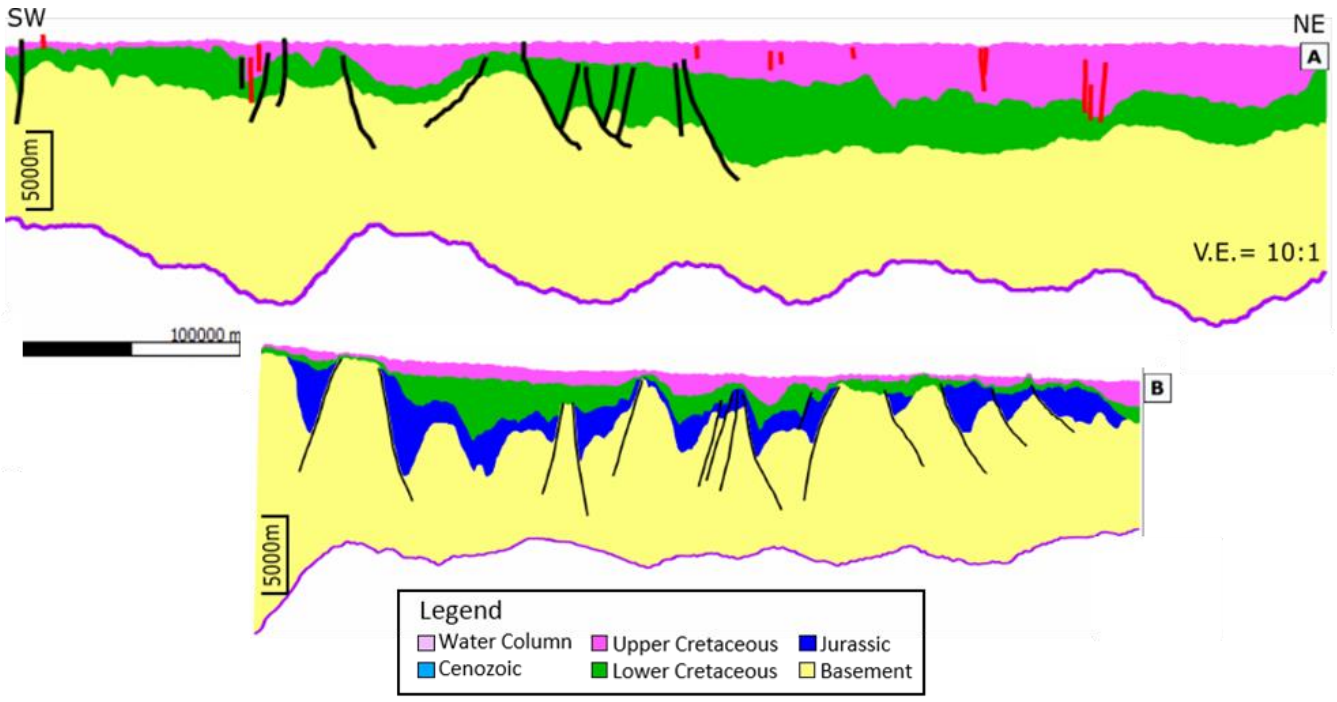


*Figure 4.6: (A) Upper Cretaceous decompaction of seismic line IRI, offshore Ireland. (B) Upper Cretaceous decompaction of seismic line NL1, offshore Newfoundland and Labrador. The black lines represent the primary faults and the red lines indicate the secondary faults. The purple line represents the Moho proxy from Welford et al. (2012).*

### 4.2.5 Upper Cretaceous Thermal Subsidence Restoration

The Upper Cretaceous unit is a post-rift sedimentary layer, therefore, thermal subsidence must be accounted for at this stage in order to accurately restore the Rockall Basin and the West Orphan Basin. The 2D Thermal Subsidence module in Move© uses a thermal subsidence model generated by McKenzie (1978) to restore the shape and paleo-depth of the seafloor. As stated, the parameters necessary to calculate and restore thermal subsidence include: the number of rifting events, age of the rifting events, the duration of syn-rift, the upper and lower stratigraphic limits of the unit that is to be restored, the beta/stretching value, the thickness of the lithosphere, the thickness of the continental crust and the densities of the mantle, the continental crust, the sedimentary rocks and the seawater. The same parameters used to restore the thermal subsidence of the Cenozoic unit were used to restore the thermal subsidence of the Upper Cretaceous unit. The only difference in parameters between the restoration of the thermal subsidence of the Cenozoic unit and the Upper Cretaceous unit is the change in the upper and lower stratigraphic limits. The Upper Cretaceous sedimentary unit has upper and lower stratigraphic limits of 66 Ma and 100 Ma, respectively, compared to the upper and lower stratigraphic limits of the Cenozoic unit, 0 and 66 Ma, respectively.

For the Upper Cretaceous period, the continental crust was restored uniformly by approximately 806 m in both the Rockall Basin and the West Orphan Basin. The results of the Upper Cretaceous thermal subsidence calculations on both the Rockall Basin and the West Orphan Basin are shown in Fig. 4.7.

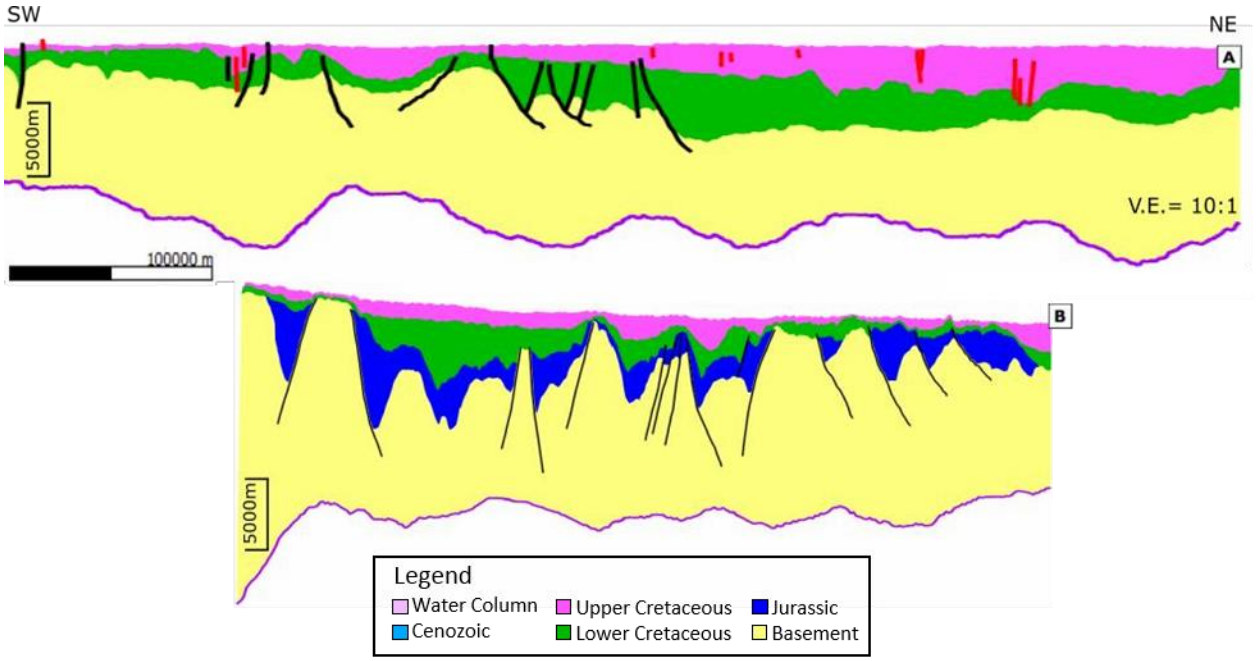


*Figure 4.7: (A) Seismic line IR1 corrected for Upper Cretaceous thermal subsidence, offshore Ireland. (B) Seismic line NL1 corrected for Upper Cretaceous thermal subsidence, offshore Newfoundland and Labrador. The black lines represent the primary faults and the red lines indicate the secondary faults. The purple line represents the Moho proxy from Welford et al. (2012).*

### 4.2.6 Lower Cretaceous Sedimentary Rock Decompaction

After restoring the effects of the Upper Cretaceous thermal subsidence, the unit was then removed, thus decompacting the underlying syn-rift, Lower Cretaceous sedimentary unit. Using the 2D Decompaction tool in Move©, the Upper Cretaceous unit was removed and the underlying units were adjusted according to the compaction curve and the porosity loss with burial (Sclater & Christie 1980). The isostatic response to unloading during the decompaction process was also accounted for again at this stage.

During the interpretation process in Petrel©, numerous primary and secondary faults were interpreted. The primary faults are those that are directly related to rifting, whereas the secondary faults likely do not account for much of the extension observed in the region. In the Rockall Basin, along seismic line IR1, the secondary faults that were associated with the Upper

Cretaceous unit (shown in red in Fig. 4.7) have been removed along with the Upper Cretaceous sedimentary rocks in order to decompact the Lower Cretaceous unit. It was appropriate to eliminate the secondary faults from the model because they have no restoration potential due to their minimal size and the lack of throw related to extension.

As previously observed in earlier decompactions, where thicker sedimentary cover was initially interpreted, a greater amount of decompaction was required (for reasons previously stated). Additionally, the topographic changes of the Lower Cretaceous horizon have been smoothed as a result of the decompaction process. The results from the decompaction of the Lower Cretaceous unit along seismic lines IR1 and NL1 are illustrated in Fig. 4.8.

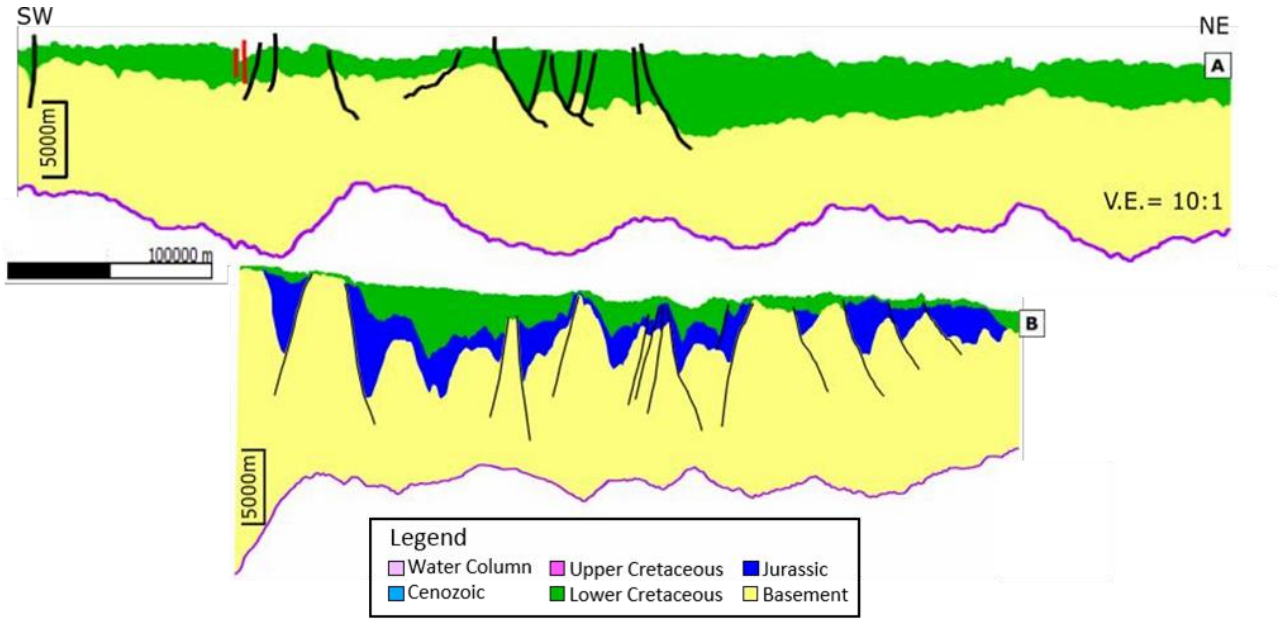


*Figure 4.8: (A) Lower Cretaceous decompaction of seismic line IRI, offshore Ireland. (B) Lower Cretaceous decompaction of seismic line NL1, offshore Newfoundland and Labrador. The black lines represent the primary faults and the red lines indicate the secondary faults. The purple line represents the Moho proxy from Welford et al. (2012).*

### 4.2.7 Jurassic Sedimentary Rock Decompaction

Due to thermal subsidence creating large changes in elevation as the lithosphere thins during rifting, thermal subsidence must be accounted for in the restoration process of post-rift

units. The Lower Cretaceous unit is a syn-rift unit, which is an accumulation of sedimentary rocks that were deposited during rifting. Therefore, no thermal subsidence calculation was required to restore the Lower Cretaceous sedimentary unit. This unit was removed and the underlying Jurassic sedimentary rocks were decompacted. Due to the fact that Jurassic sedimentary rocks were only interpreted in the Orphan Basin, only seismic lines NL1 and NL2 (and later NL3) required decompaction of the Jurassic sedimentary unit. The resultant effects of this decompaction on the Jurassic sedimentary rocks are minimal. The unit has thickened slightly and the horizon has been smoothed.

The principles of lithospheric strength depth curves are well known (e.g., Brace & Kohlstedt, 1980). At the temperatures and pressures within the uppermost crust, the yield stress for brittle failure is less than that for failure by ductile deformation mechanisms (Pérez-Gussinyé & Reston 2001). However, with increasing pressure (at depth), brittle strength increases, whereas with increasing temperature, the ductile yield stress for a given strain rate and rheology will decrease (Pérez-Gussinyé & Reston 2001). The point at which the ductile and brittle yield stresses are equal is the brittle-ductile transition. Above this transition, deformation occurs by brittle failure; below it, plastic deformation is the favoured mechanism (Pérez-Gussinyé & Reston 2001).

Following the interpretations of Gouiza *et al.* (2017) and the definition of the brittle-ductile transition zone (Pérez-Gussinyé & Reston 2001), a crustal boundary between the upper and lower crust was interpreted along all of the seismic lines in both the Rockall Basin and the West Orphan Basin. The results of the decompaction of the Jurassic sedimentary rocks and the addition of the mid-crustal boundary along NL1 are shown in Fig. 4.9.

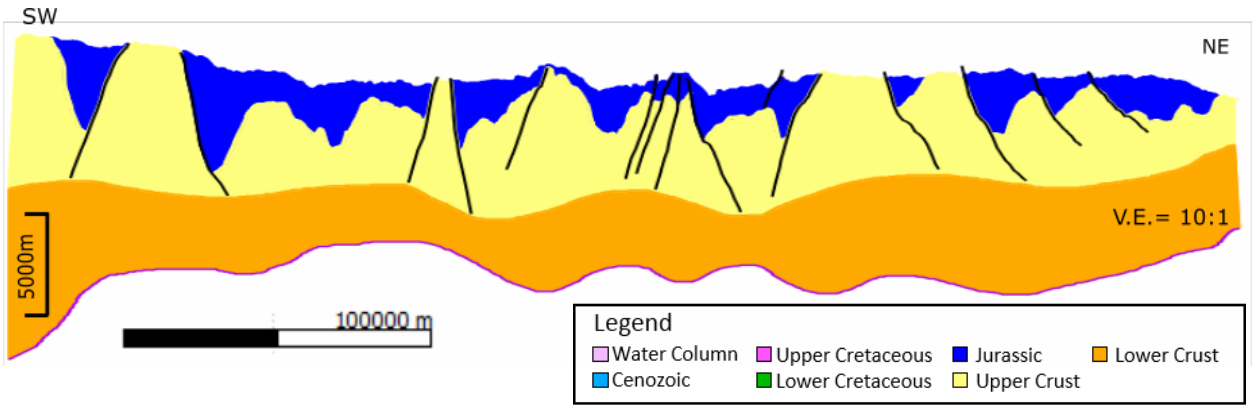


*Figure 4.9: Jurassic decompaction of seismic line NL1, offshore Newfoundland and Labrador. The mid-crustal boundary was also introduced at this stage. The yellow polygon represents the upper crust and the orange polygon represents the lower crust. The black lines represent the primary faults. Cross-sections from Gouiza e t al. (2017) helped determine the depth extent of the brittle-ductile transition used in this thesis. The purple line represents the Moho proxy from Welford et al. (2012).*

### 4.2.8 Jurassic Fault Restoration and Unfolding

Following the decompaction and the thermal subsidence restorations of seismic lines NL1 and NL2 (and later NL3), fault modelling began in the West Orphan Basin. No Jurassic sedimentary rocks were interpreted along the Irish margin, therefore seismic lines IR1 and IR2 did not require Jurassic fault restoration. Fault modelling in the West Orphan Basin was carried out in Move©. The 2D Move-on-Fault module, within Move©, was used in this thesis to restore the faults (refer to section 2.2.2.4).

Along seismic line NL1, the Jurassic faults were restored using the 2D Move-on-Fault module in Move©. Along each Jurassic fault, individual hanging walls and footwalls of the Jurassic horizon were selected and realigned in order to accurately restore the model to the beginning of the Jurassic period.

After the restoration of all of the Jurassic faults, the entire Jurassic unit was unfolded to the zero datum, thus flattening the unit. The process of unfolding a unit in Move© requires that the unit is present across the entire model. Due to the fact that the Jurassic sedimentary rocks were not interpreted across the basement highs of seismic line NL1, a thin veneer of Jurassic

sedimentary rocks were added to generate a continuous horizon. Additionally, the fault restoration process generated non-geological artifacts along the mid-crustal boundary and the Moho horizon. These artifacts were likely the result of the movement of the horizons that is necessary during the restoration process. The movement necessary to accurately restore the top horizon along the fault was mirrored in the underlying horizons, creating non-geological gaps/jumps in the horizons. To compensate, a smoothing process was used to ensure that the final model was geologically reasonable. The results of the restored, unfolded and smoothed section, with the Jurassic sedimentary unit, is shown in Fig. 4.10.

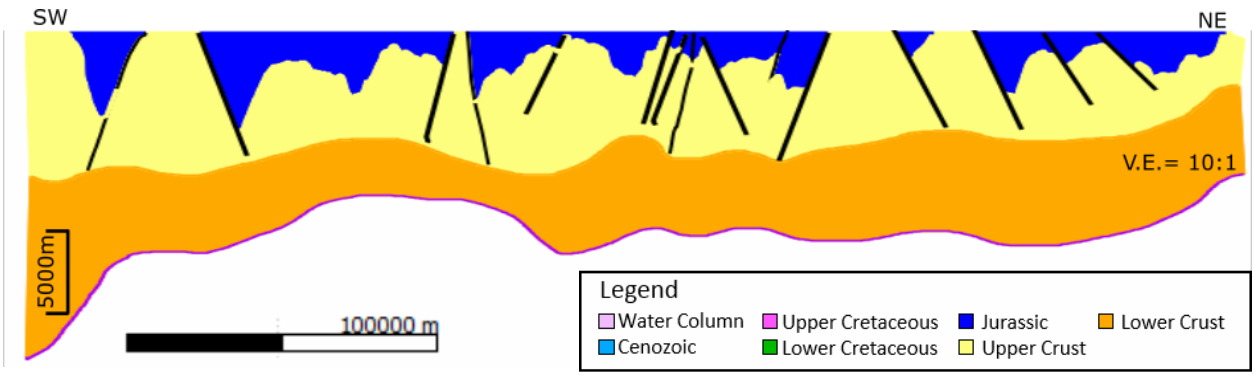


*Figure 4.10: Jurassic restoration of faults, unfolded, along seismic line NL1, offshore Newfoundland and Labrador. The black lines represent the primary faults. The purple line represents the Moho proxy from Welford et al. (2012).*

### 4.2.9 Upper Crustal Decompaction

Move© calculates the compaction that occurred, over time, of the underlying sedimentary rocks and decompacts them. Therefore, in the Rockall Basin, the lower Cretaceous unit was removed, and in the West Orphan Basin, the Jurassic unit was removed. Once the Jurassic sedimentary unit was restored along seismic lines NL1 and NL2 in the West Orphan Basin, the upper crust was decompacted across the Newfoundland-Ireland conjugate basins. The decompaction of the upper crust is justified by the assumption that metasedimentary rocks are

present in the interpreted upper crustal unit. No pre-rift sedimentary rocks were interpreted in either basin, therefore, to account for the potential decompaction of these sedimentary rocks a small porosity was assigned to the upper crustal unit to allow for minimal decompaction.

Along seismic lines NL1 and IR1, the decompaction process yielded a larger amount of restoration in areas where thicker overlying sedimentary rocks were interpreted and smaller amounts where less overlying sedimentary rock was interpreted. This is likely due to the 2D Decompaction module in Move©, as it uses porosity loss with increased burial depth to model the rock volume change. An area of thicker sedimentary cover implies that the area has a greater overall porosity and could, therefore, become more compacted over time, than an area with a lesser amount of sedimentary cover. This lateral change in decompaction can be observed along seismic line NL1 in Fig. 4.11.

As a result of the decompaction process, only the primary faults remain present in both the Rockall Basin and the West Orphan Basin. These faults are used to restore the basement to a pre-rift state. The primary faults are used to reconstruct the basin, as these faults were generated as rifting began in the basin. After restoring the faults, the model represents a pre-rift state of the basin, a primary goal of this M.Sc. thesis. As mentioned above, due to artifacts generated during the Jurassic fault restoration in Move©, a smoothing technique was applied after every step until the restoration was complete. The results of the decompaction process along seismic lines IR1 and NL1 are shown in Fig. 4.11.

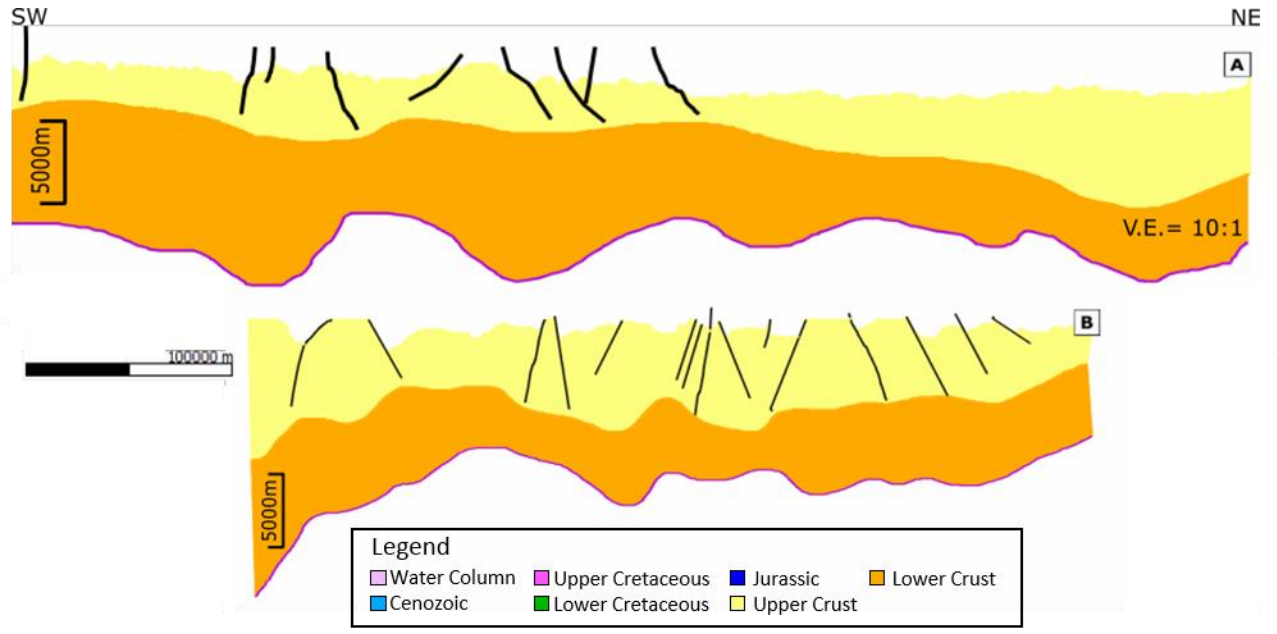


*Figure 4.11: (A) Basement decompaction along seismic line IRI, offshore Ireland, only showing continental crust. (B) Basement decompaction along seismic line NL1, offshore Newfoundland and Labrador. The black lines represent primary faults. The purple line represents the Moho proxy from Welford et al. (2012).*

### 4.2.10 Crustal Fault Restoration and Unfolding

Following the decompaction of the upper and lower crust along seismic lines NL1, NL2, IR1, IR2, and later NL3, basement fault restoration began in both the West Orphan Basin and the Rockall Basin. Using the 2D Move-on-Fault module, in Move©, each individual hanging wall and footwall adjacent to a fault were selected and restored. This process was repeated until all the primary faults, along all four seismic lines, were restored and the basins represented a pre-rift state.

After this restoration the upper crust was unfolded to the zero datum. To compensate for the artifacts generated from the fault restoration, in Move©, a smoothing technique was applied. The results of the restoration, unfolding and smoothing along the primary seismic lines IR1 and NL1, can be seen in Fig. 4.12.

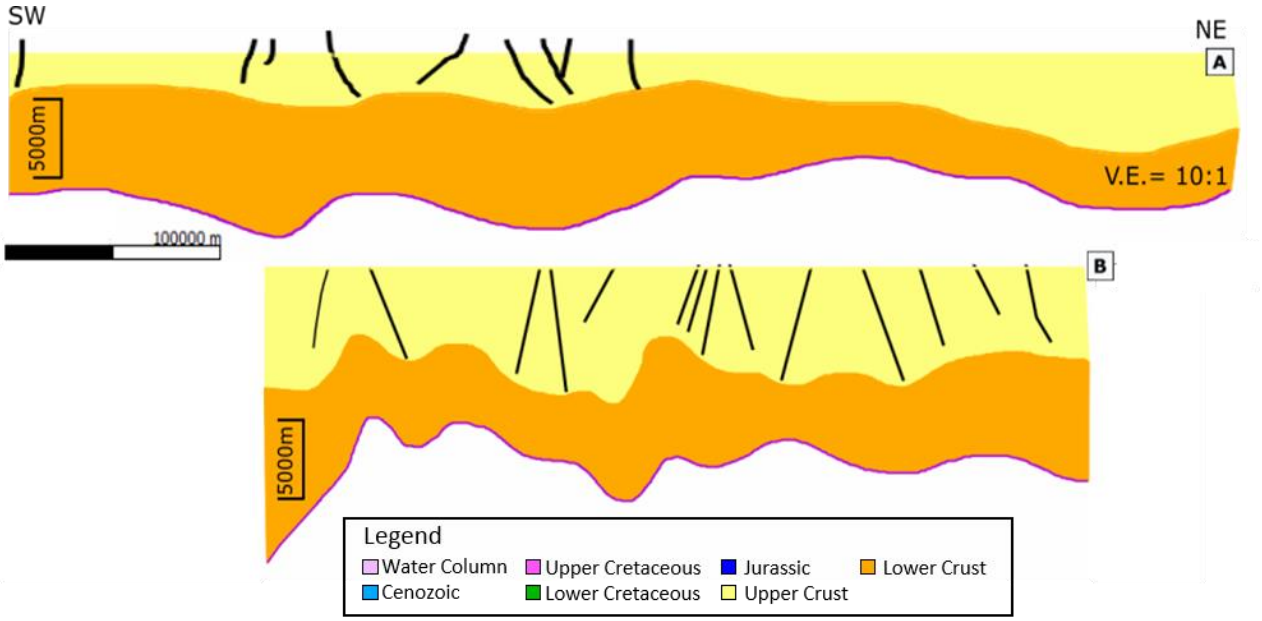


*Figure 4.12: (A) Basement fault restoration and unfolding along seismic line IRI, offshore Ireland, only showing continental crust. (B) Basement fault restoration and unfolding along seismic line NL1, offshore Newfoundland and Labrador. The black lines represent primary faults. The purple line represents the Moho proxy from Welford et al. (2012).*

### 4.3 3D Modelling

EarthByte's GPlates© software was utilized to visualize the pre-rift reconstruction of the Newfoundland-Ireland conjugate basins. GPlates© is an open-source application software that offers a wide variety of interactive visualizations of plate-tectonic reconstructions, geographic information system (GIS) functionality, and raster data visualizations. GPlates© enables both the visualization and the manipulation of plate-tectonic reconstructions and associated data through geological time. The GPlates models used in this thesis were generated by Matthews *et al.* (2016) and Müller *et al.* (2016). The main assumption made during the 3D reconstruction across the margins is that the Rockall Basin has always been conjugate to, and continuous with, the West Orphan Basin and that these restorations capture a single continuous Mesozoic basin.

Using the 3D map view in Move©, the primary and secondary seismic lines in both the Rockall Basin and the West Orphan Basin, can be zoomed, rotated and repositioned to allow for in depth analysis of the data. The location of seismic lines NL1, NL2, IR1 and IR2 were first imported into GPlates©. Seismic lines NL1 and NL2 in the Orphan Basin were attached to the nearest plate, the North American plate. As the North American plate moves through time, the seismic lines move with it, following the same pole of rotation (Kneller *et al.,* 2012 and Müller *et al.,* 1999). Seismic lines IR1 and IR2 were attached to the Eurasian plate, implying that as the Eurasian plate moves through time, the seismic lines move with it, following the same pole of rotation (Barnett-Moore *et al.*, 2016). However, it is important to note that GPlates© does not account for any internal deformation within the tectonic plates, therefore this reconstruction, across the Newfoundland-Ireland conjugate margins, is only an approximation.

At each key time period (present day, 66 Ma, 100 Ma, 145 Ma and 201 Ma), the distances between the two primary seismic lines, NL1 and IR1 were calculated. These distances were then

used in Move© to manipulate the Newfoundland margin with respect to the Irish margin throughout time, in order to geographically restore the basins to their pre-rift location.

### 4.3.1 Present Day

Using GPlates©, all of the seismic lines in both the Rockall Basin and the Orphan Basin were overlain on a modern day bathymetry map to aid in the visualization of the reconstruction. However, this bathymetry map is stationary and does not move back in time with the restoration, therefore it was only used as a reference tool for the present day models. Using the measuring tool in GPlates©, a distance of approximately 1900 km was calculated from the northeastern limit of seismic line NL1 in the West Orphan Basin to the continental crust of seismic line IR1 in the Rockall Basin (the limit of continental crust of seismic line IR1 is shown in Fig. 3.2).

In the 3D map view in Move©, seismic lines NL1 and NL2 were moved together, to a point where the northeastern extent of seismic line NL1 was 1900 km away from the southwestern extent of the continental crust of seismic line IR1. The GPlates© model and the Move© results of the movement of the seismic lines for present day are shown in Fig. 4.13.

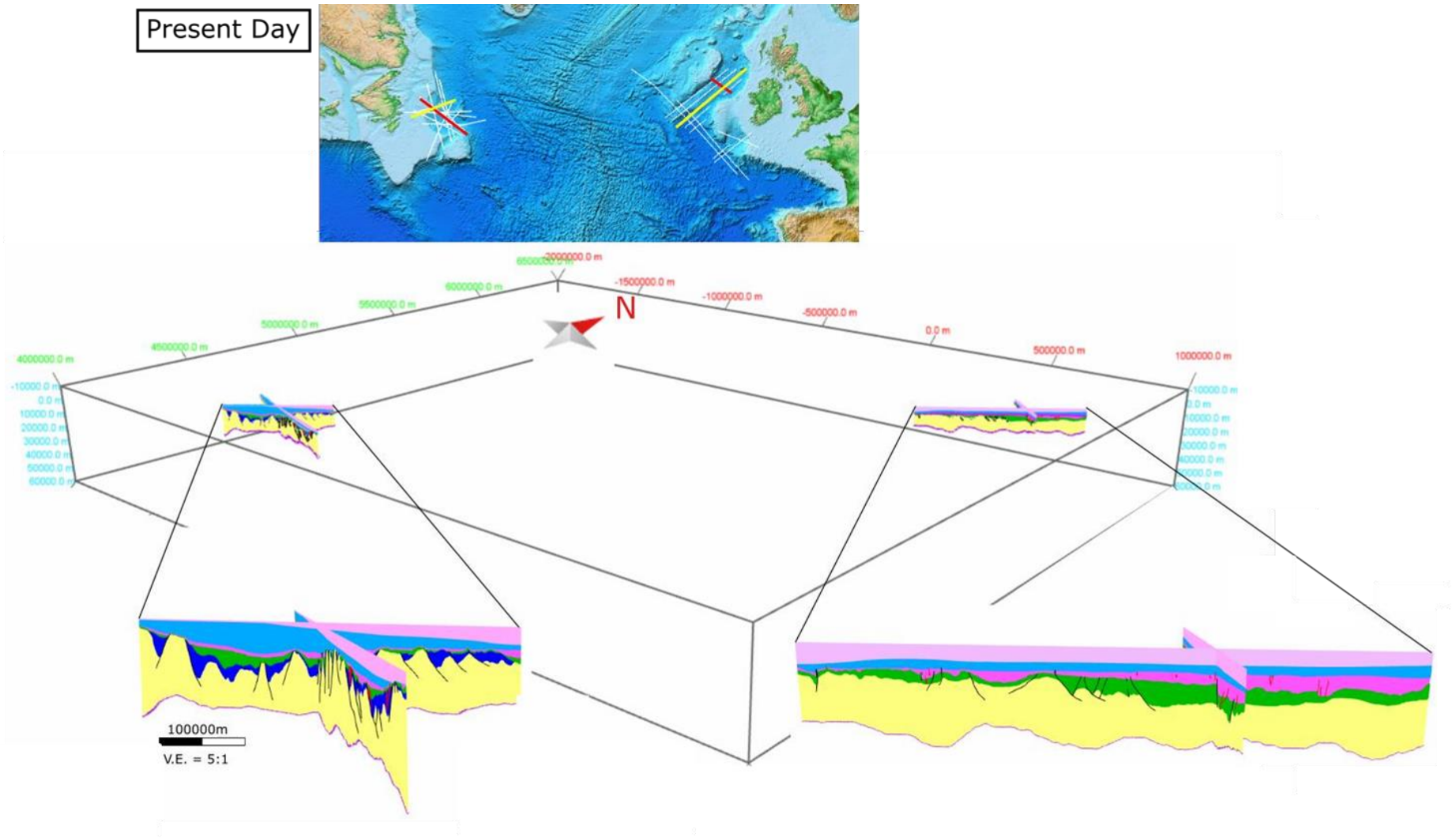


*Figure 4.13: (Top) GPlates© model of the Newfoundland-Ireland conjugate basins, present day. Background image shows bathymetry. (Bottom) 3D models of seismic lines NL1 and NL2 (left) in the Orphan Basin and 3D models of seismic lines IR1 and IR2 (right) in the Rockall Basin , present day. Black lines represent primary faults and red lines represent secondary faults. The light pink represents seawater. The light blue represents the Cenozoic unit. The dark pink represents the Upper Cretaceous unit. The green represents the Lower Cretaceous unit. The dark blue represents the Jurassic unit. The yellow represents the basement/crust. The purple line represents the Moho proxy from Welford et al. (2012).*

### 4.3.2 Cenozoic Decompaction and Thermal Subsidence Reconstruction

The focus of this thesis is on a regional and structural scale, therefore the water column was removed in a single step and the time period associated with this step remained at 0 Ma. If the focus of this thesis had been on the evolution of the petroleum systems in the basins, then the water column would have been removed in several steps, following the evolution of the paleo-water depth through time. During the removal of the water column, at 0 Ma, the Cenozoic sedimentary unit was decompacted and the thermal subsidence was restored. As previously stated, the distance between IR1 and NL1 at 0 Ma was 1900 km.

In the 3D map view in Move©, the decompacted and thermally restored Cenozoic sedimentary unit models of seismic lines NL1 and NL2 were moved together, to a point where the northeastern extent of seismic line NL1 was 1900 km away from the southwestern extent of the continental crust of seismic line IR1. The GPlates© modern day bathymetry map and the movement of seismic lines IR1, IR2, NL1 and NL2 are shown in Fig. 4.14.

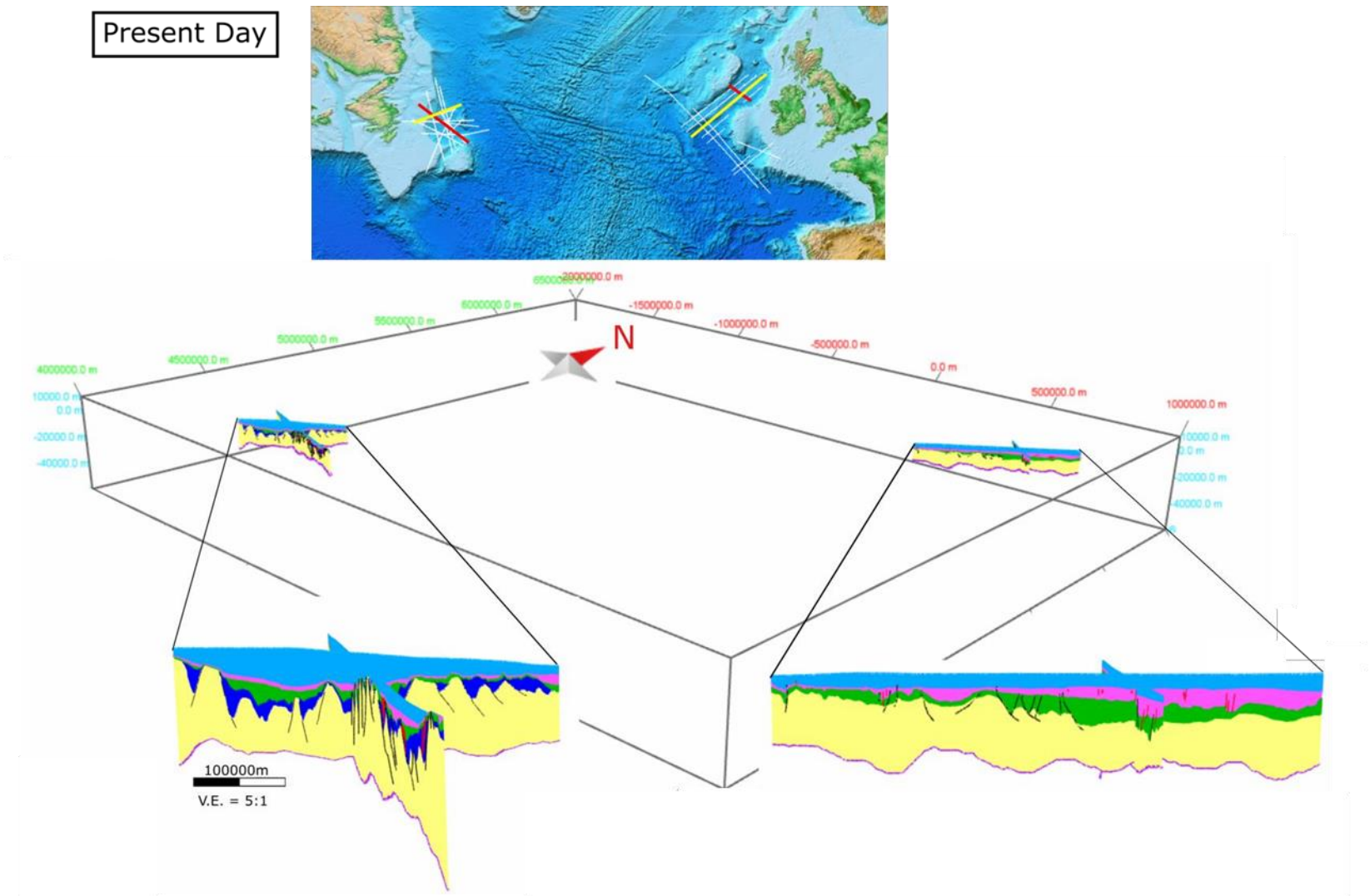


*Figure 4.14: (Top) GPlates© model of the Newfoundland-Ireland conjugate basins, present day. Background image shows modern bathymetry. (Bottom) 3D model of seismic lines NL1 and NL2 (left) in the Orphan Basin with the Cenozoic sedimentary unit decompacted. 3D model of seismic lines IR1 and IR2 (right) in the Rockall Basin with the Cenozoic sedimentary unit decompacted. Black lines represent primary faults and red lines represent secondary faults. The light blue represents the Cenozoic unit. The dark pink represents the Upper Cretaceous unit. The green represents the Lower Cretaceous unit. The dark blue represents the Jurassic unit. The yellow represents the basement/crust. The purple line represents the Moho proxy from Welford et al. (2012).*

### 4.3.3 Upper Cretaceous Decompaction and Thermal Subsidence Reconstruction

The bathymetry map previously used to aid in the visualization of the reconstruction of the Newfoundland-Ireland conjugate basins was replaced by a simple modern day coastlines shapefile. This change was necessary because the bathymetry map in GPlates© was a simple overlay and could not be reconstructed through time. However, each section of coastline could be tied to separate tectonic plates with individual poles of rotation, thus allowing the coastlines to be restored through geological time. As a result of restoring the tectonic plates, the coastlines and the seismic lines back to 66 Ma, it can be observed that the Rockall Basin and the West Orphan Basin were significantly closer together 66 Ma than they are today. During the Upper Cretaceous time period (66 Ma), it was calculated in GPlates© that seismic lines NL1 and the continental crust of IR1 were approximately 300 km apart.

Following the decompaction and thermal subsidence restoration of the Upper Cretaceous unit, the 3D map view in Move© was used to move seismic lines NL1 and NL2 to a location where NL1 was 300 km away from the continental crust of IR1. The results of the reconstructions in Move© and GPlates© can be seen together in Fig. 4.15.

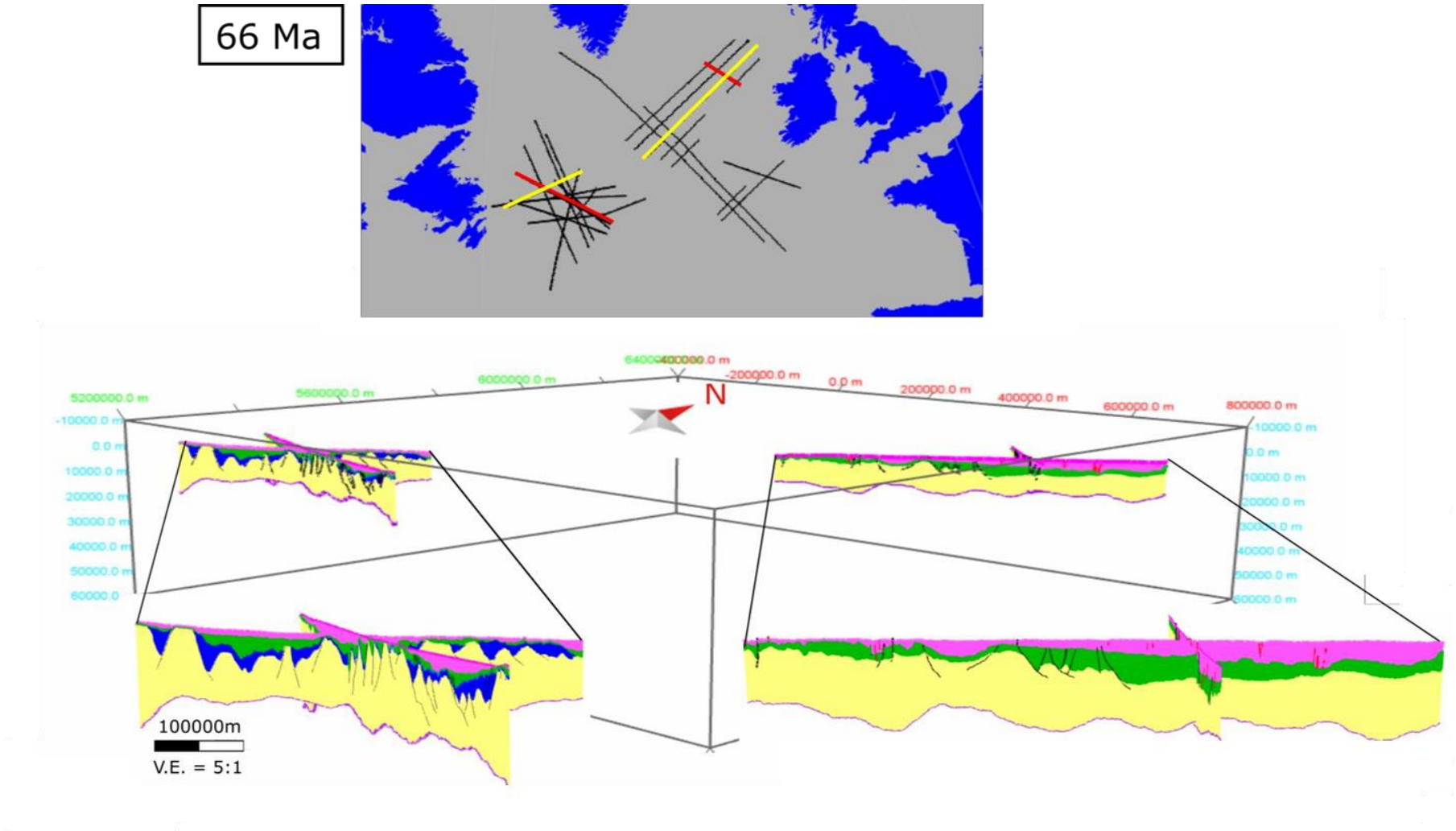


*Figure 4.15: (Top) GPlates© model of the Newfoundland-Ireland conjugate basins. Background image shows modern coastlines 66 Ma (blue polygons). (Bottom) 3D model of seismic lines NL1 and NL2 (left) in the Orphan Basin with the Upper Cretaceous sedimentary unit decompacted and thermal subsidence restored. 3D model of seismic lines IR1 and IR2 (right) in the Rockall Basin with the Upper Cretaceous sedimentary unit decompacted and thermal subsidence restored. Black lines represent primary faults and red lines represent secondary faults. The dark pink represents the Upper Cretaceous unit. The green represents the Lower Cretaceous unit. The dark blue represents the Jurassic unit. The yellow represents the basement/crust. The purple line represents the Moho proxy from Welford et al. (2012).*

### 4.3.4 Lower Cretaceous Decompaction Reconstruction

The GPlates© Lower Cretaceous reconstruction, at 100 Ma, shows that the Rockall Basin and the West Orphan Basin continue to move closer together as the North Atlantic Ocean closes. The NE extent of seismic line NL1 is approximately 60 km to the east of the southwestern extent of seismic line IR1. The seismic lines do not match up perfectly, but this margin of error can be accounted for by the fact that GPlates© does not account for any internal deformation of the plates. It is hypothesized that Flemish Cap, offshore Newfoundland and Labrador (location shown in Fig. 1.3), to the SE of the Orphan Basin, rotated approximately 43 degrees in a clockwise direction relative to Galicia Bank and Iberia during the Late Triassic to Early Cretaceous (Srivastava & Verhoef 1992, Enachescu , 2006 and Sibuet *et al.*, 2007). As a result of the rotation of Flemish Cap, there is one possible instance of internal rotation within the North American plate that is not accounted for in GPlates©. Therefore, the fact that seismic lines NL1 and IR1 are off by a margin of approximately 60 km may simply be the result of GPlates© lack of knowledge of internal deformation of the plates. Another possible explanation for the lack of cohesion between the locations of the seismic lines across the margins is that the Rockall Basin and the West Orphan Basin may not have been connected conjugate basins.

In the 3D map view in Move©, seismic lines NL1 and NL2 have been manipulated to close the distance between the Rockall Basin and the West Orphan Basin. This manipulation was done to better visualize the relationship between the thicknesses of the sedimentary rocks and the pre-rift crust across the potentially continuous basin. Assuming the margins are conjugate, following the decompaction of the Lower Cretaceous sedimentary rocks, the primary seismic lines in the Rockall Basin and the West Orphan Basin were merged together in Move©. The point of intersection of the two lines is denoted by the northeastern extent of seismic line

NL1 and the southwestern extent of the continental crust of seismic line IR1 (location shown in Fig. 3.2). The results of the reconstruction in GPlates© and the movement of the seismic lines IR1, IR2, NL1 and NL2 in Move©, can be seen in Fig. 4.16.

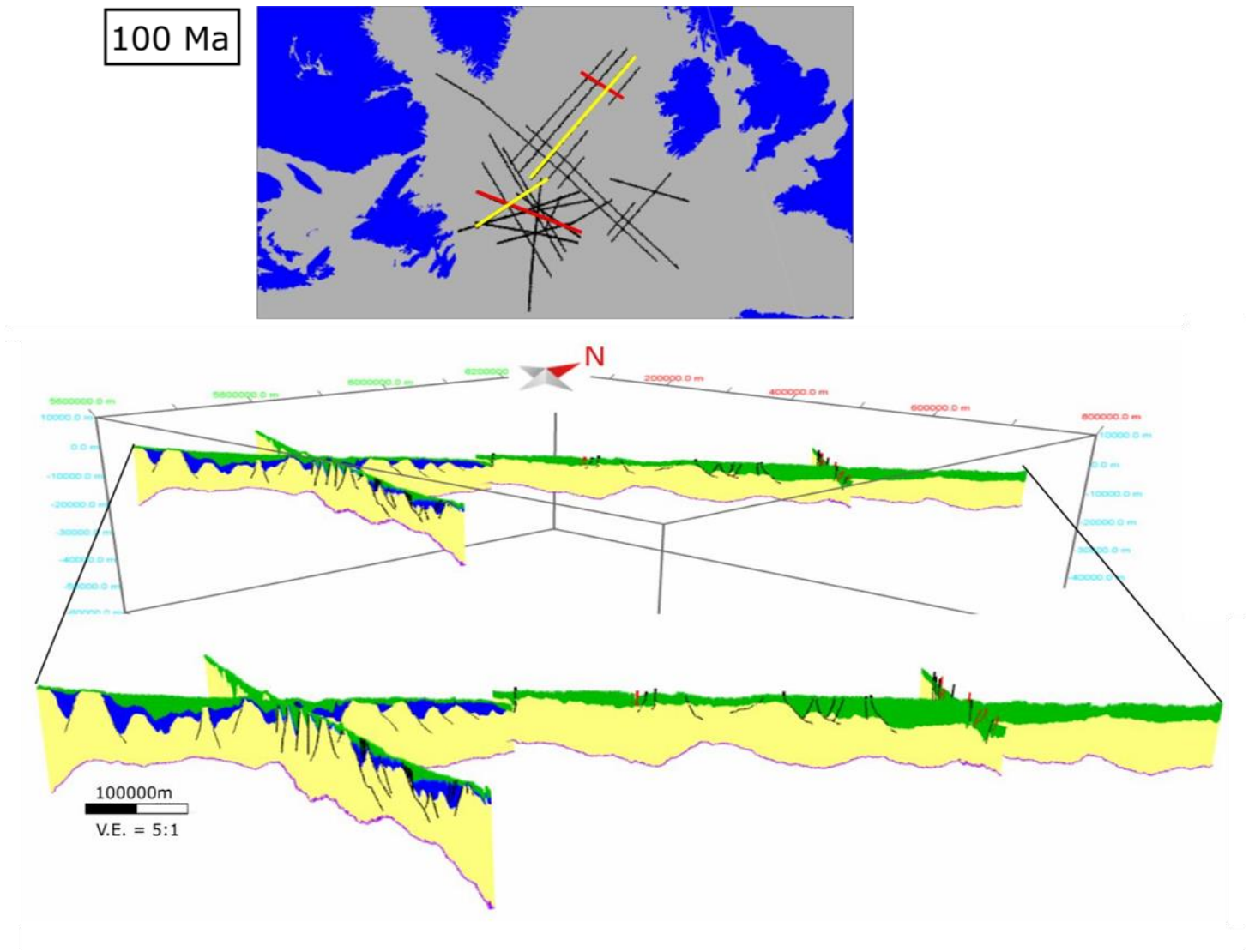


*Figure 4.16: (Top) GPlates© model of the Newfoundland-Ireland conjugate basins. Background image shows modern coastlines 100 Ma (blue polygons). (Bottom) 3D model of seismic lines NL1 and NL2 (left) in the Orphan Basin with the Lower Cretaceous sedimentary unit decompacted and thermal subsidence restored. 3D model of seismic lines IR1 and IR2 (right) in the Rockall Basin with the Lower Cretaceous sedimentary unit decompacted and thermal subsidence restored. Black lines represent primary faults and red lines represent secondary faults. The green represents the Lower Cretaceous unit. The dark blue represents the Jurassic unit. The yellow represents the basement/crust. The purple line represents the Moho proxy from Welford et al. (2012).*

### 4.3.5 Jurassic Decompaction and Fault Restoration Reconstruction

Jurassic sedimentary rocks were only interpreted in the Orphan Basin, therefore when restoring the Newfoundland-Ireland conjugate margins at 145 Ma, the decompacted upper crustal unit was used in the Rockall Basin. The mismatched distance between seismic line NL1 and seismic line IR1 has increased from the previous step. Seismic line NL1 now lies approximately 160 km to the east of IR1. As previously stated, the increasing margin of error could potentially be accounted for by the fact that GPlates© does not account for any internal deformation of the plates. Another possible explanation for the growing discord between the two primary seismic lines is that the Rockall Basin and the West Orphan Basin may not have been conjugate or continuous basins at this time.

Using the 3D map view in Move©, seismic lines NL1 and NL2, in the West Orphan Basin, remain in the merged position with seismic lines IR1 and IR2 in the Rockall Basin. After the Jurassic sedimentary unit was restored on the Newfoundland margin, seismic line NL1 was aligned with the continental crust of seismic line IR1. The point of intersection of the two lines is denoted by the northeastern extent of seismic line NL1 and the southwestern extent of the continental crust of seismic line IR1 (location shown in Fig. 3.2). The results of the reconstruction in GPlates© and the movement of the seismic lines IR1, IR2, NL1 and NL2, in Move© can be seen in Fig. 4.17.

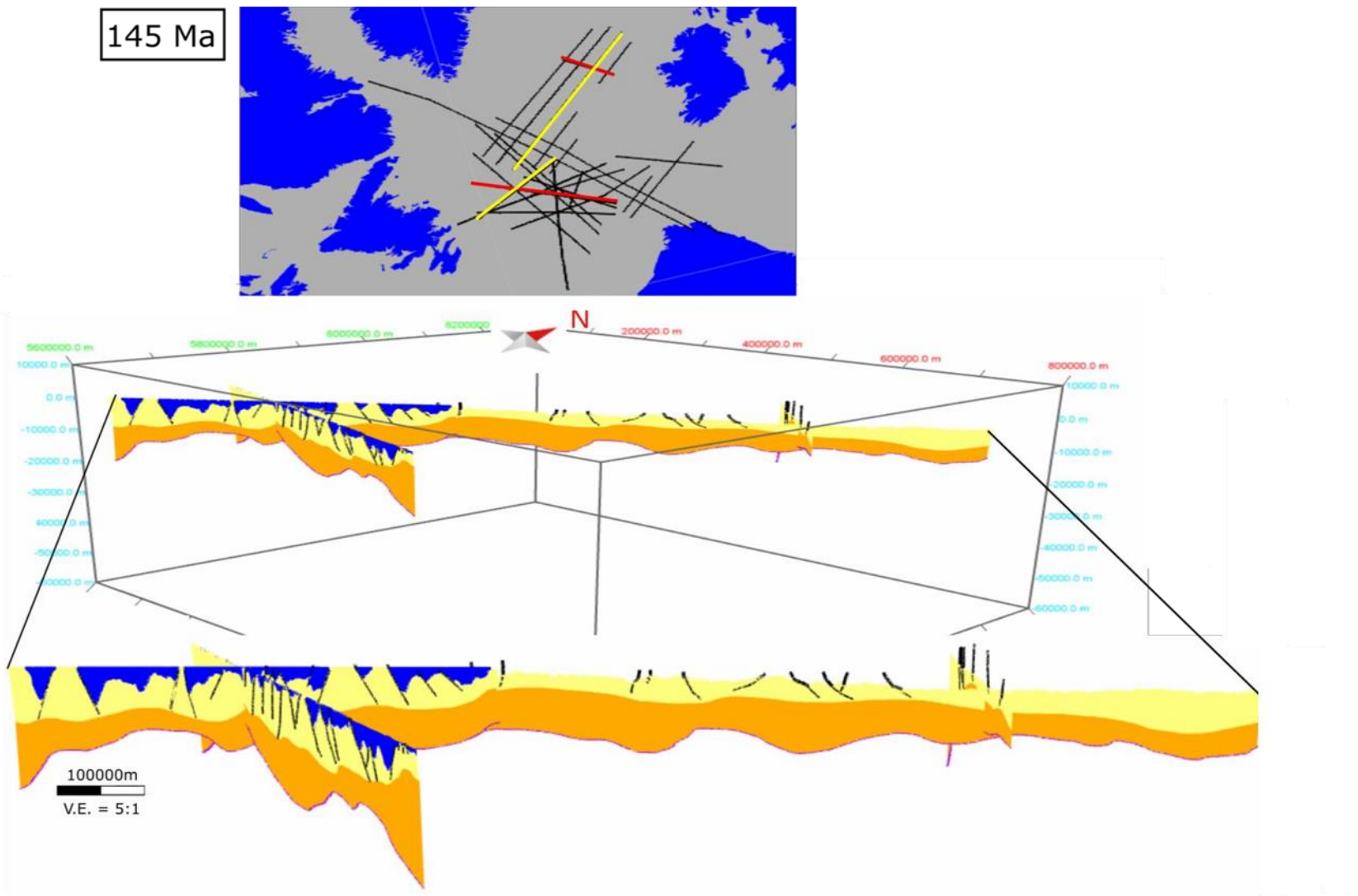


*Figure 4.17: (Top) GPlates© model of the Newfoundland-Ireland conjugate basins. Background image shows modern coastlines 145 Ma (blue polygons). (Bottom) 3D model of seismic lines NL1 and NL2 (left) in the Orphan Basin with the Jurassic sedimentary unit decompacted, restored and unfolded. 3D model of seismic lines IR1 and IR2 (right) in the Rockall Basin with the upper and lower crustal unit decompacted. Black lines represent primary faults. The dark blue represents the Jurassic unit. The yellow represents the basement. The orange represents the lower crust, bounded by the mid-crustal boundary. The purple line represents the Moho proxy from Welford et al. (2012).*

### 4.3.6 Upper Crust Decompaction and Fault Restoration Reconstruction

Observing the crustal reconstruction in GPlates©, at 201 Ma, the seismic lines in the West Orphan Basin intersect with those in the Rockall Basin. The primary line in the Rockall Basin, IR1, now intersects the secondary line in the West Orphan Basin, NL2. Multiple supplementary seismic lines from the Rockall Basin also intersect supplementary lines in the Orphan Basin at this time. The northeastern extent of seismic line NL1 now lies 280 km to the NE of the southwestern extent of the continental crust of seismic line IR1.

Following the decompaction, restoration and unfolding of the upper crustal unit in both basins, the 3D map view in Move© was used and seismic lines NL1 and NL2, in the West Orphan Basin, remain in the merged position with seismic lines IR1 and IR2 in the Rockall Basin. The four seismic lines now, at 201 Ma, depict the possible extent of a continuous Mesozoic pre-rift basin, assuming the Rockall Basin and the West Orphan Basin are conjugate basins. The 3D view of the potentially continuous pre-rift Mesozoic basin can be seen in Fig. 4.18.

## 4.4 From Modelling to Broader Understanding

Following generation of the 2D and 3D reconstructions in Move©, a thorough discussion will be presented in Chapter 5. The results and variable parameters used throughout the 2D and 3D reconstructions will be discussed in detail. Additionally, comparisons of syn-rift, post-rift and pre-rift crustal thicknesses will be analyzed across the conjugate basins in Chapter 5. Finally a possible evolutionary history of the Orphan Basin and Rockall Basin will be presented.

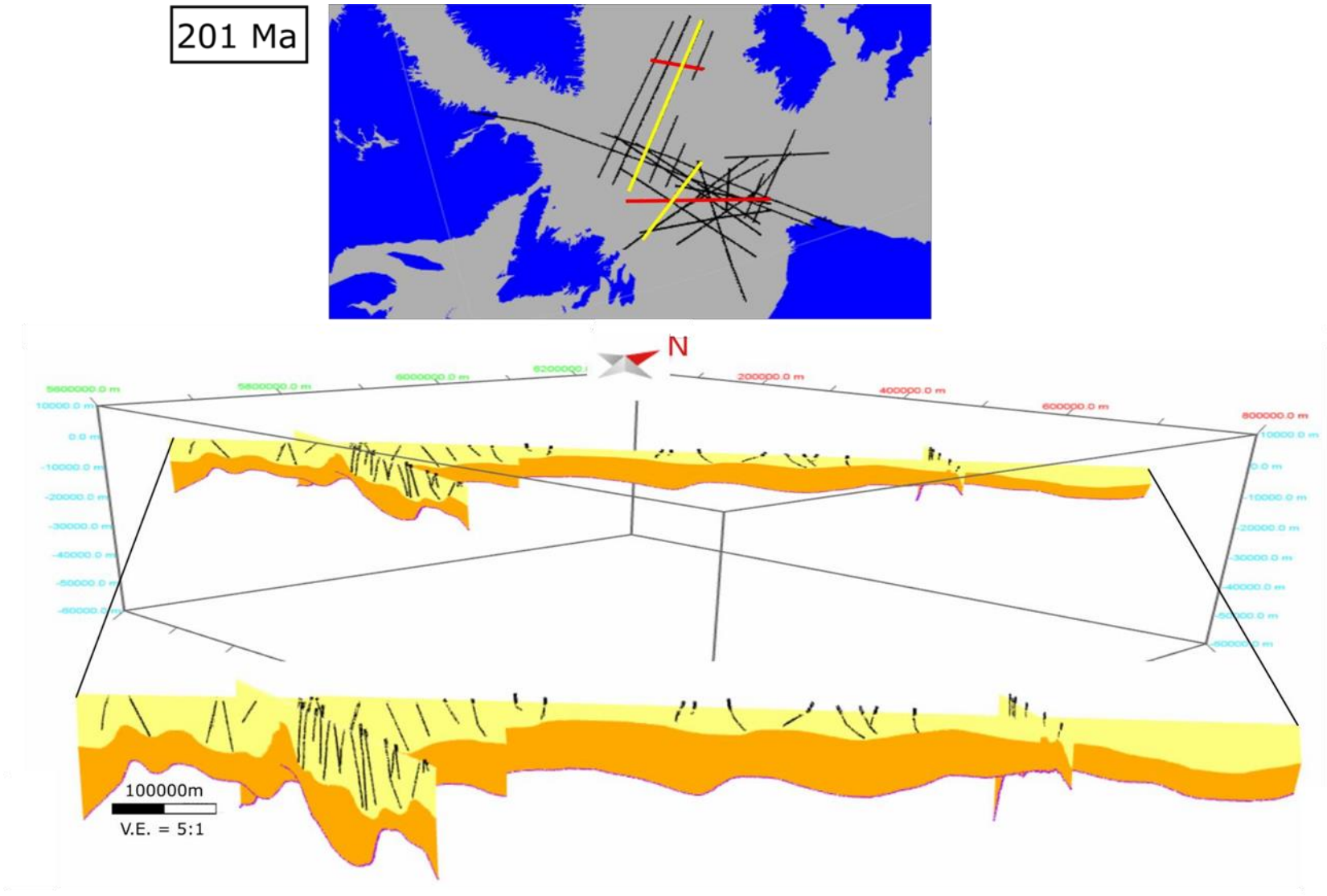


*Figure 4.18: (Top) GPlates© model of the Newfoundland-Ireland conjugate basins. Background image shows modern coastlines 201 Ma (blue polygons). (Bottom) 3D model of seismic lines NL1 and NL2 (left) in the Orphan Basin with the Basement unit decompacted, restored and unfolded. 3D model of seismic lines IR1 and IR2 (right) in the Rockall Basin with the Basement unit decompacted, restored and unfolded. Black lines represent primary faults. The yellow represents the basement. The orange represents the lower crust, bounded by the mid-crustal boundary. The purple line represents the Moho proxy from Welford et al. (2012).*

# Chapter 5: Discussion

## 5.1 Introduction

In this chapter, the techniques used during the 2D and 3D reconstructions in Move©, and the results from the Newfoundland-Ireland conjugate margins will be discussed and compared. This chapter tackles features that vary in scale and temporal evolution and will be presented in order from features that are generally localized to more regional in scale. A flowchart outlining the order of the sections in this chapter is shown in Fig. 5.1.

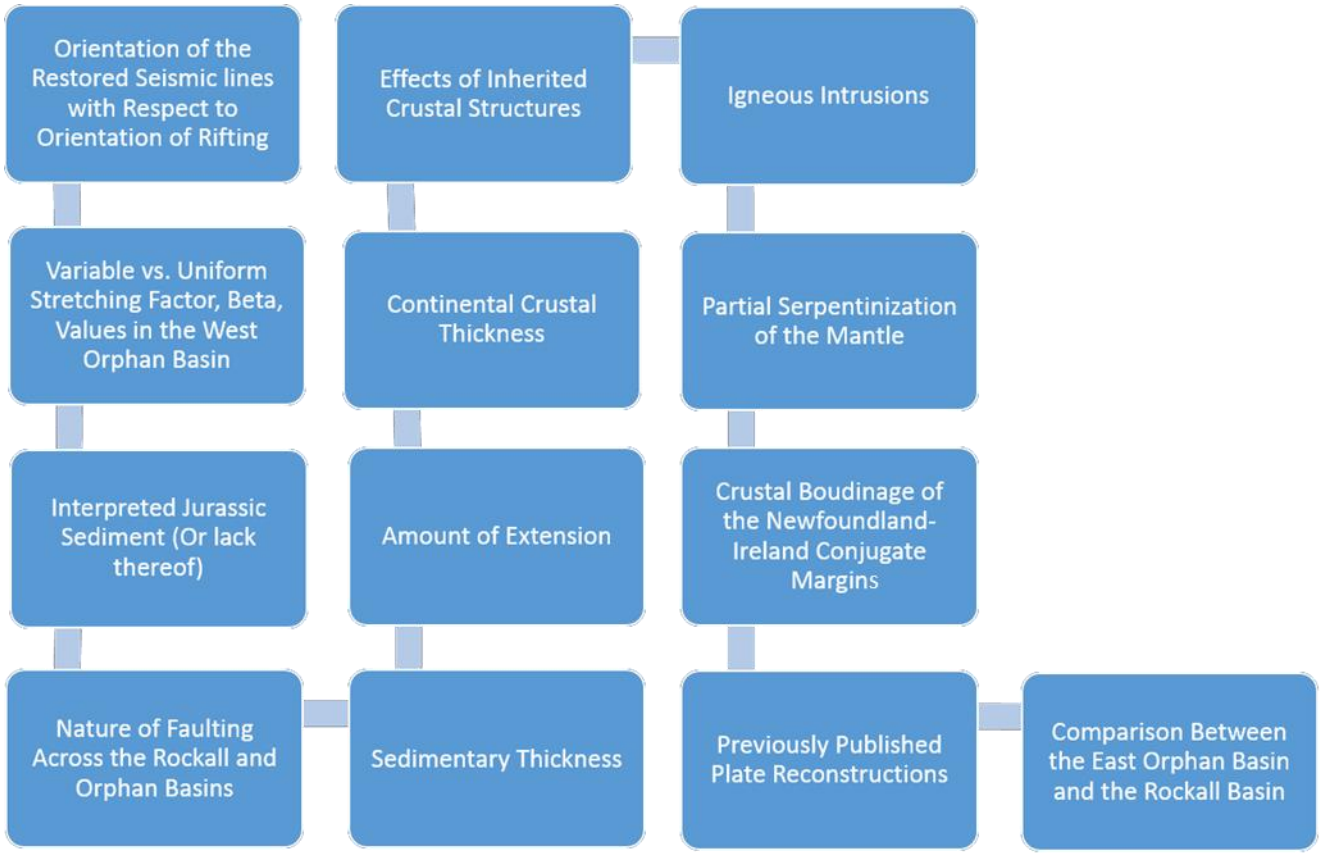


*Figure 5.1: Flowchart outlining the order of the sections in Chapter 5, from localized features to regional features.*

### 5.2 Orientation of the Restored Seismic lines with Respect to Orientation of Rifting

Due to the orientation of the seismic lines used to reconstruct the Rockall Basin and the West Orphan Basin to a pre-rift state, the basement structures and fault directions vary across the conjugate margin pair, complicating fault restoration efforts. Specifically, the main seismic line used in the West Orphan Basin, NL1, lies across strike of the rifted margin, whereas the main seismic line in the Rockall Basin, IR1, lies along strike of the rifting axis. To compensate for the variability ofthe observed faulting trends and styles across the two basins, additional intersecting seismic lines, NL2 and IR2, have been incorporated into the interpretation and analysis of this thesis. The addition of these intersecting seismic lines allows for a more direct comparison between the basins. For example, when analyzing the fault geometries of seismic line NL1, in the West Orphan Basin, a better comparison can be made in the Rockall Basin using seismic line IR2, compared to the original line, IR1. This is due to the fact that both lines NL1 and IR2 lie across strike of the rift axes, thus allowing for a more direct and accurate comparison of the fault geometries.

### 5.3 Variable vs. Uniform Stretching Factor, Beta, Values in the West Orphan Basin

The stretching factor (β) represents the ratio of final crustal thickness to the original crustal thickness and is a required parameter for the calculation of thermal subsidence. Using β value maps derived by Welford *et al.* (2012), a uniform β value of 2.0 was used across the Newfoundland-Ireland conjugate margin pair. The Rockall Basin β value map (Fig. 5.2), indicates that most of seismic line IR1 experienced a β value of 2.0, however portions of this seismic line may have experienced a higher β value, around 3.0 or 4.0. Due to the suboptimal orientation of the seismic lines used in the Rockall Basin, a lower uniform beta value was

selected. The primary seismic line in the Rockall Basin, IR1, is oriented along the strike of the rift axis, whereas the primary seismic line in the West Orphan Basin, NL1, lies across strike of the rifted margin. Thus, the lateral changes in the β value for the seismic lines of the Irish margin for this project do not provide meaningful constraints. Nonetheless, the effect of using lateral changes in the β values across the West Orphan Basin for the restoration were investigated to assess their potential significance.

Along line NL1 in the West Orphan Basin, a reconstruction with laterally variable β values was created to compare the results with the reconstruction that utilized a uniform β value of 2.0. Using the β value map adapted from Welford *et al.* (2012; Fig. 5.3), a variable β value graph was created (Fig. 5.4). These β value maps were computed based on a uniform original crustal thickness of ~30 km that may not accurately represent the pre-rift crust across the entire Newfoundland-Ireland conjugate margins. These β values were used in Move© to restore the effects of thermal subsidence during the Cenozoic and the Upper Cretaceous periods. Along seismic line NL1 in the West Orphan Basin, the lateral change in the β values resulted in a Cenozoic thermal subsidence restoration of 962 m, whereas the uniform β value of 2.0 resulted in a restoration of 740 m. Using laterally variable β values to restore the effects of thermal subsidence in the Upper Cretaceous resulted in an uplift of 1090 m, whereas using the uniform β value of 2.0 resulted in an uplift of 800 m. The restoration of seismic line NL1 using the variable β values resulted in similar final crustal thicknesses. The variable β values yielded an average pre-rift crustal thickness of 12 km, whereas the uniform β value yielded an average crustal thickness of 11.5 km. The reconstruction of seismic line NL1 using variable β values also generated a similar amount of extension as the uniform β value reconstruction, 61 km and 60 km, respectively. Similar fault geometries were also observed for the reconstruction of seismic line

NL1 using variable β values compared to a uniform β value (Fig. 5.5). Since the effects of the lateral change in the β value yielded only minimal changes in the overall reconstruction of the margin (at the regional scale), the uniform β value of 2.0 was used for both margins in this thesis. This is in agreement with the β value used in Orphan Basin in the previously published study by Gouiza *et al.* (2017). Using the same uniform β value, 2.0, in both the Rockall Basin and the West Orphan Basin also generated more consistent restorations across the conjugate margin pair.

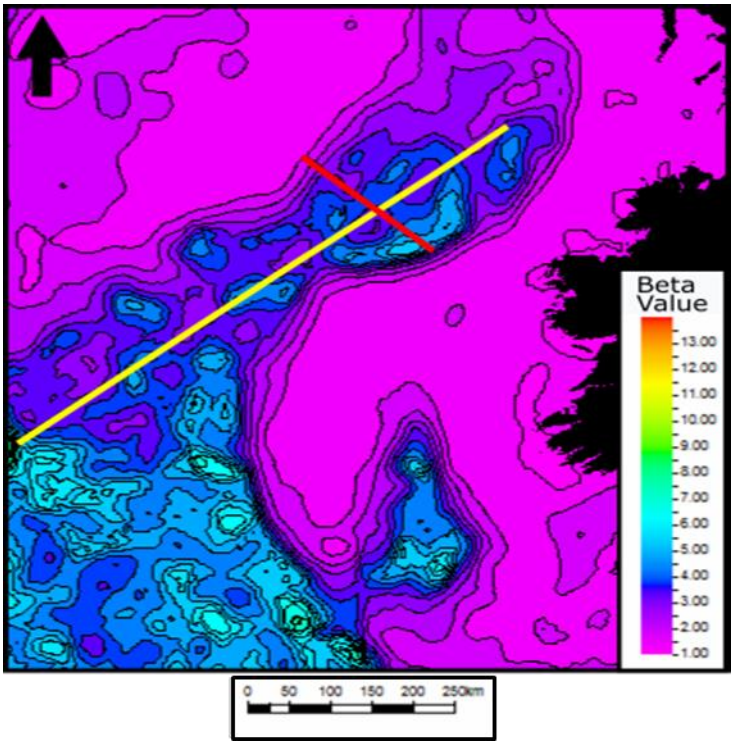


*Figure 5.2: Stretching values, β, for the Rockall Basin. The yellow line indicates seismic line IR1 and the red line indicates seismic line IR2. This figure was adapted from Welford et al. (2012).*

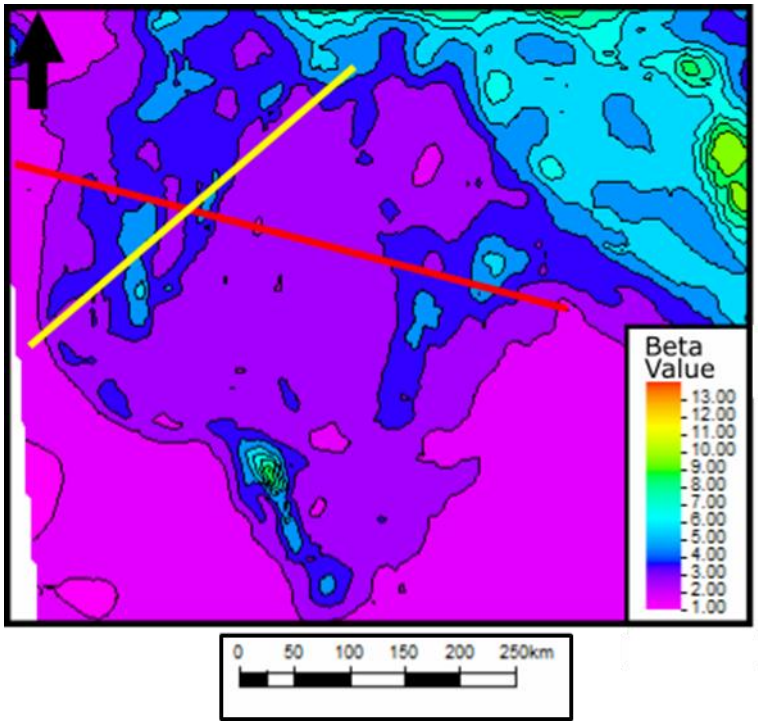


*Figure 5.3: Stretching values, β, for the Orphan Basin. The yellow line indicates seismic line NL1 and the red line indicates seismic line NL2. This figure was adapted from Welford et al. (2012).*

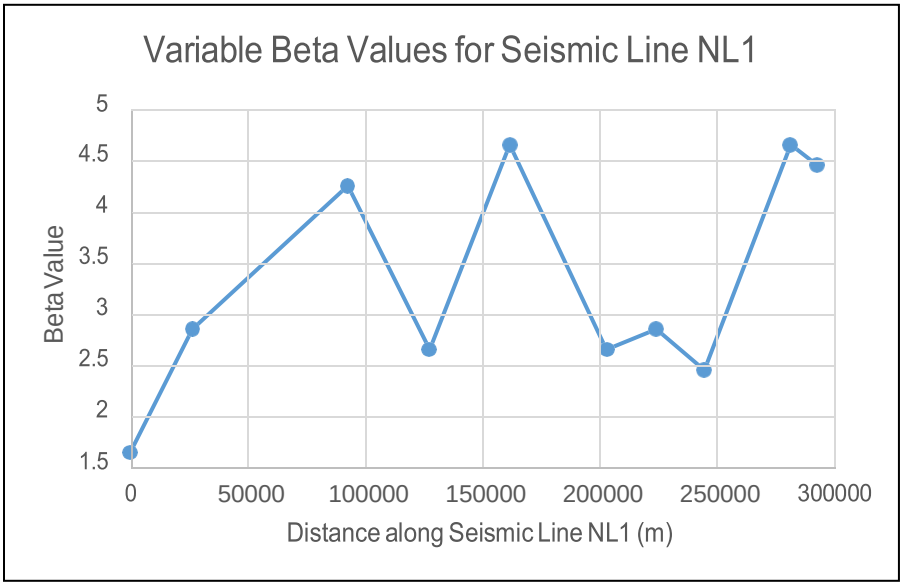


*Figure 5.4: Variable β value graph for seismic line NL1 in the West Orphan Basin showing β values versus distance along the line. Location of line shown in Fig 5 .3.*

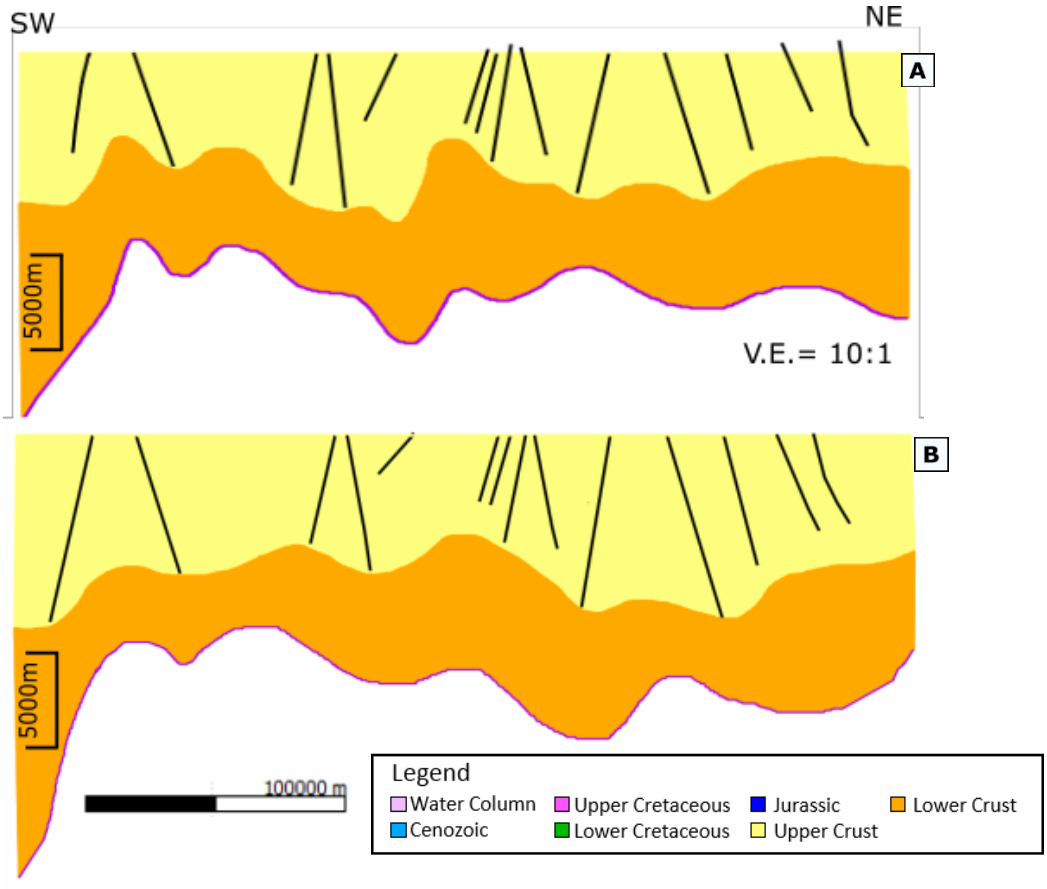


*Figure 5.5: (A) Reconstruction of seismic line NL1 using a uniform beta value of 2.0. (B) Reconstruction of seismic line NL1 using variable beta values from figure 5.4. The purple line represents the Moho proxy from Welford et al. (2012).*

## 5.4 Interpreted Jurassic Sedimentary Rocks (or lack thereof)

### 5.4.1 Orphan Basin

The amount and localization of Jurassic sedimentary formations in the West Orphan Basin has recently been debated (Lau *et al.*, 2015; Gouiza *et al.*, 2017). McCallum (personal communication, Nalcor Energy Ltd., 2018) and their prospect team have interpreted NL1 to have units of Jurassic sedimentary rocks across the entire extent of the seismic line, absent only over the basement high where the well H was drilled (location shown in Fig. 3.9). The interpretation of Jurassic sedimentary rocks in the West Orphan Basin for this thesis generally agrees with the interpretation from the team at Nalcor. For this thesis, minimal differences include missing

Jurassic sedimentary rocks over two other local basement highs in the center of the West Orphan Basin (locations shown in Fig. 3.9). Additionally, it is important to note that no wells have been drilled through units of Jurassic sedimentary rocks in the deepest extents of the West Orphan Basin, so their presence has never been proven.

Gouiza *et al.* (2017) interpreted a lack of Jurassic sedimentary rocks in the West Orphan Basin and inferred that an erosional event occurred before the second phase of rifting in the Early Cretaceous. The erosion and uplift experienced in this area is argued to be related to a failed rift system (Gouiza *et al.,* 2017). Chian *et al.* (2001) observed a large gravity anomaly high (93 mGal compared to an average of 0 mGal seaward) along the western margin of the West Orphan Basin, forming a ~100 km wide band along the outer part of the shelf. Subsidence analysis (Keen *et al.,* 1987) at well H (location shown in Fig. 3.9) indicates rapid subsidence from at least 130 to 110 Ma. This is consistent with the major pulse of extensional tectonics beginning in Middle Jurassic (160 Ma) in the Jeanne d'Arc Basin, 100 km south of the Orphan Basin. This zone may be a failed rifting center generated by continental stretching beginning in the Middle Jurassic and ending when the final Canada-Europe rift occurred in the Late Cretaceous (Chian *et al.*, 2001). As a result of the failed rift, higher density mantle material was closer to the surface which could have resulted in the erosion of Jurassic sedimentary rocks due to the added heat and uplift (Chian *et al.,* 2001). Due to the greater amount of Jurassic sedimentary rocks interpreted in this thesis, the failed rift hypothesis is not favoured.

Enachescu (2006) suggests, based on seismic data, that there is no total separation between the Orphan Basin and its southern neighbours, the Jeanne d'Arc Basin and the Flemish Pass Basin (Fig. 5.6b). Several Jurassic-aged sediment-filled troughs show communication between basins across the Cumberland Belt fault zone (location shown in Fig. 5.6a; Enachescu, 2006). These passageways have existed since the Jurassic, and possibly Triassic (Enachescu,

2006). Therefore, it is possible that the Jurassic sedimentary rocks that are currently interpreted in the Orphan Basin were deposited through sediment-filled troughs linking the Jeanne d'Arc Basin with the Orphan Basin (Enachescu, 2006).

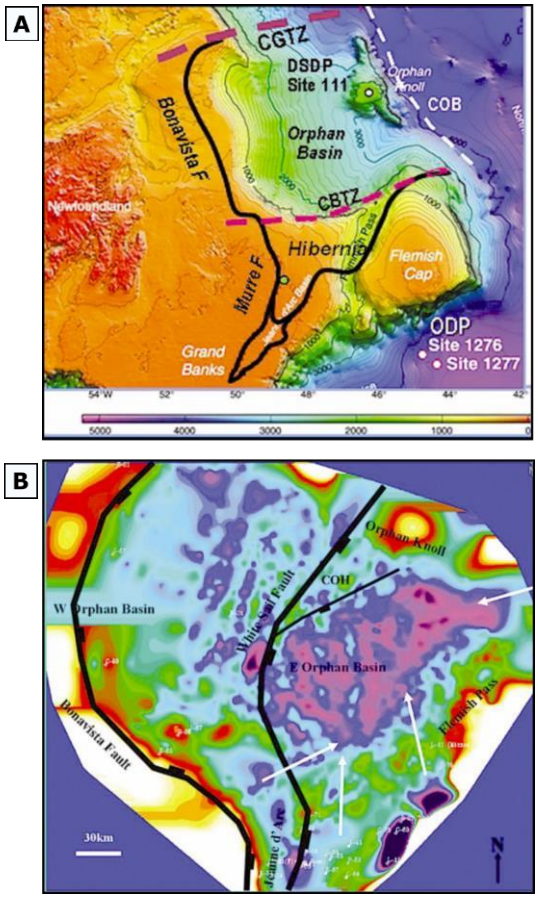


*Figure 5.6: (A) Orphan Basin location map and basin boundaries, showing location of the Cumberland Belt Transform Fault Zone (CBTZ). Other annotations include: CGTZ = Charlie Gibbs Transform Fault Zone and COB = Continent Ocean Boundary. This figure is from Enachescu (2006). (B) Time Structure of Economic Basement map over the Orphan Basin. Red and yellow are high areas outside the Orphan Basin; within the basin, green and light blues are local highs and dark blue, purple and dark purple are local lows. COH = Continental Orphan High. Arrows indicate depressions where seaway communication between the East Orphan and adjacent basins was possible during the Triassic and Jurassic.*

### 5.4.2 Rockall Basin

No Jurassic sedimentary rocks have been interpreted in the Rockall Basin in this study, due to the widespread extent of Paleogene sills that obscure the deep seismic data. However, Morewood *et al.* (2004) interpret Jurassic sedimentary rocks throughout the entire Rockall Basin. Morewood *et al.* (2004) use the results proposed by numerous authors (Shannon *et al.*, 1993; Naylor *et al.*, 1999; Stoker *et al.*, 2001; McDonnell & Shannon 2001) to interpret RAPIDS (Rockall and Porcupine Irish Deep Seismic) line 33 in the Rockall Basin (location shown in Fig. 5.7a). They identified eight layers within the seismic section: Layer 1, Late Miocene-Recent; Layer 2, Post-Middle Miocene; Layer 3, Oligocene; Layer 4, Early Tertiary; Layer 5, Cretaceous; Layer 6, Cretaceous; Layer 7, Jurassic; Layer 8, Basement (Fig. 5.7b). They use Deep Sea Drilling Project (DSDP) well 610 and a series of boreholes to place some constraints on the Neogene section in the Rockall Basin. Morewood *et al.* (2004) also use borehole data from the eastern margin of the Rockall Basin to confirm the presence of a thin Tertiary succession overlying Cretaceous and Jurassic strata (Haughton *et al.*, 2005).

RAPIDS line 33 lies approximately 100 km to the SW of seismic line IR2. Therefore, projecting the location of the potential Jurassic sedimentary rocks from RAPIDS 33 to line IR2 is only an approximation (location shown in Fig. 5.7a). Layer 1, the top of the Cenozoic unit, along RAPIDS line 33, corresponds with the top of the Cenozoic unit interpreted along seismic line IR2. Layer 5, the top of the Cretaceous unit, along RAPIDS line 33, corresponds with the top of the Upper Cretaceous unit interpreted along seismic line IR2 in the center of the basin. Toward the SE along RAPIDS line 33, the Layer 5 horizon is ~1 km deeper than the IR2 Upper Cretaceous horizon. Layer 6, representing a Mid-Lower Cretaceous horizon along RAPIDS line 33, is consistently shallower by approximately 1-1.5 km compared to the Lower Cretaceous

horizon along line IR2. Morewood *et al.* (2004) interpreted the top of Layer 7 as the top of the Jurassic unit along RAPIDS line 33. The Layer 7 Jurassic horizon lies consistently within ~ 0.5 km of the top of the Lower Cretaceous unit along line IR2 (Fig. 5.8). Layer 8, the top of the basement along RAPIDS line 33, is shallower by ~0.5-1.5 km throughout the basin, compared to the basement interpreted along line IR2. Toward the NW of seismic line IR2, the basement interpreted by Morewood *et al.* (2004) becomes shallower with a steeper gradient, compared to the interpretations for this study. This steep shallowing gradient also forces the horizons above the basement to pinch out. These discrepancies may result from the different velocity model used for the depth conversion in this study compared to the model used by Morewood *et al.* (2004). The fact that RAPIDS line 33 lies 100 km to the SW of line IR2 may also contribute to the mismatch in the interpretations for this study compared to the model generated by Morewood *et al.* (2004).

Confidence in the location of Jurassic sedimentary rocks in the model generated by Morewood *et al.* (2004) is lesser than for shallower horizons, indicated by the dashed horizon in their original image. Additionally, no wells have been drilled in the centre of the Rockall Basin to confirm or refute the presence of any Jurassic sedimentary rocks. The wells that have been drilled along the eastern margin of the Rockall Basin are in perched basins (locations shown in Fig. 2.3) and provide minimal aid in the correlation of the deep seismic data.

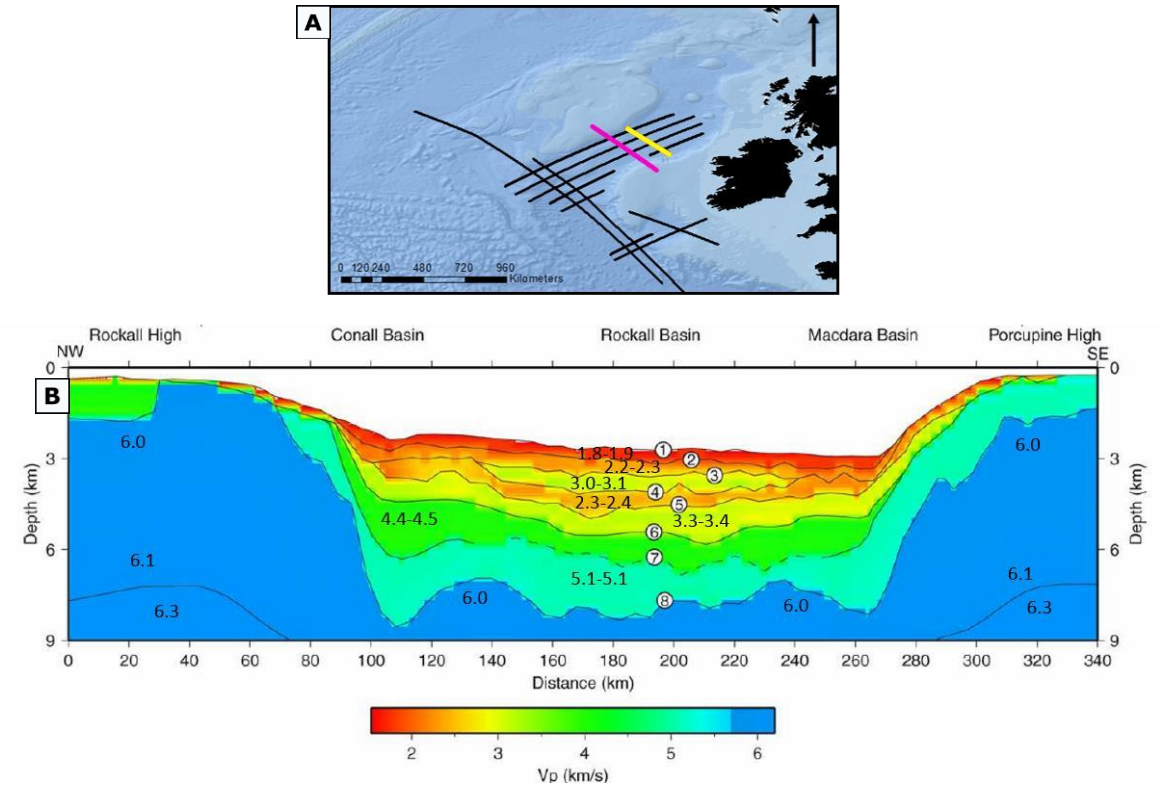


*Figure 5.7: (A) Location of RAPIDS line 33 (shown in pink) and seismic line IR2 (shown in yellow) in the Rockall Basin. (B) Velocity model of RAPIDS line 33 from Morewood et al. (2004), showing the 8 interpreted horizons and their locations in depth.*

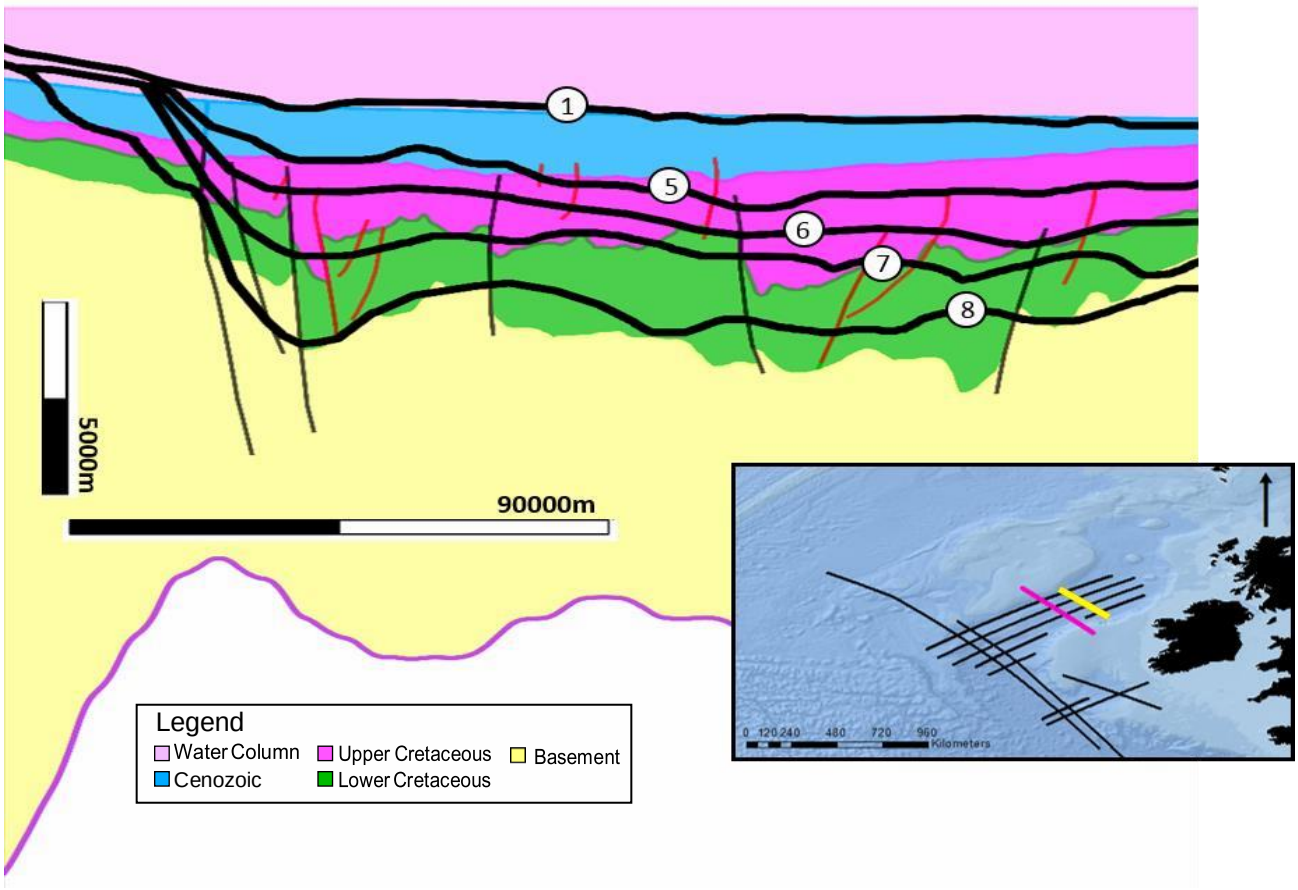


*Figure 5.8: Background image represents seismic line IR2 with interpretations and polygons from this study. Thick black lines represent interpretations from Morewood et al. (2004) of RAPIDS line 33, with circled numbers corresponding to layer numbers from figure 5.7. Inset image shows the location of RAPIDS line 33 (pink) and line IR2 (yellow) in the Rockall Basin. The purple line on the cross-section represents the Moho proxy from Welford et al. (2012).*

### 5.5 Nature of Faulting Across the Rockall and Orphan Basins

Faulting plays an important role in the formation of sedimentary basins (Lohr *et al.*, 2008). Large scale sub-surface faulting is typically identified through interpretation of 2D or 3D seismic data (McLeod *et al.*, 2000). Faults are best imaged on seismic reflection data when the seismic line is collected perpendicular to the strike of the fault surfaces (Tearpock & Brischke, 2010), as this orientation is generally across the rift axis (Ebinger *et al.*, 1999). In theory, comparing the nature and style of rifting in both the Rockall and West Orphan basins should provide additional information to aid in determining if the basins once formed a singular,

continuous Mesozoic basin.

The style and nature of faulting across the Newfoundland-Ireland conjugate margins is difficult to compare due to the orientation of the primary seismic lines with regards to the rift axis. As previously stated, seismic line NL1, in the West Orphan Basin, lies across the strike of rifting, whereas seismic line IR1, in the Rockall Basin lies along the strike of rifting. Therefore, seismic line IR2, in the Rockall Basin, is compared to seismic line NL1, in the West Orphan Basin because both lines are perpendicular to the axis of rifting.

In the West Orphan Basin, approximately four NE dipping fault blocks are observed toward the northeastern extent of seismic line NL1 (Fig. 5.9a). Three prominent fault bounded basement highs are also observed throughout the section, the largest of which is located on the continental shelf, toward the southwestern end of the section (Fig. 5.9b). There are no Jurassic sedimentary rocks interpreted over any of these basement highs, likely due to a large scale erosional event (Gouiza *et al.*, 2017). A fault-bounded seamount is interpreted in the center of seismic line NL1 (discussed later in section 5.10; Fig. 5.9c). To the northeast of the seamount, a graben structure is also interpreted along the section (Fig. 5.9c). The large variety in the fault characteristics are likely the result of the numerous rift episodes and changes in rift directions that the Orphan Basin underwent during its development (Enachescu *et al.*, 2004).

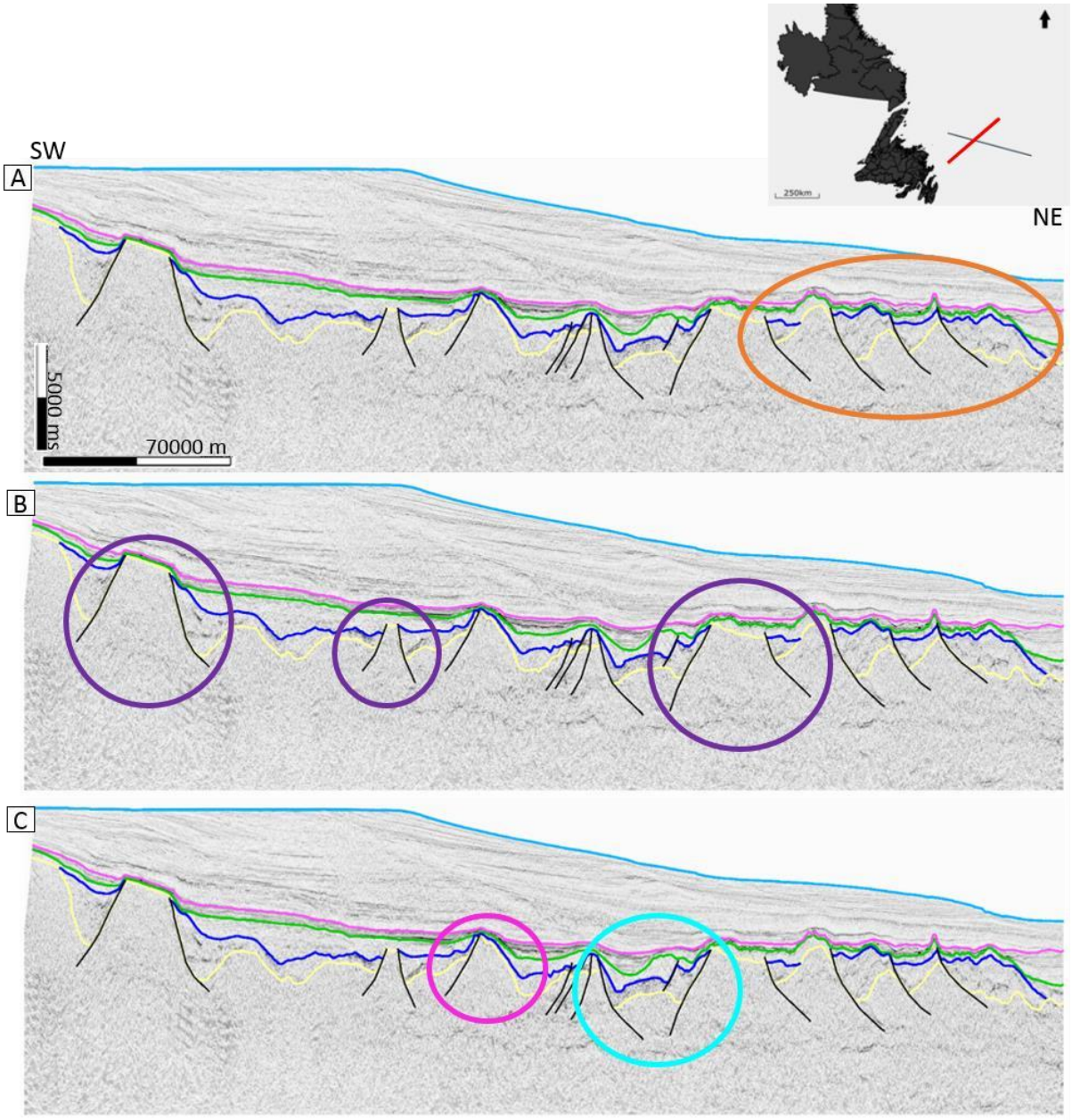


*Figure 5.9: Interpreted seismic line NL1 in the West Orphan Basin. (A) Orange oval shows the location of the NE dipping fault blocks. (B) Purple circles show the location of the prominent basement highs. (C) Pink circle shows the location of the fault-bounded seamount. The turquoise circle shows the location of the graben. Location of seismic line shown by red line on inset map.*

In the Rockall Basin, along line IR2, four SE tilted/near vertical fault blocks are observed at the NW end of the line (Fig. 5.10). Along the center of the section two vertical faults are interpreted (Fig. 5.10). Toward the SE end of the line, four NW dipping faults are interpreted (Fig. 5.10). The fault characteristics observed in the Rockall Basin are likely the results of the

numerous rift episodes that the basin experienced during its formation (Shannon, 1991).

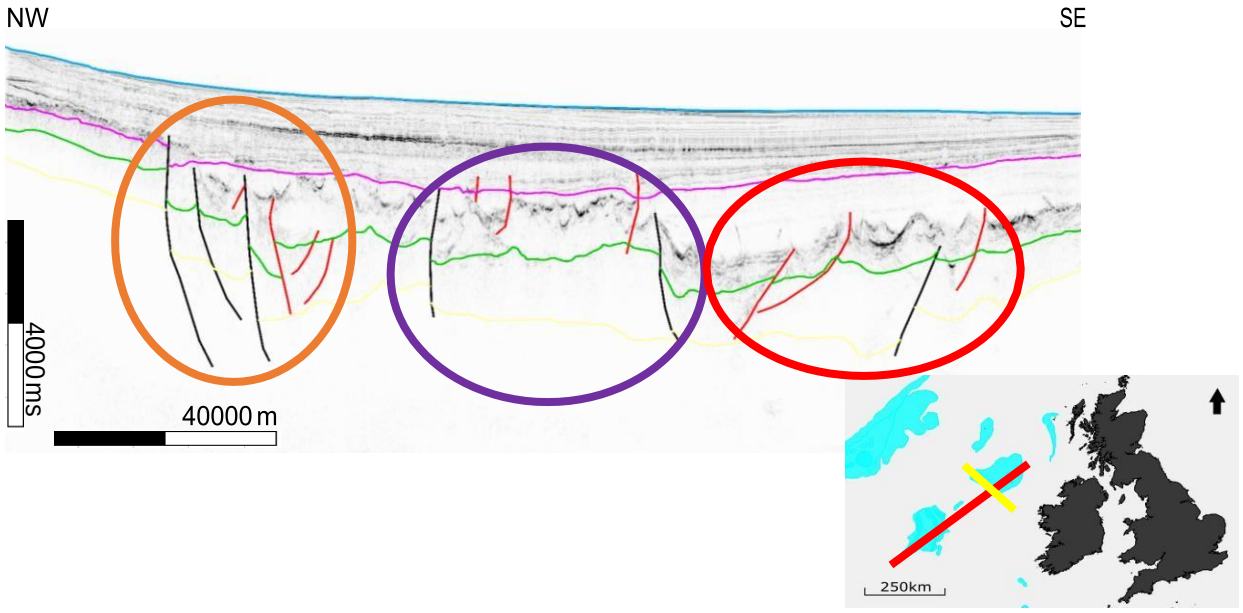


*Figure 5.10: Interpreted seismic line IR2 in the Rockall Basin, location shown on inset map as the yellow line. Orange circle indicates the location of the SE tilted faults blocks. The purple circle indicates the location of the near vertical faults. The red circle indicates the location of the NW dipping fault blocks. Location of seismic line shown by yellow line on inset map.*

Overall, few similarities in faulting style are observed perpendicular to the strike of rifting across the Newfoundland-Ireland conjugate basins. Seismic lines NL1 and IR2 both exhibit tilted fault blocks, to a varying degree. However, no seamounts, basement highs, or grabens are observed on the Irish margin. Such structures are likely present in the Rockall Basin and have not been captured by the seismic reflection data due to the obscuring sills. It isdifficult with only one seismic line in the appropriate direction, across a basin that is 1100 km long, to accurately sample the nature of the faulting within the entire basin. Therefore, while there are a few similarities in faulting style and characteristics observed across the basins, the nature of the faulting provides little evidence as to the existence of a possible continuous basin formed from the Rockall Basin and the West Orphan Basin during the Mesozoic.

### 5.6 Sedimentary Thickness

The average amount of post-rift sedimentary rock, calculated from the addition of the Cenozoic and Upper Cretaceous sedimentary units, was measured in Move©. In the West Orphan Basin, an average amount of ~ 3.7 km of post-rift sedimentary rock accumulated after rifting. In the Rockall Basin, an average amount of ~ 3.5 km of post-rift sedimentary rock accumulated after rifting. Focusing on the large-regional scale, both basins experienced a similar amount of post-rift sedimentary rock accumulation, even though the basins were drifting apart during this time. However, the average thickness of the post-rift units provides little insight into the possible connection between the two basins.

The average amount of syn-rift sedimentary rock, calculated from the Lower Cretaceous and, where applicable, the addition of the Jurassic sedimentary unit, was measured in Move©. In the West Orphan Basin, an average of ~2.4 km of syn-rift sedimentary rock accumulated during rifting. In the Rockall Basin, an average amount of ~2.4 km of syn-rift sedimentary rock was deposited. Both the West Orphan Basin and the Rockall Basin accumulated the same average amount of sedimentary rock while rifting was occurring. The similarity in the syn-rift sedimentary thicknesses implies that both basins were subjected to similar processes and accumulation rates during rifting. It also provides evidence that the Rockall Basin and the West Orphan Basin possibly formed a large continuous Mesozoic rift system.

To check on the validity of these interpreted thicknesses, the post-rift and syn-rift thicknesses of sedimentary rock were added together and compared to the known amount of sedimentary cover in each basin. Within the West Orphan Basin, according to Gouiza *et al.* (2017), there is approximately ~5-6 km of sedimentary rock. The thickness of the post-rift sedimentary rock and the syn-rift sedimentary rock accumulated in the West Orphan Basin, were

added together, ~3.7 km and ~2.4 km, respectively. The combined sedimentary thickness in the West Orphan Basin is ~ 6.1 km, which is consistent with the value suggested by Gouiza *et al.* (2017). The thickness of the post-rift sedimentary rocks and the syn-rift sedimentary rocks in the Rockall Basin were added together, ~3.5 km and ~2.4 km, respectively. The combined sedimentary thickness in the Rockall Basin is ~ 5.9 km, which is only slightly lower, than the ~6-7 km thickness suggested by Hauser *et al.* (1995) and O'Reilly *et al.* (2006). The overall similarity in the average thickness of the syn-rift sedimentary rock in the Rockall and West Orphan basins provides convincing evidence that the two basins were connected during the Mesozoic syn-rift phase.

### 5.7 Amount of Extension

The amount of extension observed from faulting, in both the Rockall and West Orphan basins, was measured in Move©. The distance from the edge of the fully restored upper crustal section to the original extent of the seismic data was measured in Move©. The distance measured represents the amount of extension, based solely on faulting, that each basin experienced throughout the reconstruction process. In the West Orphan Basin, the amount of extension observed along seismic line NL1, lying across the rift axis, was 60 km. However, the West Orphan Basin is approximately 100 km wide (Gouiza *et al.*, 2015). Therefore, the model generated for the West Orphan Basin, underestimated the amount of extension by approximately 40%. The primary seismic line in the Rockall Basin, IR1, was not used to calculate the extension in the basin because this seismic line lies along the axis of rifting. Since basins open across the rift axis and not along the rift axis, seismic line IR1 was excluded and seismic line IR2 was used instead. The amount of extension calculated along seismic line IR2 was 7.3 km. O'Reilly *et al.*

(2006) and Pérez-Gussinyé & Reston (2001) estimated that the Rockall Basin extended approximately 150-200 km. Therefore, the model generated in the Rockall Basin underestimated the amount of extension by approximately 95%.

Numerous authors have reported similar extensional discrepancies across rifted margins (Driscoll & Karner, 1998; Sibuet, 1992; Davis & Kusznir, 2004; Gouiza *et al.*, 2017). Explanations for the extension discrepancy fall into two broad categories. One suggests that only a fraction of the faulting has been recognized and thus the brittle extension has been massively underestimated (Reston, 2005). The other category proposes that the observed faulting is close to the total amount of brittle extension and that the lower crust has locally been thinned far more than the brittle upper crust (Sibuet, 1992; Driscoll and Karner, 1998; Kusznir et al., 2005), a mechanism known as depth-dependent stretching (DDS) (Reston, 2007b).

The first explanation for the discrepancy in extension is that only a fraction of the faulting has been recognized. One possible explanation for the lack of interpreted faults is that the youngest faults cut across earlier faults, obscuring them. This is known as polyphase faulting (Reston, 2007b). Normal faults form at dips of ~65º–70°, like those seen in both the Rockall and West Orphan basins. The faults then rotate during subsequent extension and lock up at dips of >30° (Reston, 2007b). These faults correspond to a stretching factor of just below 2 (the value assumed for both the Rockall and West Orphan basins) and are then replaced by a second generation of faults (Reston, 2007b; Fig. 5.11). However, Gouiza *et al.* (2017) state that fault geometries, syn-rift stratigraphy and basement structures imaged on the seismic data do not provide evidence that polyphase faulting occurred in the Orphan Basin.

An equally effective way of producing an apparent extensional discrepancy would be failure to recognize large-offset normal faults that flexurally rotate to sub horizontal (Lavier &

Manatschal, 2006) and may form the top of the basement over tens of kilometres (Reston, 2007b). The dimensions of such faults can easily be overlooked on seismic data. Furthermore, both the flexural unloading of the footwall and continuing extension can lead to polyphase faulting, cutting the exhumed footwall into smaller blocks (Reston, 2007b). Distributed deformation, sometimes described as sub seismic faulting, may lead to the amount of extension being underestimated by as much as 50% (Marrett & Allmendinger, 1992).

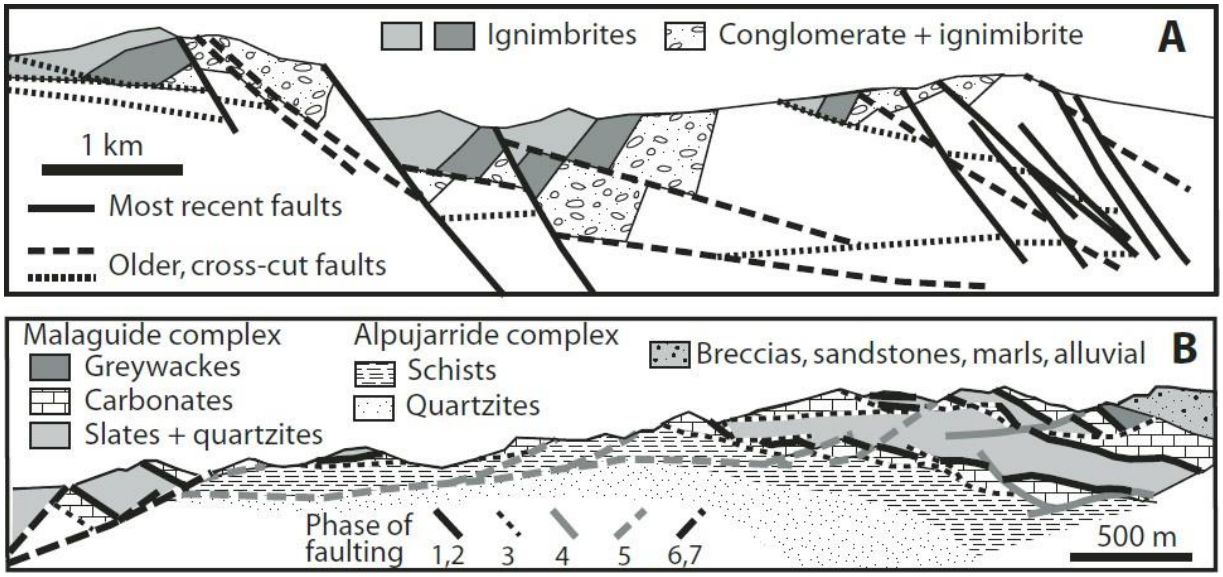


*Figure 5.11: Examples of polyphase faulting exposed on land (no vertical exaggeration). (A) Simple polyphase faulting produces complex geometries. (B) Radial extension has thinned this section from 20 km to 1 km through 7 phases of extensional faulting. Note that earlier faults tend to define lithological contacts and so would not be easily recognizable as faults on seismic data (Reston, 2007b).*

The second explanation for the extensional discrepancy is a mechanism known as depth-dependent stretching (DDS; Reston, 2007b). A degree of crustal DDS is to be expected as it is unlikely that the crust would extend perfectly uniformly. However, the problem with invoking DDS to explain the extension discrepancy is the extreme amount of DDS required (Reston, 2007b). Davis & Kusznir (2004) state that an extensional discrepancy may be resolved by the presence of a region farther toward the ocean with an extension discrepancy of opposite polarity

so that the equality of the horizontal integral of extension is maintained. This would require that somewhere oceanward the upper continental crust is strongly stretched and thinned by an amount greater than deeper material (Davis & Kusznir 2004). Gouiza *et al.* (2017) compared lower and upper crustal thinning against whole crustal thinning and showed that upper crustal thinning factors are higher for the continental shelf and the Flemish Cap (i.e., domains with the thickest crust), whereas lower crustal thinning factors are higher in the East and West Orphan basins (i.e., domains with the thinnest crust). This is consistent with the findings of Lau *et al.* (2015) and Watremez *et al.* (2015) who constrained the Orphan Basin crust using wide-angle seismic profiling. These observations are clear evidence of DDS within the crust. These observations are also indicative of ductile flow within the lower crust, mainly underneath domains of localized upper crustal brittle deformation, namely the East and West Orphan basins (Gouiza *et al.,* 2017). In the Rockall Basin, during the Eocene, the observed rapid thermal subsidence is consistent with an episode of Late Cretaceous-Early Tertiary DDS (Hauser *et al.,* 1995; Tate *et al.,* 1999).

### 5.8 Continental Crustal Thickness

The initial crustal thickness of the Newfoundland-Ireland conjugate margins was assumed to be 30 km (Welford *et al.,* 2012; Gouiza *et al.,* 2017). The average pre-rift crustal thickness, based on the Move© models generated in this study, for the West Orphan Basin, was 12.3 km and was 8.5 km in the Rockall Basin. This discrepancy between the assumed and observed pre-rift crustal thickness is possibly the result of missing deformation that was not accounted for (i.e., polyphase faulting and DDS, as previously discussed). Over time, younger faults imprint over older faults, therefore erasing the rifting history that was preserved in them (Reston, 2007a). The reconstructions done in this study can only restore the faults that are visible

on the seismic data. As a result, older faults and sub-parallel faults, generated by large-scale folding, are not interpreted and therefore, cannot aid in the restoration process.

Alternatively, the original assumption that the pre-rift continental crust was initially 30 km thick across the Newfoundland-Ireland conjugate margins may be inaccurate. The unstretched crust beneath mainland Ireland is approximately 30 km thick (Lowe & Jacob 1989; Hauser *et al.,* 2008). Similarly, the crust beneath the Porcupine Bank (O'Reilly *et al.,* 2006) and the Rockall Bank (Vogt *et al.,* 1998) is suggested to be 30 km thick. Since there is no evidence for significant crustal extension in these areas, Welford *et al.* (2012) regarded 30 km as the thickness of the unstretched crust for the Irish margin. On the Newfoundland margin, the areas of unstretched crust are variable (30 km beneath Flemish Cap (Funck *et al.,* 2003); 36 km beneath the Grand Banks (Lau *et al.,* 2006); 40 km for the onshore Avalon zone, 45 km for the Proterozoic Grenville province of Western Newfoundland (Hall *et al.,* 1998; Welford *et al., 2012*)). Welford *et al.* (2012) used the thickness of the crust under Flemish Cap to assume that the initial crustal thickness in the Orphan Basin was approximately 30 km. However, it is possible that the initial thickness of the continental crust was different than previously thought.

### 5.9 Effects of Inherited Crustal Structures

Another source of uncertainty in quantifying the characteristics of the pre-rift crust is inheritance. Manatschal *et al.* (2015) state that for hyperextended rift systems that developed over the Variscan lithosphere, like the Newfoundland-Ireland conjugate margins, inherited structures were important in controlling strain on a local scale and very early in the rift system. They also conclude that mantle composition and mantle processes occurring before and during rifting may control the rheology of the mantle, the mantle budget, the thermal structure and the localization of deformation during late stages of continental crust attenuation and lithospheric

breakup, while early stages are controlled by upper crustal inherited structures (Manatschal *et al.,* 2015). The Mesozoic North Atlantic rift formed on remnants of the Palaeozoic Caledonian–Appalachian orogeny, as well as the Variscan orogeny, which resulted in the closure of the Iapetus Ocean (Dewey & Kidd, 1974). This closure led to continental collision, crustal and probably lithospheric thickening (imbrication of multiple terranes), crustal uplift, and erosion (Williams 1984; 1995; McKerrow *et al.,* 2000). The closing of the Iapetus Ocean also stitched together the distinct basement terranes that make up the Newfoundland and Irish margins considered in this study (Haworth & Keen, 1979; Williams 1984; 1995). Migration of rifting suggests that variations in thickness and/or rheology, inherited from the pre-Mesozoic Caledonian–Appalachian orogeny, may have played a crucial role in the tectonic evolution of the Mesozoic North Atlantic basins (Gouiza *et al.,* 2017) (i.e., the Rockall and West Orphan basins).

### 5.10 Igneous Intrusions

The Newfoundland margin is widely regarded as a nonvolcanic/magma poor rifted margin (Reston, 2009). Magmatic activity appears to have been minimal within the Orphan Basin, although some studies suggest the presence of Cretaceous igneous features, such as seamounts, along the outer edge of Orphan Knoll and in the West Orphan Basin (Grant & McAlpine, 1990; Enachescu *et al*., 2005; Whittaker *et al*., 2012; Pe-Piper *et al*., 2013). The Charlie Gibbs Volcanic Province (CGVP) is located to the north of the West Orphan Basin (location shown in Fig. 5.17). The CGVP likely formed during the Late Cretaceous, as seafloor spreading propagated northward into the region and hot asthenosphere experienced decompression melting as it came closer to the surface (Keen *et al.,* 2014). Keen *et al.* (2014) suggest that, since there is no evidence of an anomalously hot mantle below the region, melting was focused within the near-vertical fault zone complex created by the Charlie Gibbs Fracture

Zone (CGFZ). Large strains near the western termination of the CGFZ may have further concentrated melt in that region.

Seismic lines NL1 and NL2 lie to the south of the CGVP, therefore, minimal seamounts were interpreted in the West Orphan Basin. However, Alex Peace (personal communication, 2018), interpreted multiple seamounts in the area. In this study, in the center of seismic line NL1, near the junction with NL2, a large potential seamount was interpreted based on the onlapping nature of the shallower horizons toward the seamount. This seamount was bounded to the SW by a singular fault (Fig. 5.12). The location of this interpreted seamount agrees with that of the Peace interpretation (Fig. 5.12), however that interpretation does not include the bounding fault. Toward the northeastern extent of seismic line NL1 (locations shown in Figs. 5.13 and 5.14), numerous fault bounded potential seamounts were interpreted in this study, compared to the un-faulted seamounts interpreted in the area by Peace.

Keen *et al.* (2014) interpreted and mapped numerous seamounts within the CGVP (Fig. 5.15). Their interpretation of the seamounts on the seismic data occasionally included faults bounding one side of the seamounts (Fig. 5.16). These fault-bounded seamounts interpreted by Keen *et al.* (2014) are very similar to the seamounts interpreted for this study.

Interpretation of seismic data is highly subjective and while it is important to recognize alternative interpretations of the data, for this project the areas of interest in the NE of the West Orphan Basin continue to be interpreted as fault blocks or possibly fault-bounded seamounts. Additionally, the results of the reconstruction of the West Orphan Basin would only be mildly affected by altering the interpretations.

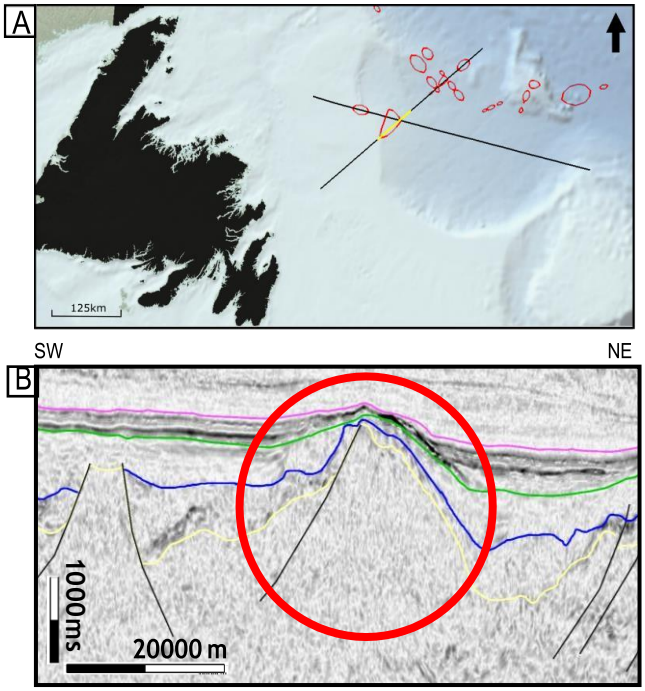


*Figure 5.12: (A) Seismic lines NL1 and NL2 in the Orphan Basin (black lines). Red polygons indicate the location of interpreted seamounts by Alex Peace (personal communication, 2018). Yellow line indicates the zoomed in location of B. (B) Zoomed in view of seismic line NL1 depicting the interpreted seamount.*

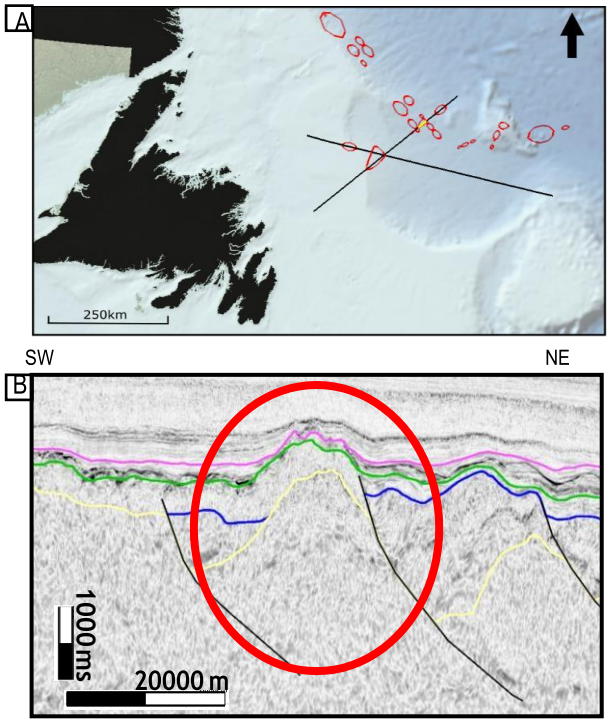


*Figure 5.13: (A) Seismic lines NL1 and NL2 in the Orphan Basin (black lines). Red polygons indicate the location of interpreted seamounts by Alex Peace (personal communication, 2018). Yellow line indicates the zoomed in location of B. (B) Zoomed in view of seismic line NL1. Red circle indicates the extent of the interpreted seamount.*

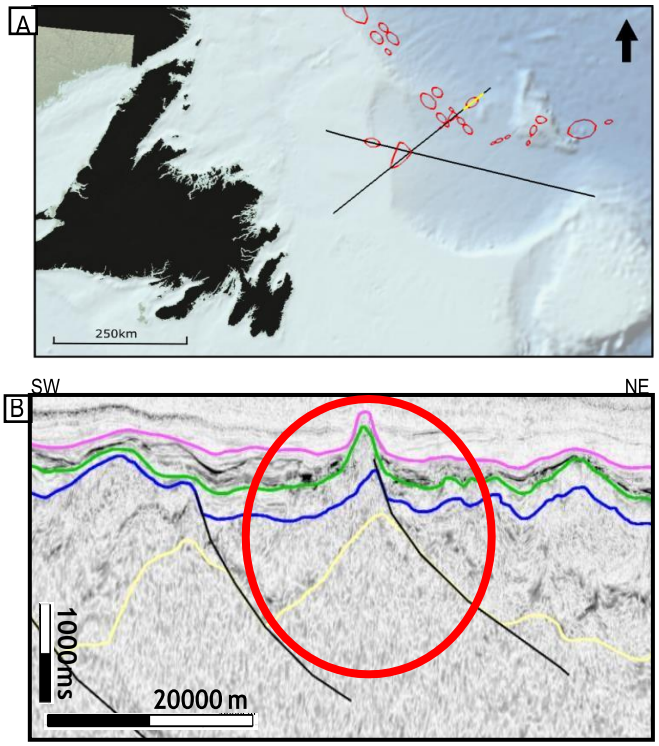


*Figure 5.14: (A) Seismic lines NL1 and NL2 in the Orphan Basin (black lines). Red polygons indicate the location of interpreted seamounts by Alex Peace (personal communication, 2018). Yellow line indicates the zoomed in location of B. (B) Zoomed in view of seismic line NL1. Red circle indicates the extent of the interpreted seamount.*

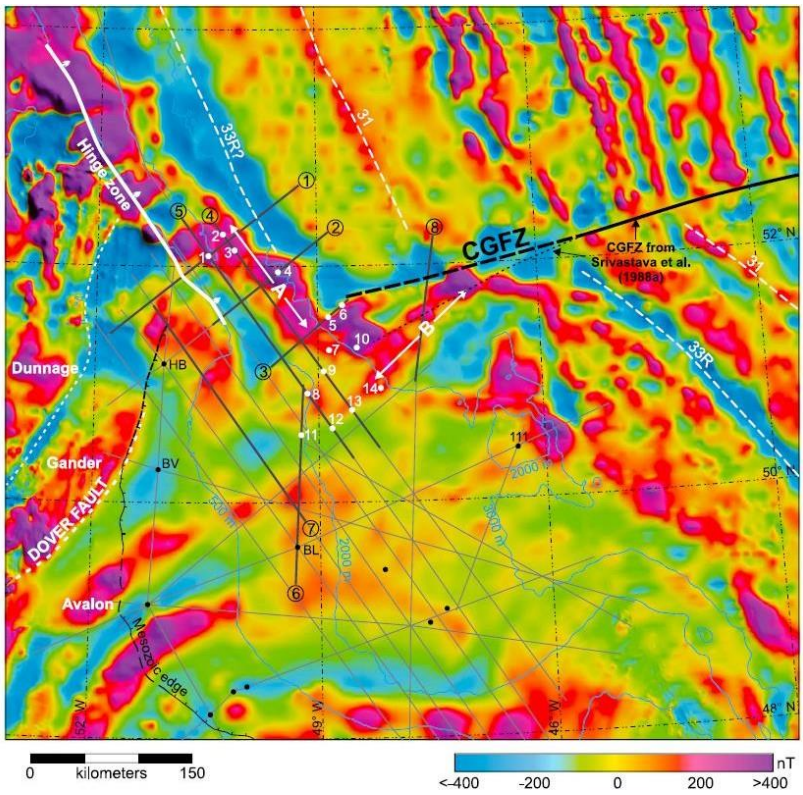


*Figure 5.15: Magnetic anomaly map of the Orphan Basin. The numbered white dots represent the apexes of the seamounts in the CGVP. The grey lines represent the seismic lines in the area. This figure is from Keen et al. (2014).*

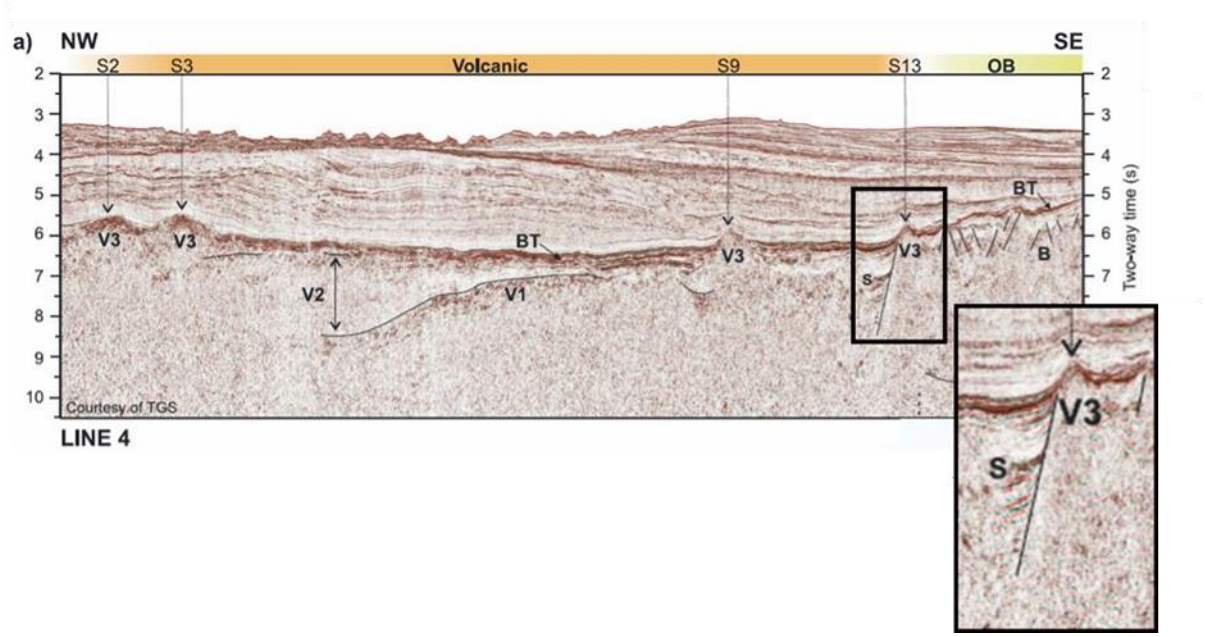


*Figure 5.16: Interpreted seismic line 4 from Keen et al. (2014). Zoomed in box shows seamount number 13 (location shown in Fig.5.15), of a fault-bounded seamount.*

A number of episodes of igneous activity have been recorded in the Rockall Basin, primarily in the Early Cretaceous and the Paleogene (Shannon *et al.,* 2006). The Barra Volcanic Ridge System (BVRS) has been interpreted as one of the main Early Cretaceous volcanic centers in the Irish North Atlantic (Shannon *et al.,* 2006). Paleogene igneous activity is represented in the Rockall Basin by a series of volcanic cones along the eastern margin of the basin (Haughton *et al.,* 2005) and a set of sills, dykes and lava flows in the central part of the basin (Shannon *et al.,* 2006).

Keen *et al. (*2014) suggest that the CGVP on the Newfoundland margin may correspond to an equivalent magnetic province in the Rockall Basin region, the BVRS. They go on to suggest that these conjugate features are similar in shape and almost coalesce at Chron 34 (Fig. 5.17). As Srivastava *et al.* (1988) demonstrated, one of the Barra Volcanic Ridges in the southern Rockall Basin is collinear with the eastern end of the CGVP at Chron 34 and these spatial correlations of the two conjugate provinces suggest a common origin (Keen *et al.,* 2014). Scrutton & Bentley (1988) suggested that the BVRS represents incipient seafloor spreading in the southern Rockall Basin, emplaced along faults bounding basement highs (Gernigon *et al.,* 2004). Similarly, Keen *et al.* (2014) suggested that the CGVP used older faults as conduits to focus magmatism, possibly along reactivated Appalachian/Caledonian trends.

Keen *et al.* (2014) propose a history for the development of the Newfoundland-Ireland conjugate margins beginning in the Early Cretaceous. During the Early Cretaceous, the Rockall and West Orphan basins were actively rifting and represented a linked system (Ady & Whittaker, 2012). The southern boundary of the CGVP and a branch of the BVRS may represent an accommodation zone within the West Orphan/Rockall Basin system that developed through reactivation of pre-existing faults (Keen *et al.,* 2014). Rifting ended in Aptian time in the West

Orphan and Rockall basins. From Aptian to Santonian time there was a major reorganization of plates as seafloor spreading propagated northward from the Newfoundland Basin in the south to the CGVP in the north (Keen *et al.*, 2014). By Santonian time, plate motions were accommodated by transform motion along the CGFZ (Keen *et al.*, 2014). The fault zone along the trend of the southern boundary of the CGVP was no longer active as movements shifted to align with the plate motion direction along the CGFZ (Keen *et al.*, 2014).

Overall, the similar structure and location of both the CGVP and the BVRS are suggestive of a possible Mesozoic connection between the Rockall and West Orphan basins (Fig. 5.17). The tectonic plate reconstruction performed by Skogseid *et al.* (2010), as well as the developmental history of the region provided by Keen *et al.* (2014), provide further evidence to support this possible connection.

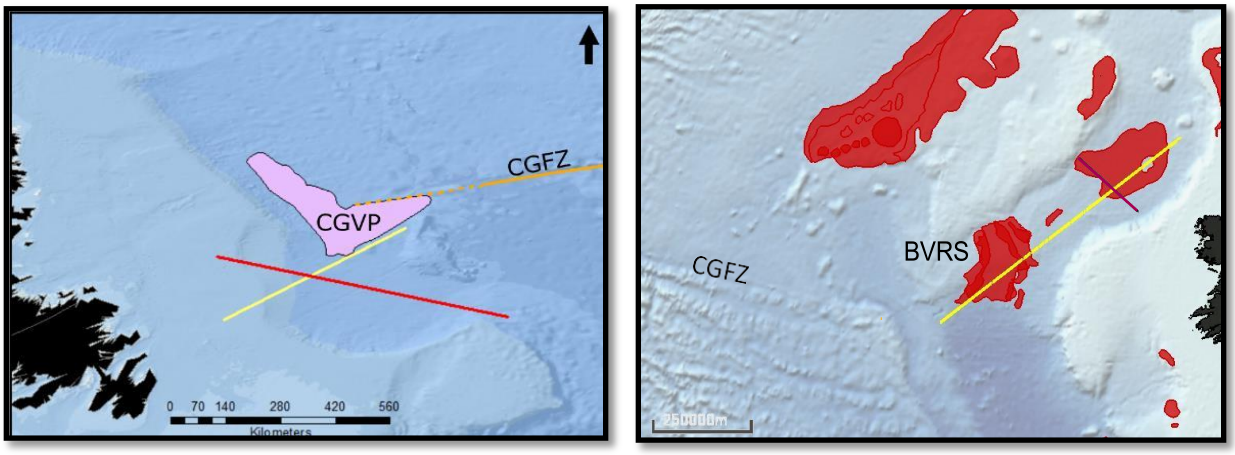


*Figure 5.17: Location of the Charlie Gibbs Fracture Zone (CGFZ) across the Newfoundland-Ireland conjugate margin pair. (Left) the location of the Charlie Gibbs Volcanic Province (CGVP) and its relation to the CGFZ, the West Orphan Basin and the seismic lines of this study. (Right) the location of the CGFZ and its relation to the Barra Volcanic Ridge System (BVRS), the Rockall Basin and the seismic lines of this study.*

### 5.11 Partial Serpentinization of the Mantle

Serpentinization of the mantle occurs along hyper-extended continental margins when large amounts of syntectonic cooling during extension lead to the downward migration of the brittle/ductile transition zone in the crust and the propagation of faults into the shallow mantle lithosphere (O'Reilly *et al.,* 1996). The lowered brittle/ductile transition, as well as the deeper faults, facilitate the seawater circulation necessary to serpentinize the shallow mantle (O'Reilly *et al.,* 1996). The interaction of the water and the mantle must occur near the end of the syn-rift phase of development, when extensional fractures are open and provide permeability (O'Reilly *et al.,* 1996). Rheological changes in the lithosphere as rifting progressed likely played a key role in the process of fracture growth (O'Reilly *et al.,* 1996).

O'Reilly *et al.* (1996) observed a shallow low-velocity layer within the mantle beneath the Rockall Basin. They presented a differential stretching model for the development of the Rockall Basin that explained the shallow mantle structure as a zone of partially serpentinized upper mantle peridotites. O'Reilly *et al.* (1996) infer that syntectonic heat loss led to the rheological coupling between the crust and sub-crustal lithosphere as the primary (pre-extensional) intracrustal brittle/ductile transition zone was destroyed. Finally, they conclude that this coupling led to vertical fracture propagation through the Moho into the shallow mantle, facilitating seawater circulation and hydration of the shallow mantle, thus serpentinizing the mantle.

Welford *et al.* (2010) generated a 3-D density anomaly model of the Irish Atlantic continental margin from a regional inversion of free air gravity data. Along the northeast trending axis of the Rockall Basin, Welford *et al.* (2010) found that the Moho depth from both the seismic data and the gravity inversion shows a gradual deepening from 12 km down to 18 km

in the northeast. The variation may correspond to different amounts of igneous intrusions, possibly related to the formation of oceanic crust (Scrutton 1986; Bentley & Scrutton 1988), exhumed serpentinized mantle (O'Reilly *et al.,* 1996) or different basement/crustal terranes (Welford *et al.,* 2010).

In contrast, for the Orphan Basin, there is no evidence of a zone of partially serpentinized mantle beneath the thinned crust (Chian *et al.,* 2001; Lau *et al.,* 2015). The limited crustal scale seismic refraction data in the West Orphan Basin show significant thinning of the crust to 6-8 km, but typically unaltered mantle velocities are modelled beneath the crust (Chian *et al.,* 2001). The resolved serpentinized mantle beneath the Rockall Basin (O'Reilly *et al.,* 1996; 2006; Reston *et al.,* 2001) is thought to have required an initially strong lithosphere based on recent geodynamic models (Huismans & Beaumount 2011; Welford *et al.,* 2012). The lack of evidence for serpentinized mantle beneath the Orphan Basin, based on more limited seismic refraction modelling (Chian *et al.,* 2001), would require a weak lower crustal layer and rupture within the mantle lithosphere based on the same geodynamic models (Huismans & Beaumount 2011; Welford *et al.,* 2012).

The lack of serpentinized mantle beneath the Orphan Basin does not necessarily mean that its crust differs greatly from the crust onthe Irish margin, but rather that the Irish crust failed more abruptly as the serpentinized mantle beneath it acted as a ductile detachment (Welford *et al.,* 2012). Relatively weaker lower crust may exist on both margins, with the main difference between rifting styles ofthe two margins being due to the localization of rifting and the ability of the rifting to generate crustal-scale faults that could allow seawater to propagate into the uppermost mantle (Welford *et al.,* 2012). The results of the study carried out by Welford *et al.* (2012) suggest a fundamental difference in the rheological properties of the lithosphere between

the Orphan Basin and the Rockall Basin. They infer that, although the rheological variations may be due to differences in the original crustal compositions of the margins, it is also possible that the rheological variations developed because of the manner in which rifting was focused on each margin. Ultimately, focused rifting on the Irish margin led to deeper fractures, highly thinned crust and serpentinization of the mantle between strong, rheologically more robust, blocks (Welford *et al.,* 2012). On the Newfoundland margin, extension was accommodated over a broader area, therefore not allowing faults to penetrate as deep, with the weakest crustal layer controlling the formation of the massive Orphan Basin without any significant serpentinization of the uppermost mantle (Welford *et al.,* 2012).

### 5.12 Crustal Boudinage of the Newfoundland-Ireland Conjugate Margins

If it is assumed that the West Orphan Basin evolved as a linked basin to the Rockall Basin, then it is possible that the East Orphan Basin evolved along with the Porcupine Basin. The juxtaposition and possible link between the East Orphan Basin and the Porcupine Basin have been previously investigated (Srivastava & Verhoef 1992; Knott *et al.,* 1993; Louden *et al.,* 2004, Enachescu, 2006). Between both pairs of possible conjugate margin basins lie continental highs. The Orphan Knoll, between the East and West Orphan basins, and the Porcupine Bank, between the Rockall and Porcupine basins. The juxtaposition of thick continental fragments and thinned crust may represent some kind of regional, crustal-scale, boudinage effect, present on both margins (Fig. 5.18).

The Orphan Knoll lies at the eastern edge of the Orphan Basin and is presumed to be a continental fragment, beyond which lies the continent-ocean transition (Keen *et al.* 1987). The Deep Sea Drilling Project (DSDP) site 111 drilled the Orphan Knoll to a depth of 250 m below

the seabed. The well drilled through coarse sandstones and shales at the base, that were determined to be Jurassic with nearby source beds of late Paleozoic age, indicating that the Orphan Knoll is a continental fragment (Chian *et al.*, 2001).

The Porcupine Bank represents an extension of the Irish Mainland Shelf and bounds the Rockall Basin to the southeast, separating it from the Porcupine Basin (Hauser *et al.*, 1995). The Porcupine Bank is a continental block that has a crustal thickness of approximately 30 km (O'Reilly *et al.*, 2006; Welford *et al.*, 2010).

A rough plate reconstruction, based solely on closing the North Atlantic Ocean at the magnetic anomaly M0 time (Srivastava & Verhoef 1992; Skogseid 2010) shows the West Orphan Basin, the Orphan Knoll and the East Orphan Basin forming a multibasin rift systemthat is continuous with the Rockall Basin, the Porcupine Bank and the Porcupine Basin, respectively (Fig. 5.18). The Orphan Knoll feature could be considered to be a portion of Porcupine Bank, detached from it after most of the Orphan Basin had formed and after a rift jump during the North Atlantic opening (Enachesu *et al.*, 2005). Therefore, it is possible that East Orphan Basin, the Orphan Knoll and the West Orphan Basin are conjugate equivalents to the Porcupine Basin, the Porcupine Bank and the Rockall Basin, respectively.

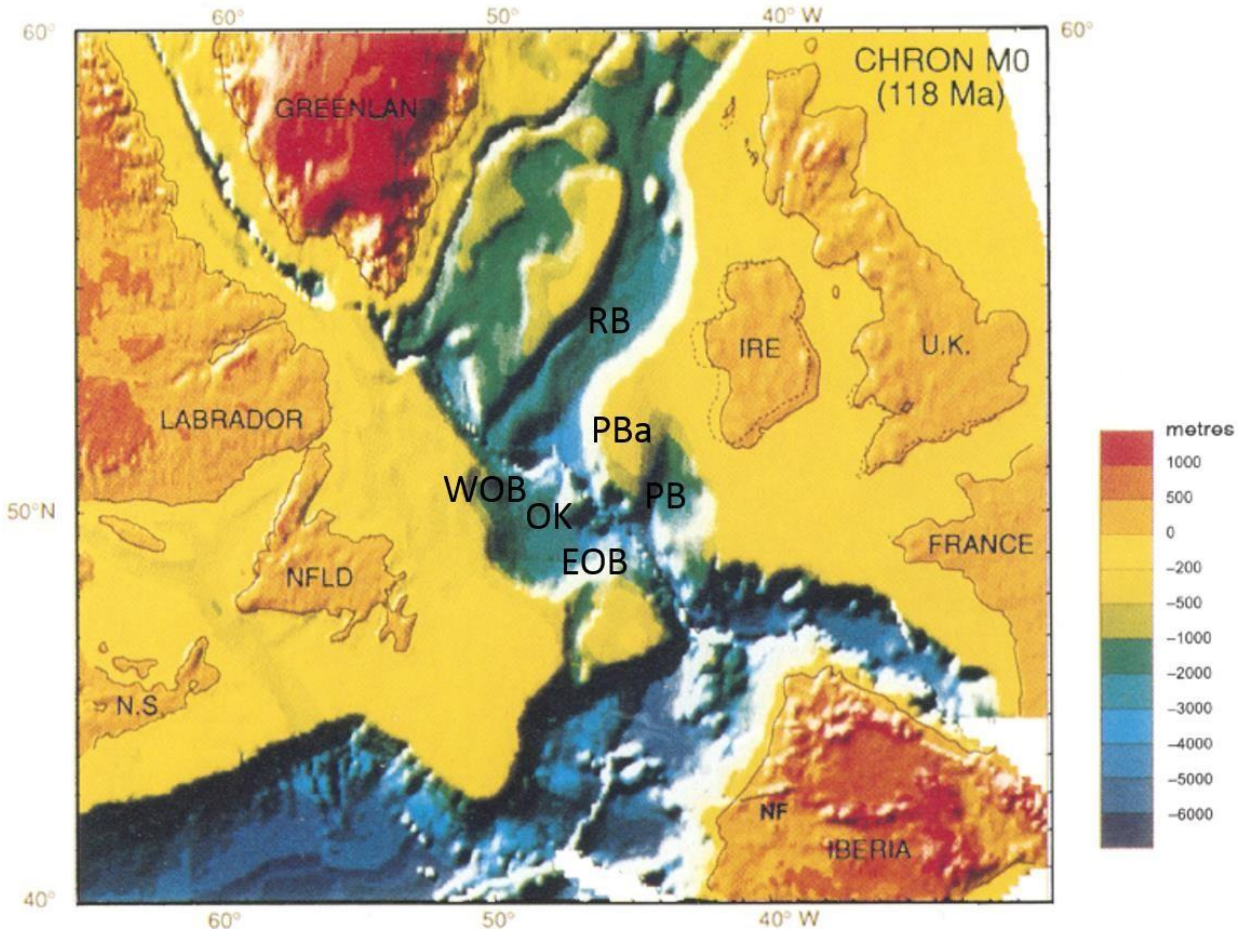


*Figure 5.18: Plate reconstruction of the North Atlantic at the magnetic anomaly M0 time, showing the juxtaposition of thick continental blocks and thinned crust. Background indicates bathymetry. RB, Rockall Basin; PBa, Porcupine Bank; PB, Porcupine Basin; EOB, East Orphan Basin; OK, Orphan Knoll; WOB, West Orphan Basin. Image adapted from Srivastava & Verhoef (1992).*

### 5.13 Previously Published Plate Reconstructions

Rigid plate paleoreconstructions of the North Atlantic Ocean to a time prior to lithospheric break-up and the formation of oceanic crust show that the East and West Orphan sub-basins were juxtaposed against the Porcupine and the Rockall basins, respectively (Srivastava & Verhoef 1992; Knott *et al.,* 1993; Louden *et al.,* 2004; Enachescu, 2006). Separation of the Irish continental margin from its conjugate pair, the northern Flemish Cap/Orphan Basin region of Newfoundland, Canada, occurred during the Mid-Late Cretaceous

(Tucholke *et al.*,1989; Hopper *et al.*, 2006; Lundin & Doré, 2011; Lau *et al.*, 2015) and comparable stratigraphic, structural, and crustal syn-rift evolution would be expected (Gouiza *et al.*, 2017). Keen *et al.* (2014) suggest that in Early Cretaceous time, there was simultaneous rifting in the Labrador Sea and in the Rockall and the Orphan basins. This would have created a complex triple point, with movement between the North American, Rockall, and European plates (Bull & Masson, 1996).

Skogseid *et al.* (2010) utilized a proprietary 4D modelling software package to perform kinematic plate reconstructions of the North Atlantic margins. This restoration focused on the role of the Orphan Basin, as well as the rotation of the Flemish cap away from the Bonavista platform, during the opening of the North Atlantic. The reconstruction generated at 180 Ma by Skogseid *et al.* (2010) suggests that the Rockall Basin and the East Orphan Basin are aligned and can be linked into the Jeanne d'Arc Basin (Fig. 5.19a). At 140 Ma, the eastward relative motion of the Flemish Cap and the East Orphan Basin with respect to the Eurasian side caused the Rockall Basin to abandon its linkage with the East Orphan Basin (Skogseid *et al.*, 2010). At this stage, the West Orphan Basin was established from a westward rift axis jump and southward propagation, which cut across the East Orphan Basin and Jeanne d'Arc Basin (Fig. 5.19b; Skogseid *et al.*, 2010). The Porcupine Basin appears to align with the East Orphan Basin at this time. At 120 Ma, the reconstruction performed by Skogseid *et al.* (2010) shows the final stage in the tectonic development of the Orphan Basin (Fig. 5.19c). The shape of the West Orphan Basin – Flemish Pass rift and the angle of rotation chosen imply only a moderate N-S shear motion approaching the southern tip of the rift (Skogseid *et al.*, 2010). Skogseid *et al.* (2010) conclude that the Rockall Basin developed as the main Mesozoic NE Atlantic rift center and it is interpreted to have been directly linked into the two-stage opening of the East and West Orphan basins.

The results of the kinematic plate reconstruction carried out by Skogseid *et al.* (2010) conflict with the results of the reconstruction performed by the Matthew *et al. (*2016) and Müller *et al.* (2016) GPlates© model efforts. The results of the reconstruction performed by Matthew *et al. (*2016) and Müller *et al.* (2016) can be seen in Chapter 4, sections 4.3.1 – 4.3.6. Based on the present-day location of the seismic lines, their model shows that the Rockall Basin was possibly never continuous with the Orphan Basin. However, if a possible connection was to be assumed from their reconstruction, only the West Orphan Basin would have been connected to the Rockall Basin.

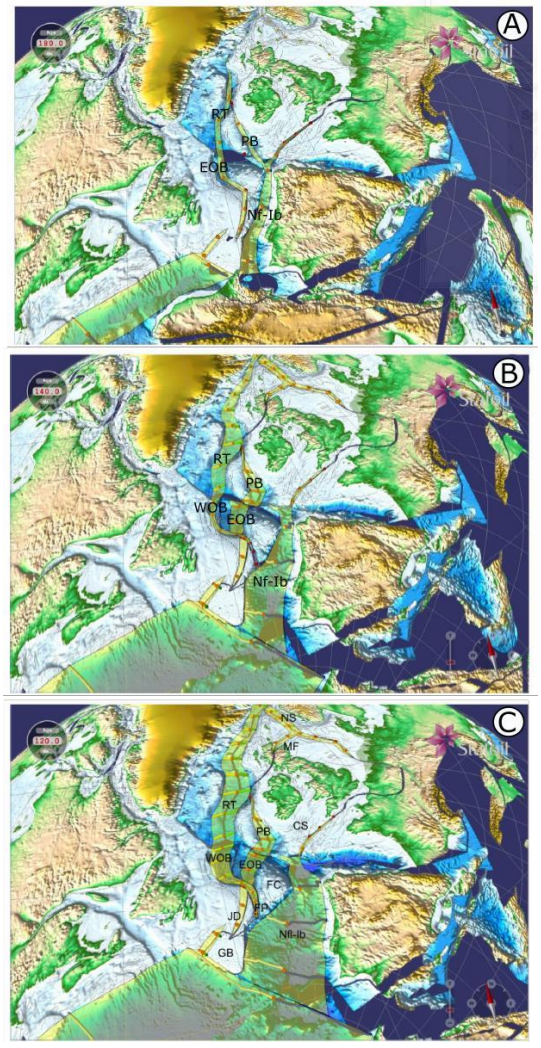


*Figure 5.19: Time steps in the plate kinematic modelling linking the Mesozoic N and NE Atlantic rifting from Skogseid et al. (2010). (A) 180 Ma, early basin formation. (B) 140 Ma, where Rockall Basin has abandoned the linkage to the East Orphan Basin and the West Orphan Basin is established. (C) 120 Ma, showing the final reconstruction of the Orphan Basin development. The total magnitude of extension along rift zones is shown by yellow shading. RT: Rockall Trough (or Basin), PB: Porcupine Basin, WOB: West Orphan Basin, EOB: East Orphan Basin, NF-Ib: Newfoundland – Iberia, FC: Flemish Cap, GB: Grand Banks, CS: Celtic Sea, JD: Jeanne d'Arc Basin, FP: Flemish Pass*

A recent paper published by Nirrengarten *et al.* (2018) focuses on the southern North Atlantic rifted margins. They investigated the partitioning and propagation of deformation in hyper-extended rift systems using kinematic modelling in GPlates©. They combined 3D gravity inversion results with local structural, stratigraphic and geochronological constraints on the rift deformation history. The restoration of the Newfoundland-Ireland conjugate margins was not the

primary focus of the paper. However, they generated a GPlates© model that restored the two basins and showed a possible evolutionary link where the Rockall Basin was initially conjugate to the East Orphan Basin and later the West Orphan Basin (Fig. 5.20). Nirrengarten *et al.* (2018) included continental micro-blocks that enabled the partitioning of the deformation between the different rift segments (i.e., the East Orphan Basin, Orphan Knoll, the West Orphan Basin, Flemish Cap, the Rockall Basin, the Rockall Bank, the Porcupine Basin and the Porcupine Bank).

While the evolutionary history of the three basins was similar to that proposed by Skogseid *et al.* (2010), the reconstruction generated by Nirrengarten *et al.* (2018) involved different timing than the reconstruction performed by Skogseid *et al.* (2010). The continental-block polygons created in the Nirrengarten *et al.* (2018) reconstruction are rigid and do not deform as extension occurs, creating inaccuracies within the model. Also, numerous rift events, specifically the extensional events related to the two main rift episodes in the Orphan Basin, the Late Jurassic and Early Cretaceous, were excluded from this model. Additionally, the rigid polygons do not appear in the reconstruction until after rifting is assumed to have ceased in the specific area of the microplate. Therefore, the appearance of the polygon in the model may not accurately represent the timing of the possible connection between the conjugate basins.

The reconstruction generated by Nirrengarten *et al.* (2018) shows the possible connection of the Rockall Basin and the East Orphan Basin at approximately 120 Ma (Fig. 20b). At approximately 110 Ma, the Rockall Basin appears to be conjugate to the West Orphan Basin. Skogseid *et al.* (2010) predicted that the Rockall Basin was likely conjugate to the East Orphan Basin as early as 180 Ma and that the Rockall Basin became conjugate to the West Orphan Basin around 140 Ma. As previously mentioned, the inconsistencies in the timing of the appearance of

the polygons in the Nirrengarten *et al.* (2018) model are likely due to the fact that the polygons do not appear until after rifting has ceased and not all relevant rifting events have been accounted for. Therefore, the timing of events from Skogseid *et al.* (2010) is likely more accurate than those from the reconstruction performed by Nirrengarten *et al.* (2018).

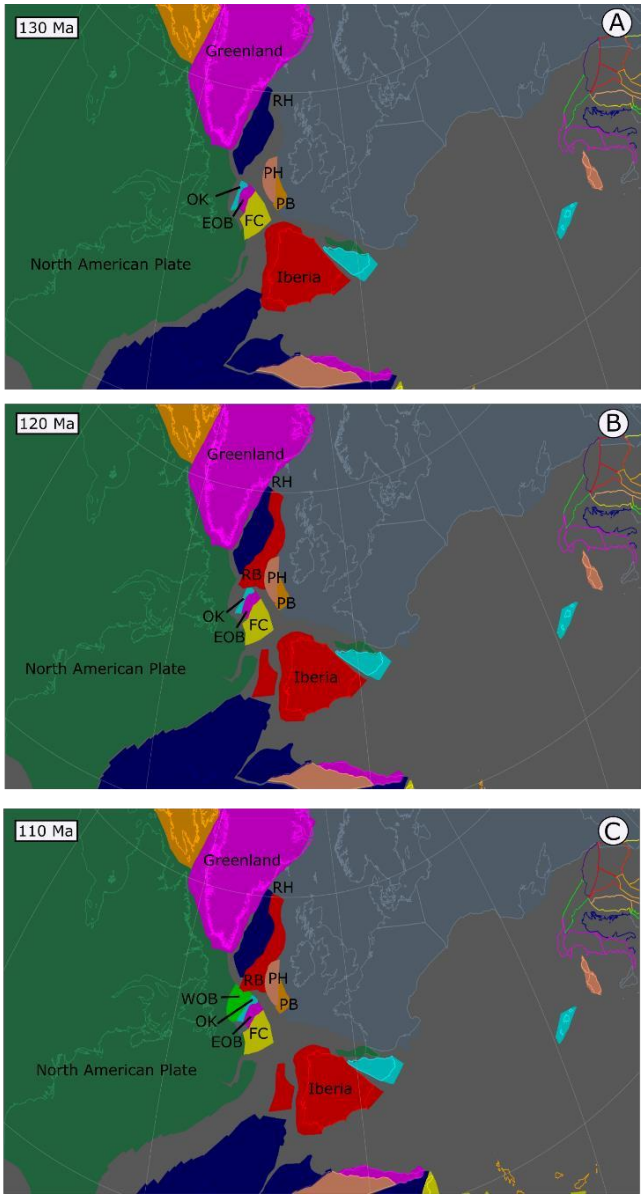


*Figure 5.20: Plate tectonic reconstruction from Nirrengarten et al. (2018). (A) 130 Ma, depicting the East Orphan Basin not conjugate to the Porcupine Basin. The West Orphan Basin and the Rockall Basin polygons have not appeared yet. (B) 120 Ma, the Rockall Basin polygon has appeared and is potentially conjugate to the East Orphan Basin. The West Orphan Basin polygon has not appeared. (C) 110 Ma, the West Orphan Basin polygon has appeared and is potentially continuous with the Rockall Basin. RH: Rockall High; RB: Rockall Basin; PH: Porcupine High; PB: Porcupine Basin; WOB: West Orphan Basin; OK: Orphan Knoll; EOB: East Orphan Basin; FC: Flemish Cap*

### 5.13.1 Previously Published Plate Reconstructions Determined from Magmatic Events

Using seismic and potential field data, Keen *et al.* (2014) mapped an offshore igneous province, termed the Charlie-Gibbs Volcanic Province (CGVP), showing the presence of a variety of volcanic features, including sills, lava flows, and volcanic highs occurring north of the West Orphan Basin, on the Newfoundland continental margin near the Charlie-Gibbs Fracture Zone (CGFZ; Fig. 5.21). The seamounts present in the CGVP are suggested to be Late Cretaceous in age (Keen *et al.,* 2014). On the conjugate Irish margin, the Barra Volcanic Ridge System (BVRS), located in the southern Rockall Basin, has been estimated to be Early Cretaceous in age (Kimbell *et al.,* 2010). The BVRS may represent an accommodation zone within the West Orphan/Rockall Basin system that developed through reactivation of pre-existing faults, with volcanism beginning later in Santonian times (Keen *et al.,* 2014). This volcanism occurs within an overall nonvolcanic margin setting and probably represents magmatism along an oblique strike-slip fault zone of considerable structural complexity in a region where Rockall Basin was once joined to West Orphan Basin until the Mid to Late Cretaceous (Keen *et al.,* 2014; Fig. 5.21).

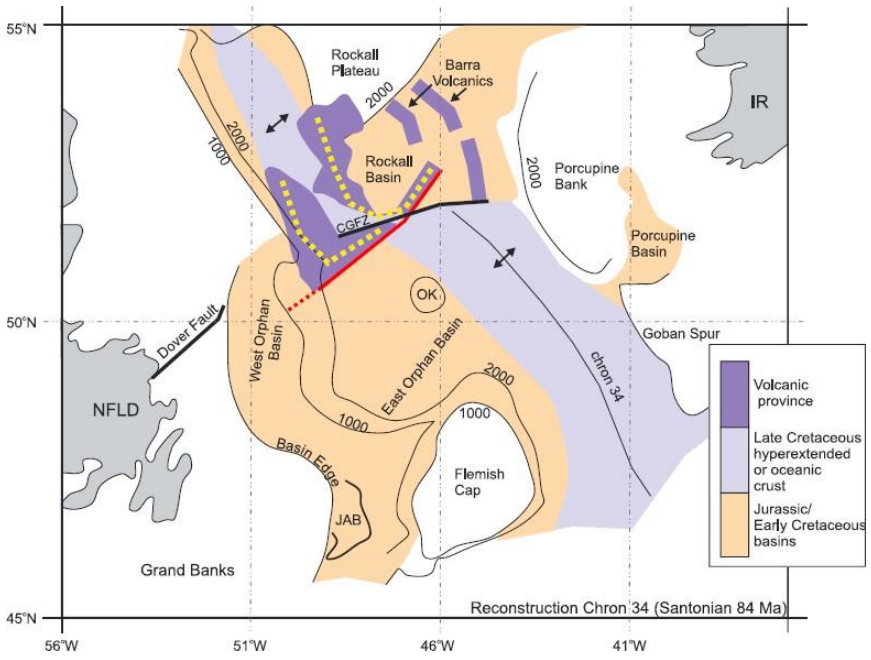


*Figure 5.21: Plate tectonic reconstruction at chron 34 from Srivastava et al. (1988). The CGVP north of the Orphan Basin and the volcanic features that appear conjugate in Rockall Basin are shown and highlighted with yellow dotted lines. The Barra Volcanic Ridges are shown, one of which aligns with the Southern Branch of the CGVP, along the trend indicated by the red solid line. The dotted red line is the location of the truncation of the deep crustal reflectors in the Orphan Basin. This trend is oblique to the trend of the CGFZ, shown as a solid black line. Bathymetric contours are in metres. NFLD: Newfoundland, IR: Ireland, JAB: Jeanne d'Arc basin, OK: Orphan Knoll. Image from Keen et al. (2014), adapted from Welford et al. (2012) and Kimbell et al. (2 010).*

Lau *et al.* (2015) compare crustal sections for the Orphan and Rockall basins, constrained by seismic velocity and gravity models (Morewood *et al.*, 2005; O'Reilly *et al.*, 2006). Each of the basins is asymmetrical and the two systems across the Atlantic share the same juxtaposition of a narrower eastern zone versus a wider western zone of hyperextended crust (<10 km). This further supports a connection between the Rockall Basin and West Orphan Basin and between the Porcupine Basin and East Orphan Basin during rifting (Lau *et al.*, 2015). The Newfoundland margin developed in response to numerous rift episodes in a variety of directions, at least one of which likely affected the Irish margin (Lau *et al.*, 2015). The Irish margin also developed as a result of numerous episodes of rifting in a variety of directions, at least one of which likely affected the Newfoundland margin (Lau *et al.*, 2015). One additional rift episode affected the

Irish margin, possibly related to the separation of Greenland from Europe, however this extensional event is beyond the scope of this M.Sc. thesis.

### 5.14 Comparison between the East Orphan Basin and the Rockall Basin

As previously mentioned, Skogseid *et al.* (2010) used a 4D modelling software package, proprietary to Equinor©, to perform kinematic plate reconstructions of the North Atlantic margins. This restoration focused on the role that the Orphan Basin played in the opening of the North Atlantic. The reconstruction generated at 180 Ma suggests that the Rockall Basin and the East Orphan Basin are aligned and can be linked into the Jeanne d'Arc Basin. At 140 Ma, the relative eastward motion of the Flemish Cap and the East Orphan Basin with respect to the Eurasian side caused the Rockall Basin to abandon the linkage with the East Orphan Basin in favour of the West Orphan Basin via a westward rift axis jump and southward propagation of extension (Skogseid *et al.,* 2010). Skogseid *et al.* (2010) conclude that the Rockall Basin developed as the main Mesozoic NE Atlantic rift center, directly linked into the two-stage opening of the East and West Orphan basins.

If the plate reconstruction model generated by Skogseid *et al.* (2010) is correct, then similarities between the East Orphan Basin and the Rockall Basin should be present. To accurately compare the two basins, a reconstruction of the East Orphan Basin was carried out in Move© following the same methodology as the reconstructions performed in the Rockall Basin and in the West Orphan Basin. Seismic interpretations for the East Orphan Basin were generously provided by Larry Sandoval (personal communication, 2018). The same reconstruction workflow was followed for seismic line NL3 in the East Orphan Basin (location shown in Fig. 5.22), within Move©. The reconstruction included: converting the seismic horizons

and associated faults from the time domain to the depth domain, decompacting the Cenozoic sedimentary unit and accounting for thermal subsidence, decompacting the Upper Cretaceous unit and accounting for thermal subsidence, decompacting the Lower Cretaceous unit, decompacting, restoring faults and unfolding the Jurassic unit and decompacting, restoring faults and unfolding the Upper Crust. Selected results of these reconstructions, along with the reconstruction from the West Orphan Basin and the Rockall Basin are shown in 3D alongside the reconstructions generated by Skogseid *et al.* (2010; Figs. 5.23a, 5.24a and 5.25a).

The 2D reconstruction of seismic line NL3, in the East Orphan Basin, resulted in the calculation of an average pre-rift crustal thickness of ~8.7 km, compared to the ~12.3 km of pre-rift crust observed in the West Orphan Basin. The thickness of the pre-rift crust in the East Orphan Basin is very similar to the average thickness of pre-rift crust in the Rockall Basin, 8.5 km (Table 5.1). The similarities observed for the pre-rift crustal thicknesses between the East Orphan Basin and the Rockall Basin can be explained if the two basins were connected during this time, ~180 Ma. This finding is in agreement with the model presented by Skogseid *et al.* (2010) and the comparison can be seen in Fig. 5.23.

The 2D reconstruction of seismic line NL3, in the East Orphan Basin, resulted in the calculation of an average syn-rift sedimentary thickness of ~3.8 km. This value is significantly higher than the syn-rift thicknesses recorded in the West Orphan Basin and the Rockall Basin, with both having an average thickness of ~2.4 km (Table 5.1). Therefore, it is likely that during the North Atlantic rifting events that occurred at ~160-140 Ma (Shannon, 1991), the Rockall Basin abandoned its linkage to the East Orphan Basin and became conjugate to the West Orphan Basin. This change in the Rockall Basin's linkage from the East to the West Orphan Basin could

potentially explain the discrepancy in syn-rift sedimentary rock thickness observed between the Rockall Basin and the East Orphan Basin and the similarities observed between the West Orphan Basin and the Rockall Basin. The exact timing of the linkage switch of the Rockall Basin, from the East to the West Orphan Basin, is difficult to quantify due to the lack of Jurassic sedimentary rocks interpreted in the Rockall Basin. If any Jurassic sedimentary rocks were interpreted in the Rockall Basin, the thicknesses could be compared across the margins and a more complete timeline could be generated. However, no Jurassic sedimentary rocks were interpreted in the Rockall Basin due to the quality of the deep seismic data. Therefore, it is difficult to state whether the linkage switch of the Rockall Basin from the East to the West Orphan Basin happened around 160 Ma, during the Late Jurassic, as the West Orphan Basin began to open (Enachescu *et al.,* 2004) or around 140 Ma, after Jurassic rifting had ceased across the margins (Mackenzie *et al.*, 2002; Lau *et al*., 2015). Since the age constraints for this study are not accurate enough to specify a time period of the linkage switch, the time period used by the model generated by Skogseid *et al.* (2010) was chosen, 140 Ma (Fig. 5.24).

Skogseid *et al.* (2010) state that the reason that the Rockall Basin abandoned its linkage with the East Orphan Basin was due to the eastward relative motion of the Flemish Cap and the East Orphan Basin with respect to the Irish margin. Therefore, it is likely that, as the East Orphan Basin rotated further east following the motion of the Flemish Cap, the Rockall Basin remained in place, due to the presence of a weaker, more accessible rift zone. As rifting propagated westward from the East Orphan Basin during the Late Jurassic, the West Orphan Basin began to open (Enachescu *et al.,* 2004). This potentially put the Rockall Basin in a closer proximity to a weaker rifting zone, the West Orphan Basin, therefore causing the linkage switch.

At 120 Ma, the Rockall Basin and the West Orphan Basin likely remained connected based on the similarities in syn-rift thicknesses observed in this study, until the North Atlantic began to open around 100 Ma (Shannon 1991; Doré *et al.,* 1997). This finding is in agreement with the model presented by Skogseid *et al.* (2010) and the comparison can be seen in Fig. 5.25.

Along seismic line NL3 in the East Orphan Basin, an average of ~3.8 km of post-rift sedimentary rock is interpreted. This is similar to the thickness of the post-rift sedimentary rock observed in the West Orphan Basin, ~3.7 km (Table 5.1). It is expected that the East and West Orphan basins experienced similar amounts of post-rift sedimentary rock deposition because the two sub-basins were connected. Following rifting, the East and West sub-basins evolved in a relatively similar manner (Enachescu *et al.,* 2004). The average post-rift thickness in the Rockall Basin is ~3.4 km. This value is similar to that observed across the Orphan Basin as a whole, although post-rift thicknesses are expected to be slightly different as the basins evolved independently following the opening of the North Atlantic (Shannon 1991; Naylor & Shannon, 2005).

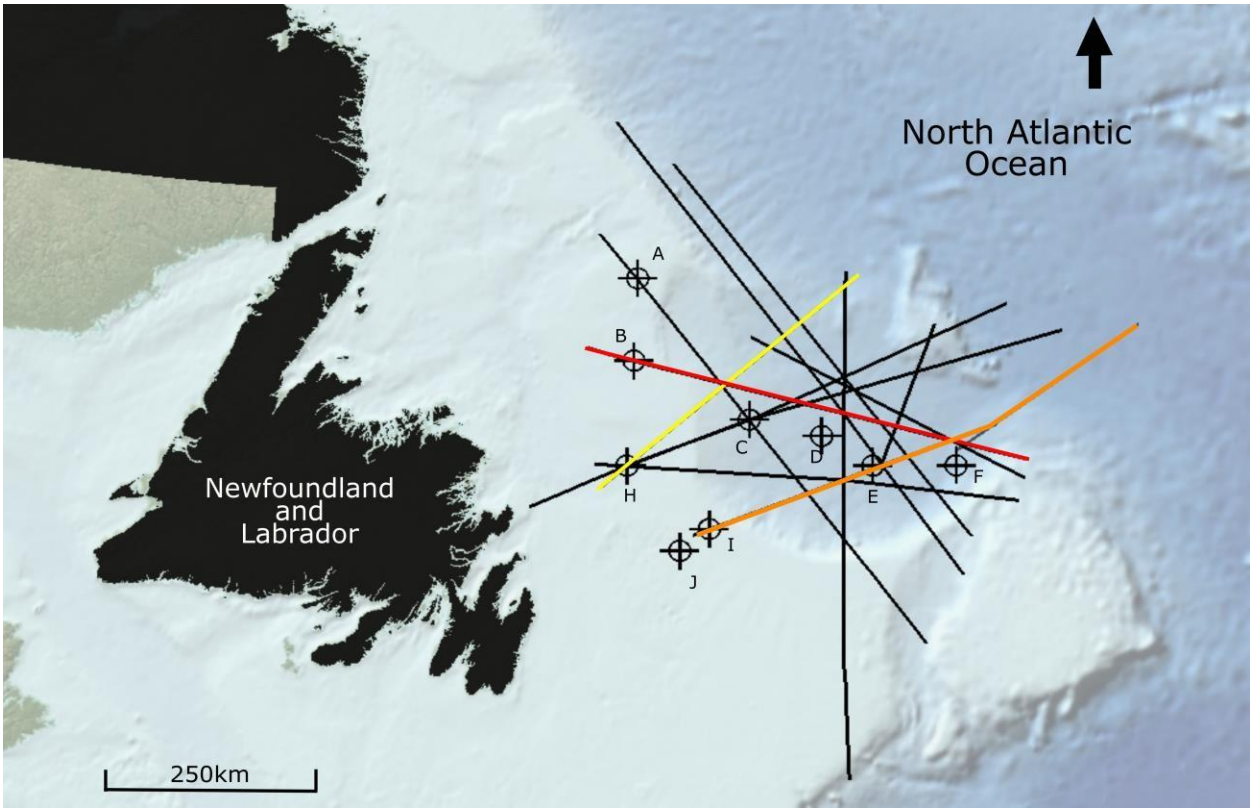


*Figure 5.22: Location of the Orphan Basin seismic lines. Seismic line NL3 is shown as the orange line, it is a compilation of two seismic lines that have been joined together. Seismic line NL1 is shown as the yellow line and seismic line NL2 is shown as the red line.*

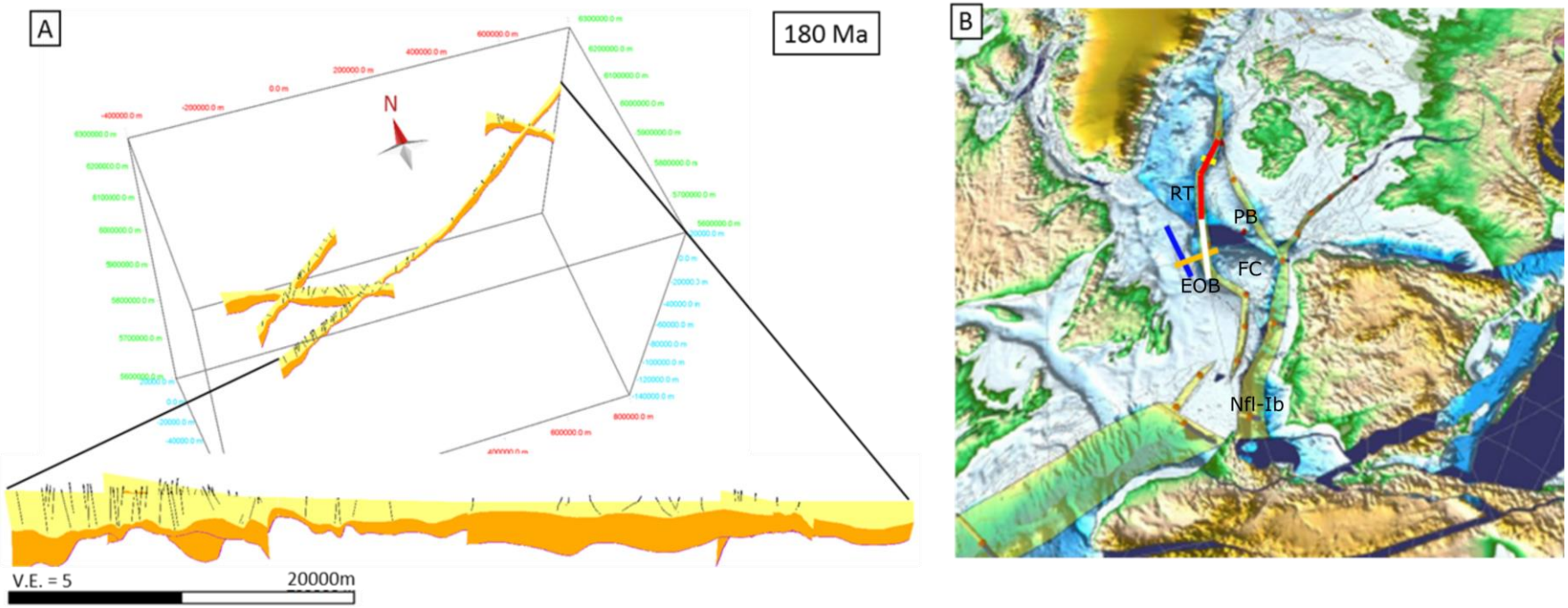


*Figure 5.23: (A) 3D reconstruction of the East and West Orphan basins and the Rockall Basin at 180 Ma. Zoomed in view shows seismic line NL3 in the East Orphan Basin conjugate to seismic line IR1 in the Rockall Basin. Black lines represent primary faults. The yellow represents the basement/upper crust. The orange represents the lower crust, bounded by the mid -crustal boundary. The purple line represents the Moho proxy from Welford et al. (2012). (B) 2D reconstruction from Skogseid et al. (2010), with the locations of the main seismic lines shown. IR1 is shown as the red line, IR2 is shown as the yellow line, NL3 is shown as the white line, NL2 is shown as the orange line and NL1 is shown as the blue line. Note the locations of these lines are an approximation, as the Skogseid et al. (2010) model is owned by Equinor and not available for academic use. EOB: East Orphan Basin; FC: Flemish Cap; Nfl-Ib: Newfoundland-Iberia rift zone; RT: Rockall Trough; PB: Porcupine Basin.*

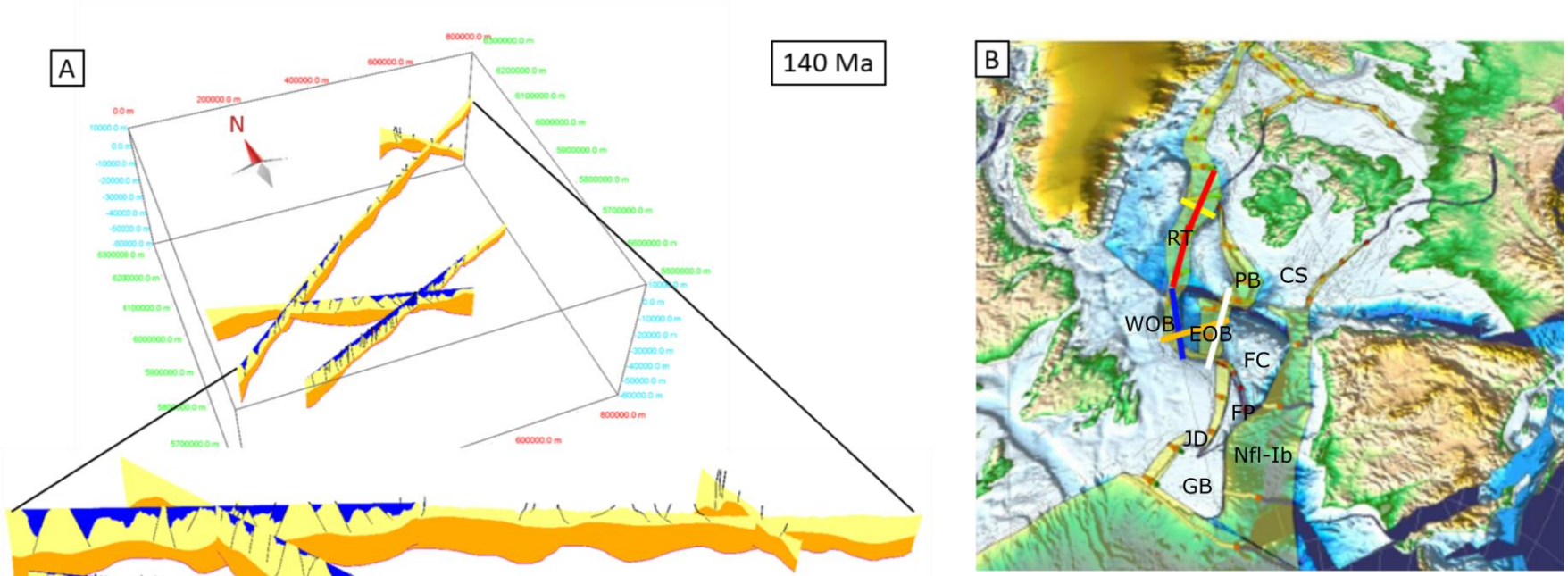


*Figure 5.24: (A) 3D reconstruction of the East and West Orphan basins and the Rockall Basin at 140 Ma. Zoomed in view shows seismic line NL1 in the West Orphan Basin is now conjugate to seismic line IR1 in the Rockall Basin. Black lines represent primary faults. The dark blue represents the Jurassic unit. The yellow represents the basement/upper crust. The orange represents the lower crust, bounded by the mid-crustal boundary. The purple line represents the Moho proxy from Welford et al. (2012). (B) 2D reconstruction from Skogseid et al. (2010), with the locations of the main seismic lines shown. IR1 is shown as the red line, IR2 is shown as the yellow line, NL3 is shown as the white line, NL2 is shown as the orange line and NL1 is shown as the blue line. Note the locations of these lines are an approximation, as the Skogseid et al. (2010) model is owned by Equinor and not available for academic use. GB: Grand Banks; CS: Celtic Sea; EOB: East Orphan Basin; FC: Flemish Cap; FP: Flemish Pass; JD: Jeanne d'Arc Basin; Nfl-Ib: Newfoundland-Iberia rift zone; RT: Rockall Trough; PB: Porcupine Basin; WOB: West Orphan Basin.*

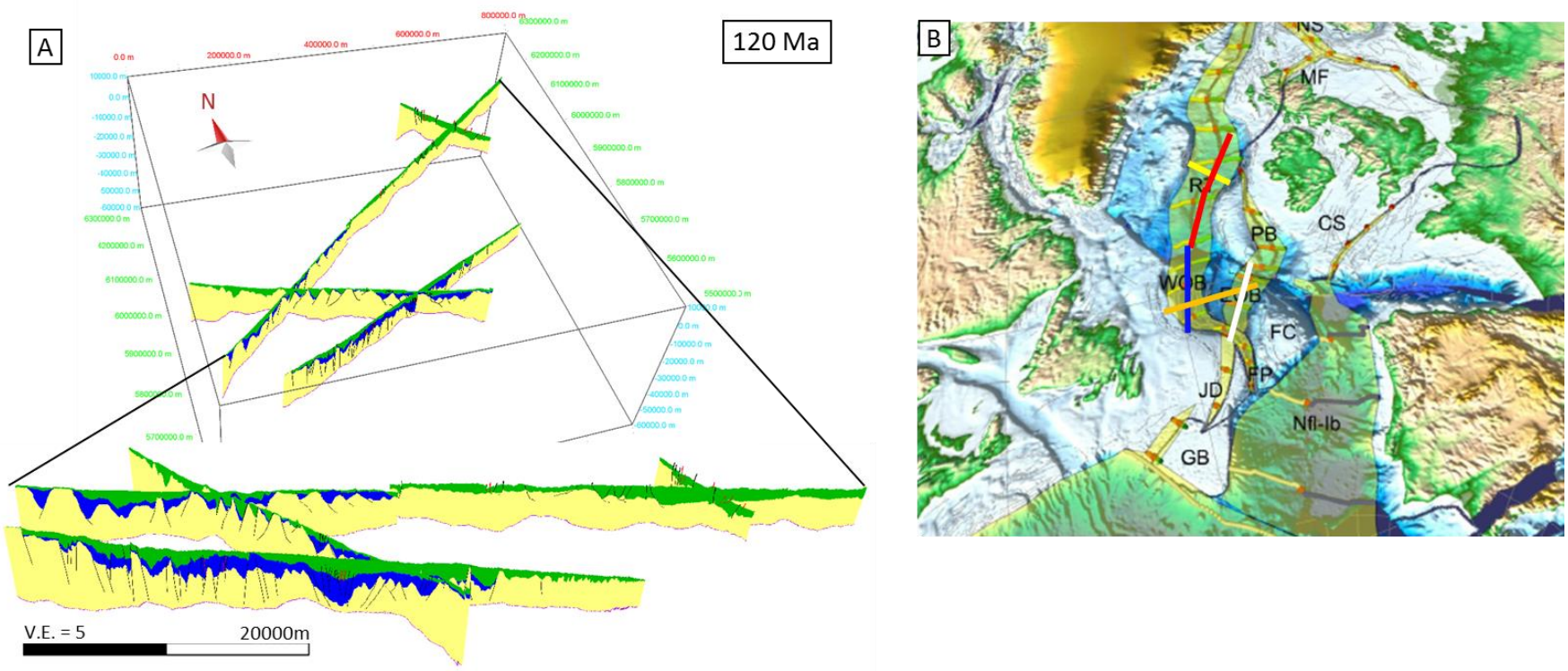


*Figure 5.25: (A) 3D reconstruction of the East and West Orphan basins and the Rockall Basin at 120 Ma. Zoomed in view shows seismic line NL1 in the West Orphan Basin conjugate to seismic line IR1 in the Rockall Basin. Black lines represent primary faults and red lines represent secondary faults. The green represents the Lower Cretaceous unit. The dark blue represents the Jurassic unit. The yellow represents the basement/crust. The purple line represents the Moho proxy from Welford et al. (2012). (B) 2D reconstruction from Skogseid et al. (2010), with the locations of the main seismic lines shown. IR1 is shown as the red line, IR2 is shown as the yellow line, NL3 is shown as the white line, NL2 is shown as the orange line and NL1 is shown as the blue line. Note the locations of these lines are an approximation, as the Skogseid et al. (2010) model is owned by Equinor and not available for academic use. GB: Grand Banks; CS: Celtic Sea; EOB: East Orphan Basin; FC: Flemish Cap; FP: Flemish Pass; JD: Jeanne d'Arc Basin; MF: Morray Firth Basin; Nfl-Ib: Newfoundland-Iberia rift zone; NS: North Sea Basin; RT: Rockall Trough; PB: Porcupine Basin; WOB: West Orphan Basin.*

| | West Orphan Basin | East Orphan Basin | Rockall Basin |
|---|---|---|---|
| Average thickness of pre-rift crust | 12.3 km | 8.6 km | 8.5 km |
| Average thickness of syn-rift sedimentary rock | 2.4 km | 3.8 km | 2.4 km |
| Average thickness of post-rift sedimentary rock | 3.7 km | 3.8 km | 3.4 km |

*Table 5.1: Average thicknesses of the pre-rift crust, the syn-rift sedimentary rock and the post-rift sedimentary rock in the West and East Orphan basins and the Rockall Basin. Values measured from 2D reconstructions generated in Move ©.*

Overall, the results of the 2D and 3D reconstructions across the Newfoundland-Ireland conjugate margins generated for this M.Sc. project are in good agreement with the reconstruction model presented by Skogseid *et al.* (2010), as well as the model generated by Nirrengarten *et al.* (2018). It is possible that the Rockall Basin was originally conjugate to the East Orphan Basin, explaining the similarities observed in the average thickness of the pre-rift crust. However, the East Orphan Basin began rotating further to the east, while the Rockall Basin remained relatively in place. During this time, the West Orphan Basin began to form and offered a weaker, more accessible rifting zone in closer proximity to the Rockall Basin and a linkage switch was made. The Rockall Basin potentially remained conjugate to the West Orphan Basin during rifting, explaining the similarities in the syn-rift thicknesses, until the opening of the North Atlantic. However, it is important to note that this is only one possible explanation for the reconstruction of the Newfoundland-Ireland conjugate margins.

# Chapter 6: Conclusion and Future Work

## 6.1 Conclusion

Three scenarios are envisaged to explain the evolutionary history of the Newfoundland-Ireland conjugate margins with respect to the Rockall Basin and the Orphan Basin: 1) the Rockall Basin was never conjugate to, or continuous with, the West Orphan Basin; 2) the Rockall Basin was always conjugate to, and continuous with, the West Orphan Basin; 3) the Rockall Basin was originally conjugate to, and continuous with, the East Orphan Basin, but became conjugate to, and continuous with, the West Orphan Basin.

Based on the results from this thesis, the evidence to support the first scenario is minimal given similarities in sedimentary rock and crustal thicknesses. Thus, the remaining uncertainty lies in the interplay between the Rockall Basin and both the East and West Orphan basins through time.

While the nature of faulting was difficult to characterize across the West Orphan Basin and the Rockall Basin, minimal similarities were observed. This was likely due to the orientation of the seismic lines and the lack of seismic coverage within the Rockall Basin. Seismic lines NL1 and IR2 both exhibit tilted fault blocks, to a varying degree. However, no seamounts, basement highs, or grabens are observed on the Irish margin. These structures are likely present in the Rockall Basin but have not been captured by the seismic reflection data due to the interference from shallower widespread sills. Therefore, while there are a few similarities in faulting styles observed across the two margins, the nature of the faulting cannot be used to definitively tie the Rockall Basin to the West Orphan Basin given the currently available data.

An additional asymmetry across the margins is the fact that the Rockall Basin is known to be underlain by serpentinized mantle whereas the Orphan Basin is not (O'Rielly *et al.*, 1996;

Chian *et al.,* 2001; Lau *et al.,* 2015). The lack of serpentinized mantle beneath the Orphan Basin does not necessarily mean that its crust differed greatly from the crust on the Irish margin, but rather that the Irish crust failed more abruptly as the serpentinized mantle beneath it acted as a ductile detachment (Welford *et al.,* 2012).

The GPlates© reconstruction generated by Matthews *et al.* (2016) and Müller *et al.* (2016) shows the possibility that the West Orphan Basin and the Rockall Basin were never conjugate, continuous basins. Their reconstruction places the Rockall Basin further to the north than the West Orphan Basin. However, the GPlates© model generated by Matthews *et al.* (2016) and Müller *et al.* (2016) does not account for any internal deformation of the plates. It is possible that by accounting for this deformation, the Rockall and West Orphan basins would align.

The evidence suggesting that the Rockall Basin and the West Orphan Basin are conjugate, continuous basins includes the simple closing of the North Atlantic Ocean and fitting together of the basins (Srivastava & Verhoef 1992; Knott *et al.*, 1993; Louden *et al.*, 2004; Enachescu, 2006; Welford *et al.,* 2012). Closing the North Atlantic Ocean using seafloor magnetic anomalies results in the West Orphan Basin lying adjacent to the Rockall Basin, and the East Orphan Basin lying adjacent to the Porcupine Basin (Srivastava & Verhoef, 1992; Knott *et al,* 1993; Louden *et al.,* 2004; Enachescu, 2006; Welford *et al.*, 2012). Between both pairs of possible conjugate basins lie a continental high, the Orphan Knoll, between the East and West Orphan basins and the Porcupine Bank, between the Rockall and Porcupine basins. This along-margin regional boudinage effect of the juxtaposition of thinner basinal crust against thicker crust in a continental high to thinner basinal crust again, is similar on both margins. Therefore, it is possible that East Orphan Basin, the Orphan Knoll and the West Orphan Basin are conjugate to, and continuous with, the Porcupine Basin, the Porcupine Bank and the Rockall Basin,

respectively.

It has also been determined that to the north of the West Orphan Basin lies the Charlie Gibbs Volcanic Province (CGVP), located along the western extent of the Charlie Gibbs Fracture Zone (CGFZ) in the North Atlantic (Keen *et al.,* 2014). Within the Rockall Basin lies the Barra Volcanic Ridge System (BVRS), the volcanic province lies within proximity to the eastern extent of the CGFZ (Shannon *et al.,* 2006). Overall, the similar structure and location to the CGFZ of both the CGVP and the BVRS provide evidence of a possible Mesozoic connection between the Rockall and West Orphan basins.

The evidence to support scenarios two and three was generated from the 2D and 3D reconstructions in Move©. The primary evidence comes from the calculations of the thicknesses of the post-rift and syn-rift sedimentary packages and the pre-rift crust across the East and West Orphan basins and the Rockall Basin. The thickness of the post-rift sedimentary rock is similar in the East and West Orphan Basins, ~3.7 – 3.8 km, as expected. Within the Rockall Basin the thickness of the post-rift sedimentary rock is slightly less, ~3.4 km. However this variance would be expected in both the second and third scenarios because the basins evolved independently following the opening of the North Atlantic Ocean. The thicknesses of the syn-rift sedimentary package in the West Orphan Basin and the Rockall Basin are both ~2.4 km, compared to a significantly thicker syn-rift package in the East Orphan Basin of ~3.8 km. The similar syn-rift thicknesses imply that the West Orphan Basin and the Rockall Basin were likely connected during rifting. This observation agrees with both scenarios two and three. However, the evidence for scenario three becomes stronger when analyzing the thickness of the pre-rift crust. In the East Orphan Basin, an average crustal thickness of ~8.6 km for the pre-rift crust was calculated. In the

Rockall Basin, an average crustal thickness of ~8.5 km for the pre-rift crust was calculated. These values are strikingly similar compared to the ~12.3 km of pre-rift crust observed in the West Orphan Basin. Therefore it is possible that the East Orphan Basin was connected to the Rockall Basin as rifting began.

Overall, the most plausible scenario, from evidence generated in this thesis, is that the Rockall Basin was originally conjugate to, and continuous with, the East Orphan Basin before rifting began, explaining the similarities observed in the average thickness of the pre-rift crust. However, the East Orphan Basin began rotating further to the east due to the rotation of Flemish Cap, while the Rockall Basin remained relatively in place (Skogseid *et al.,* 2010). During this time, the West Orphan Basin began to form and offered a more accessible and weaker rifting zone in closer proximity to the Rockall Basin such that a linkage switch was made (Skogseid *et al.,* 2010). The Rockall Basin potentially remained conjugate to, and continuous with, the West Orphan Basin during the remaining rifting episodes, explaining the similarities observed in the syn-rift thicknesses. This conclusion is in agreement with the kinematic plate reconstruction presented by Skogseid *et al.* (2010), as well as the model generated by Nirrengarten *et al.* (2018).

The overall goal of this M.Sc. project was to create a Newfoundland-Ireland conjugate margin basin model from a single seismic megatransect that could be restored to a pre-rift state. This thesis successfully created the aforementioned basin model and restored multiple megatransects to a pre-rift state. This thesis also demonstrated that there were complications with the restoration between the West Orphan Basin and the Rockall Basin. These complications were successfully mitigated through the additional analysis and comparison between the East Orphan Basin and the Rockall Basin. Finally, this thesis successfully presented a scenario for the closing of the North Atlantic Ocean and the formation of continuous Mesozoic basins

between the East and West Orphan Basins and the Rockall Basin.

### 6.2 Future Work

Future work across the Newfoundland-Ireland conjugate margins should include the generation of a plate tectonic reconstruction model that accurately depicts the movement of the West Orphan Basin, Orphan Knoll, East Orphan Basin, Rockall Basin, Porcupine Bank and Porcupine Basin individually. This will allow for a more accurate reconstruction of the Newfoundland-Ireland conjugate margins and may provide additional insights into questions that were beyond the scope of this thesis, for example where the Orphan Knoll came from. Additionally, new seismic refraction data acquisition in both the Orphan Basin and the Rockall Basin would greatly improve the confidence in the seismic interpretations in the study area. The ability to see beneath the igneous intrusions within the Rockall Basin would likely greatly impact the seismic interpretation and therefore the reconstruction of the basin. Although it is not economically feasible for purely scientific purposes, drilling wells into the deepest extents of both the Rockall and Orphan basins would allow for more well ties to be made. This would result in more confidence in the seismic interpretations and therefore more confidence in the reconstruction as a whole.

## Bibliography


Ady, B., & R. C. Whittaker, (2012). A new kinematic plate reconstruction of the North Atlantic between Ireland and Canada, in Third Central and North Atlantic Conjugate Margins Conference (Abstracts), pp. 2–3, PIPCo RSG Ltd., Dublin, Ireland.

Barnett-Moore, N., Müller, D. R., Williams, S., Skogseid, J., & Seton, M., (2016). A reconstruction of the North Atlantic since the earliest Jurassic. *Basin Research, 30,* 160-185. doi:10.1111/bre.12214

Brace, W. F., & D. L. Kohlstedt, (1980). Limits on lithospheric stress imposed by laboratory experiments, J. Geophys. Res., 85, 6248-6252.

Brune, S., Heine, C., Clift, P. D., & Pérez-Gussinyé, M., (2017). Rifted margin architecture and crustal rheology: Reviewing Iberia-Newfoundland, Central South Atlantic, and South China Sea. *Marine and Petroleum Geology, 79,* 257-281. doi: 10.1016/j.marpetgeo.2016.10.018

Buck, W.R., (2007). Dynamic Processes in Extensional and Compressional Settings – the Dynamics of Continental Breakup and Extension. In: Treatise on Geophysics, vol. 6. Crust and Lithosphere Dynamics.

Buck,W.R., Lavier, L.L., Poliakov, A.N.B., (1999). How to make a rift wide. philos. Trans. R. Soc. Lond. Ser. A Mathematical Phys. Eng. Sci. 357 (1753), 671e690.

Buiter, S.J.H., Huismans, R.S., Beaumont, C., (2008). Dissipation analysis as a guide to mode selection during crustal extension and implications for the styles of sedimentary basins. J. Geophys. Research-Solid Earth 113 (B6), B06406. doi: 10.1029/2007jb005272

Bugeja, R., (2011). Crustal Attenuation in the region of the Maltese Islands using Coda Wave Decay (Doctoral dissertation). Retrieved from https://www.um.edu.mt/_data/assets/pdf_file/0012/160032/dissertation.pdf

Bull, J. M., & D. G. Masson, (1996). The southern margin of the Rockall Plateau: Stratigraphy, Tertiary volcanism and plate tectonic evolution, J. Geol. Soc., 153, 601–612. doi: 10.1144/gsjgs.153.4.0601

Chian, D., Louden, K. E., & Reid, I. (1995). Crustal structure of the Labrador Sea conjugate margin and implications for the formation of nonvolcanic continental margins. *Journal of Geophysical Research: Solid Earth, 100*(B12), 24239-24253. doi:10.1029/95jb02162

Chian, D., Reid, I. D., & Jackson, H. R., (2001). Crustal structure beneath Orphan Basin and implications for nonvolcanic continental rifting. *Journal of Geophysical Research: Solid Earth, 106*(B6), 10923 10940. doi: 10.1029/2000jb900422

Corfield, S., Murphy, N., & Parker, S., (1999). The structural and stratigraphic framework of the Irish Rockall Trough. Petroleum Geology of Northwest Europe: Proceedings of the 5th Conference, 407-420. doi: 10.1144/0050407

Crocker, E.E. & Shannon, P.M., (1987). The evolution and hydrocarbon prospectivity of the Porcupine Basin, offshore Ireland. *In:* BROOKS, J. & GLENNIE, K.W. (eds) *Petroleum Geology of North West.*

Davis, M. & Kusznir, N.J., (2004). Depth-dependent lithospheric stretching at rifted continental margins. In: Karner, G.D. (Ed.), Proceedings of NSF Rifted Margins Theoretical Institute. Columbia University Press, pp. 92–136. doi: 10.7312/karn12738-005

Dewey JF, Kidd WSF, (1974). Continental collisions in the Appalachian– Caledonian orogenic belt: variations related to complete and incomplete suturing. Geology 2:543–546. doi: 10.1130/0091-7613(1974)2<543:ccitao>2.0.co;2

Doré, A. G., Lundin, E. R., Jensen, L. N., Birkeland, Ø., Eliassen, P. E., & Fichler, C., (1997). Principal tectonic events in the evolution of the northwest European Atlantic margin. *Petroleum Geology of Northwest Europe: Proceedings of the 5th Conference.* doi: 10.1144/0050041

Driscoll, N.W. & Karner, G.D., (1998). Lower crustal extension across the Northern Carnarvon basin, Australia: evidence for an eastward dipping detachment. Journal of Geophysical Research 103, 4975–4991. doi: 10.1029/97jb03295

Ebinger, C.J.; Jackson J.A.; Foster A.N.; Hayward N.J., (1999). "Extensional basin geometry and the elastic lithosphere" (PDF). Philosophical Transactions of the Royal Society A. The Royal Society. 357 (1753): 741–765. doi: 10.1098/rsta.1999.0351

Eddy, M. P., Jagoutz, O., & Ibañez-Mejia, M. (2017). Timing of initial seafloor spreading in the Newfoundland-Iberia rift. *Geology*, *45*(6), 527-530. doi:10.1130/g38766.1

Enachescu, M.E., (2006). Structural setting and petroleum potential of the Orphan Basin, offshore Newfoundland and Labrador, Recorder, 31(2), 5–13.

Enachescu, M., S. Kearsey, V. Hardy, J.-C. Sibuet, J. Hogg, S. Srivastava, A. Fagan, T. Thompson, and R. Ferguson, (2005). Evolution and petroleum potential of Orphan Basin, offshore Newfoundland, and its relation to the movement and rotation of Flemish Cap based on plate kinematics of the North Atlantic, in Petroleum Systems of Divergent Continental Margin Basins, Proceedings of the 25th Annual GCSSEPM Foundation Bob F. Perkins Research Conference, 2005 (CD format only), edited by P. J. Post *et al*., pp. 75–131, Bureau of Economic Geology, University of Texas, Austin, Tex. doi: 10.5724/gcs.05.25.0075

Enachescu, M.E., Meyer, K. & Hogg, J., (2004). East Orphan Basin: Structural setting and evolution with seismic and potential field arguments. *Canadian Society of Exploration Geophysicists (CSEG)Annual Convention, Expanded Abstracts.*

England, R. W., & Hobbs, R. W. (1997). The structure of the Rockall Trough imaged by deep seismic reflection profiling. Journal of the Geological Society, 154(3), 497-502. doi: 10.1144/gsjgs.154.3.0497

Fleitout, L., Froidevaux, C., (1982). Tectonics and topography for a lithosphere containing density heterogeneities. Tectonics 1 (1), 21e56. doi: 10.1029/tc001i001p00021

Fossen, H., (2016). Structural geology. Cambridge: Cambridge University Press.

Funck, T., Hopper, J.R., Larsen, H.C., louden, K.E., Tucholke, B.E. & Holbrook, W.S., (2003). Crustal structure of the ocean–continent transition at Flemish Cap: seismic refraction results. Journal of Geophysical Research, 108, B11. doi: 10.1029/2003jb002434

Gernigon, L., C. Ravaut, P. M. Shannon, A. Chabert, B. M. O'Reilly, and P. W. Readman, (2004). Contrasting styles between the structure and the magmatism of the West and South Hatton/Rockall Margins (North Atlantic Igneous Province), Eos Trans. AGU, 85(47), Fall Meeting Program, Abstract #V51B-0567.

Grant, A. C., & K. D. McAlpine, (1990). The continental margin around Newfoundland, in Geology of the Continental Margin of Eastern Canada, Geology of Canada, No. 2, edited by M. J. Keen and G. L. Williams, pp. 239–292, Geol. Surv. of Canada, Ottawa, Ont. doi: 10.1130/dnag-gna-i1.239

Gouiza, M., Hall, J., & Bertotti, G., (2015). Rifting and pre-rift lithosphere variability in the Orphan Basin, Newfoundland margin, Eastern Canada. *Basin Research*, *27*(4), 367-386. doi: 10.1111/bre.12078

Gouiza, M., Hall, J., & Welford, J. K., (2017). Tectono-stratigraphic evolution and crustal architecture of the Orphan Basin during North Atlantic rifting. International Journal of Earth Sciences, 106(3), 917-937. doi: 10.1007/s00531-016-1341-0

Hall, J., Marillier, F. & Dehler, S.A., (1998). Geophysical studies of the structure of the Appalachian orogen in the Atlantic borderlands of Canada. Canadian Journal of Earth Sciences, 35, 1205–1221. doi: 10.1139/cjes-35-11-1205

Haughton P, Praeg D, Shannon P, Harrington G, Higgs K, Amy L, Tyrrell S, Morrissey T., (2005). First results from shallow stratigraphic boreholes on the eastern flank of the Rockall Basin, offshore western Ireland. In: guss AG, Vining B (eds) Petroleum geology: North-West Europe and global perspectives— proceedings of the 6th petroleum geology conference. Geological Society, London, pp 1077–1094. doi: 10.1144/0061077

Hauser, F., O'Reilly, B.M., Jacob, A.W.B., Shannon, P.M., Makris, J. & Vogt, U., (1995). The crustal structure of the Rockall Trough: differential stretching without underplating. Journal of Geophysical Research, 100, 4097–4116. doi: 10.1029/94jb02879

Hauser, F., O'Reilly, B., Readman, P., Daly, J. & van den Berg, R., (2008). Constraints on crustal structure and composition within a continental suture zone in the Irish Caledonides from shear wave wide-angle reflection data and lower crustal xenoliths, Geophys. J. Int., 175, 1254– 1272. doi: 10.1111/j.1365-246x.2008.03945.x

Haworth, R. T., (1977). The continental crest northeast of Newfoundland and its ancestral relationship to the Charlie Fracture Zone, *Nature*, 266, 246-249. doi: 10.1038/266246a0

Haworth, R.T. & Keen, C.E., (1979). The Canadian Atlantic margin: a passive continental margin encompassing an active past. Tectonophysics, 59, 83–126. doi: 10.1016/0040-1951(79)90040-4

Hopper, J. R., Funck, T., Tucholke, B. E., Louden, K. E., Holbrook, W. S., & Larsen, H. C., (2006). A deep seismic investigation of the Flemish Cap margin: implications for the origin of deep reflectivity and evidence for asymmetric break-up between Newfoundland and Iberia. *Geophysical Journal International*, *164*(3), 501-515. doi: 10.1111/j.1365-246x.2006.02800.x

Huismans, R. & Beaumont, C., (2011). Depth-dependent extension, two-stage breakup and cratonic underplating at rifted margins. Nature, 473, 74–78. doi: 10.1038/nature09988

Keen, C. E., & Barrett, D. L., (1981). Thinned and subsided continental crust on the rifted margin of Eastern Canada: crustal structure, thermal evolution and subsidence history. *Geophysical Journal International*, *65*(2), 443-465. doi: 10.1111/j.1365 246x.1981.tb02721.x

Keen, C. E., & Dehler, S. A., (1993). Stretching and subsidence: Rifting of conjugate margins in the North Atlantic Region. *Tectonics*, *12*(5), 1209-1229. doi: 10.1029/93tc00915

Keen, C. E., Dafoe, L. T., & Dickie, K., (2014). A volcanic province near the western termination of the Charlie-Gibbs Fracture Zone at the rifted margin, offshore northeast Newfoundland. Tectonics, 33(6), 1133-1153. doi: 10.1002/2014tc003547

Keen, C.E., G.S. Stockmal, H. Wellsink, G. Quinlan, and B. Mudford, (1987). Deep crustal structure of the rifted margin northeast of Newfoundland results from LITHOPROBE East, Can. J. Earth Sci., 24, 1537-1549. doi: 10.1139/e87-150

Kimbell, G., Ritchie, J., & Henderson, A. (2010). Three-dimensional gravity and magnetic modelling of the Irish sector of the NE Atlantic margin. Tectonophysics, 486(1-4), 36-54. doi: 10.1016/j.tecto.2010.02.007

Kneller, E. A., Johnson, C. A., Karner, G. D., Einhorn, J., & Queffelec, T. A., (2012). Inverse methods for modelling non-rigid plate kinematics: Application to mesozoic plate reconstructions of the Central Atlantic. *Computers & Geosciences*, *49*, 217-230. doi: 10.1016/j.cageo.2012.06.019

Knott, S.D., Burchell, M.T., Jolley, E.J., Fraser, A.J., (1993). Mesozoic to Cenozoic plate reconstructions of the North Atlantic and hydrocarbon plays of the Atlantic margins. In: Parker, J.R. (Ed.), Petroleum Geology of Northwest Europe: Proceedings of the 4th Conference. The Geological Society, London, pp. 953–974.

Kusznir, N.J., Hunsdale, R., Roberts, A.M., and SIMM Team, (2005). Norwegian margin depth dependent stretching, in Doré, A.G., and Vining, B.A., eds., Petroleum geology: Northwest Europe and global perspectives—Proceedings of the 6th Petroleum Geology Conference: Geological Society [London], Petroleum Geology Conferences Ltd., p. 767 783.

Lamb, S. & Watts, A., (2010). The origin of mountains – imlications for the behaviour of the Earth's lithosphere. *Current Science, 99(12), 1699- 1718.*

Landes, M., Ritter, J. R., Readman, P. W., & Oreilly, B. M., (2005). A review of the Irish crustal structure and signatures from the Caledonian and Variscan Orogenies. Terra Nova, 17(2), 111- 120. doi: 10.1111/j.1365-3121.2004.00590.x

Lane, A. C., (1932). Pratt And Airy And Isostasy. Science, 76(1959), 53-54. doi: 10.1126/science.76.1959.53

Lau, K.W.H., Louden, K.E., Funck, T., Tucholke, B.E., Holbrook, W.S., Hopper, J.R. & Larsen, H.C., (2006). Crustal structure across the Grand Banks–Newfoundland Basin continental margin—I. Results from a seismic refraction profile. Geophysical Journal International, 167, 127–156. doi: 10.1111/j.1365-246x.2006.02988.x

Lau, K. H., Watremez, L., Louden, K. E., & Nedimović, M. R., (2015). Structure of thinned continental crust across the Orphan Basin from a dense wide-angle seismic profile and gravity data. *Geophysical Journal International, 202*(3), 1969-1992. doi: 10.1093/gji/ggv261

Lavier, L.L. & Manatschal, G., (2006). A mechanism to thin the continental lithosphere at magmapoor margins: Nature, v. 440, p. 324–328

Lohr, T., Krawczyk, C. M., Tanner, D. C., Samiee, R., Endres, H., Thierer, P. O., Oncken, O., Trappe, H., Bachmann, R., Kukla, P. A. (2008): Prediction of subseismic faults and fractures: Integration of three-dimensional seismic data, three-dimensional retrodeformation, and well data on an example of deformation around an inverted fault. AAPG Bulletin, 92, 4, 473-485. doi: 10.1306/11260707046

Louden, K.E., Tucholke, B.E. & Oakey, G.N., (2004). Regional anomalies of sediment thickness, basement depth and isostatic crustal thickness in the North Atlantic Ocean, Earth planet. Sci. Lett., 224(1–2), 193–211. doi: 10.1016/j.epsl.2004.05.002

Lowe, C. & Jacob, A.B., (1989). A north-south seismic profile across the Caledonian Suture zone in Ireland, Tectonophysics, 168, 297–318. doi: 10.1016/0040-1951(89)90224-2

Lundin, E.R. & Doré, A.G., (2011). Hyperextension, serpentinization, and weakening: a new paradigm for rifted margin compressional deformation, Geology, 39(4), 347–350. doi: 10.1130/g31499.1

Mackenzie, G., Shannon, P., Jacob, A., Morewood, N., Makris, J., Gaye, M., & Egloff, F., (2002). The velocity structure of the sediments in the southern Rockall Basin: results from new wide-angle seismic modelling. *Marine and Petroleum Geology, 19*(8), 989 1003. doi: 10.1016/s0264-8172(02)00133-2

Magee, C., Jackson, C. A., & Schofield, N., (2014). Diachronous sub-volcanic intrusion along deep-water margins: insights from the Irish Rockall Basin. Basin Research, 26(1), 85 105. doi: 10.1111/bre.12044

Manatschal, G., Lavier, L., & Chenin, P. (2015). The role of inheritance in structuring hyperextended rift systems: Some considerations based on observations and numerical modeling. *Gondwana Research, 27*(1), 140-164. doi:10.1016/j.gr.2014.08.006

Marrett, R., & Allmendinger, R., (1992). Amount of extension on "small" faults: An example from the Viking graben: Geology, v. 20, p. 47– 50. doi: 10.1130/0091 7613(1992)020<0047:aoeosf>2.3.co;2

Matthews, K. J., Maloney, K. T., Zahirovic, S., Williams, S. E., Seton, M., & Müller, R. D. (2016). Global plate boundary evolution and kinematics since the late Paleozoic. *Global and Planetary Change, 146*, 226-250. doi:10.1016/j.gloplacha.2016.10.002

McDonnell, A., & Shannon, P. M. (2001). Comparative Tertiary stratigraphic evolution of the Porcupine and Rockall basins. In P. M. Shannon, P. D. W. Haughton, & D. V. Corcoran (Eds.), The Petroleum Exploration of Ireland's Offshore Basins. The Geological Society of London, Special Publication, 188, 323–344. doi: 10.1144/gsl.sp.2001.188.01.19

McKenzie, D., (1978). Some Remarks on the Development of Sedimentary Basins: Earth and Planetary Science, Letters, 40, p.25-32. doi: 10.1016/0012-821x(78)90071-7

McKerrow WS, Niocaill CM, Dewey JF., (2000) The Caledonian Orogeny redefined. J Geol Soc 157:1149–1154. doi: 10.1144/jgs.157.6.1149

McLeod, A. E., N. H. Dawers, and J. R. Underhill, (2000). The propagation and linkage of normal faults; insights from the Strathspey-Brent-Statfjord fault array, northern North Sea, Processes and controls in the stratigraphic development of extensional basins, v. 12; 3-4: Oxford, United Kingdom, Blackwell Science, p. 263-284. doi: 10.1111/j.1365-2117.2000.00124.x

Morewood, N. C., Mackenzie, G. D., Shannon, P. M., O'Reilly, B. M., Readman, P. W., & Makris, J., (2005). The crustal structure and regional development of the Irish Atlantic margin region. Petroleum Geology: North-West Europe and Global Perspectives Proceedings of the 6th Petroleum Geology Conference, 1023-1033. doi: 10.1144/0061023

Morewood, N., Shannon, P., & Mackenzie, G., (2004). Seismic stratigraphy of the southern Rockall Basin: comparison between wide-angle seismic and normal incidence reflection data. *Marine and Petroleum Geology, 21*(9), 1149-1163. doi: 10.1016/j.marpetgeo.2004.07.006

Müller, R. D., Royer, J., Cande, S. C., Roest, W. R., & Maschenkov, S., (1999). Chapter 2 New constraints on the late cretaceous/tertiary plate tectonic evolution of the caribbean. *Sedimentary Basins of the World Caribbean Basins,* 33-59. doi:10.1016/s1874 5997(99)80036-7

Müller, R.D., Seton, M., Zahirovic, S., Williams, S.E., Matthews, K.J., Wright, N.M., Shephard, G.E., Maloney, K.T., Barnett-Moore, N., Hosseinpour, M., Bower, D.J. & Cannon, J. 2016. Ocean Basin Evolution and Global-Scale Plate Reorganization Events Since Pangea Breakup, Annual Review of Earth and Planetary Sciences, vol. 44, pp. 107

Naylor, D., & Shannon, P. M., (2005). The structural framework of the Irish Atlantic Margin. Geological Society, London, Petroleum Geology Conference series, 6(1), 1009-1021. doi: 10.1144/0061009

Naylor, D., Shannon, P., & Murphy, N. (1999). *Irish Rockall Basin region: A standard structural nomenclature system*. Dublin: Petroleum Affairs Div., Dept. of the Marine and Natural Resources.

Nirrengarten, M., Manatschal, G., Tugend, J., Kusznir, N., & Sauter, D., (2018). Kinematic Evolution of the Southern North Atlantic: Implications for the Formation of Hyperextended Rift Systems. Tectonics. doi:10.1002/2017tc004495

O'Reilly, B. M., Hauser, F., Jacob, A. W. B., Shannon, P. M., Makris, J. & Vogt, U., (1996). The lithosphere below the Rockall Trough: wide-angle seismic evidence for extensive serpentinisation. *Tectonophysics,* 255, 1-23. doi: 10.1016/0040-1951(95)00149-2

O'Reilly, B., Hauser, F., Ravaut, C., Shannon, P., & Readman, P., (2006). Crustal thinning, mantle exhumation and serpentinization in the Porcupine Basin, offshore Ireland: Evidence from wide angle seismic data. *Journal of the Geological Society, 163*(5), 775 787. doi: 10.1144/0016-76492005-079

Pe-Piper, G., S. Meredyk, Y. Zhang, D. J. W. Piper, and E. Edinger, (2013). Petrology and tectonic significance of seamounts within transitional crust east of Orphan Knoll, offshore eastern Canada, Geo. Mar. Lett., 33, 433–447. doi: 10.1007/s00367-013 0342-2

Pérez-Gussinyé, M., & Reston, T. J., (2001). Rheological evolution during extension at nonvolcanic rifted margins: Onset of serpentinization and development of detachments leading to continental breakup. *Journal of Geophysical Research: Solid Earth, 106*(B3), 3961-3975. doi: 10.1029/2000jb900325

Péron-Pinvidic, G., Manatschal, G., & Osmundsen, P. T., (2013). Structural comparison of archetypal Atlantic rifted margins: A review of observations and concepts. *Marine and Petroleum Geology, 43*, 21-47. doi: 10.1016/j.marpetgeo.2013.02.002

Prodehl, C. & Mooney, W., (2012). Exploring the Earth's crust — history and results of controlled source seismology. The Geological Society of America Memoir, 208, p. 764.

Reston, T. J., (2007a). The formation of non-volcanic rifted margins by the progressive extension of the lithosphere: the example of the West Iberian margin. *Geological Society, London, Special Publications, 282*(1), 77-110. doi: 10.1144/sp282.5

Reston, T., (2007b). Extension discrepancy at North Atlantic nonvolcanic rifted margins: Depth dependent stretching or unrecognized faulting? Geology, 35(4), 367. doi: 10.1130/g23213a.1

Reston, T., (2009). The structure, evolution and symmetry of the magma-poor rifted margins of the North and Central Atlantic: A synthesis. Tectonophysics, 468(1-4), 6-27. doi: 10.1016/j.tecto.2008.09.002

Reston, T.J., Pennell, J., Stubenrauch, A., Walker, I. & Pérez-Gussinyé, M., (2001). Detachment faulting, mantle serpentinization, and serpentinite–mud volcanism beneath the Porcupine Basin, southwest of Ireland. Geology, 29, 587–590. doi: 10.1130/0091 7613(2001)029<0587:dfmsas>2.0.co;2

Reston, T.J., Krawczyk, C.M. & Klaeschen, D., (1996). The S reflector west of Galicia (Spain): evidence from prestack depth migration for detachment faulting during continental breakup, *J. geophys. Res.*, 101, 8075–8091. doi: 10.1029/95jb03466

Roberts, D.G., Ginzberg, A., Nunn, K., McQuillin, R., (1988). The structure of the Rockall Trough from seismic refraction and wide-angle reflection measurements. Nature 332, 632–635. doi: 10.1038/332632a0

Schulmann, K., Catalán, J. R., Lardeaux, J. M., Janoušek, V., & Oggiano, G., (2014). The Variscan orogeny: extent, timescale and the formation of the European crust. *Geological Society, London, Special Publications, 405*(1), 1-6.

Sclater, J. & Christie, P., (1980). Continental Stretching--Explanation of Post-Mid-Cretaceous Subsidence of Central North Sea Basin: ABSTRACT. AAPG Bulletin, 64. doi: 10.1306/2f919201-16ce-11d7-8645000102c1865d

Scrutton, R., (1986). The geology, crustal structure and evolution of the Rockall Trough and the Faeroe-Shetland Channel, Proc. R. Soc. Edinburgh, 88B, 7–26.

Scrutton, R., & Bentley, P., (1988). Major Cretaceous volcanic province in southern Rockall Trough. Earth and Planetary Science Letters, 91(1-2), 198-204. doi: 10.1016/0012 821x(88)90161-6

Shannon, P. M., (1991). The development of Irish offshore sedimentary basins. Journal of the Geological Society, 148(1), 181-189.

Shannon, P. M., Jacob, A. W., O'Reilly, B. M., Hauserr, F., Readman, P. W., & Makris, J., (1997). Structural setting, geological development and basin modelling in the Rockall Trough. *Petroleum Geology of Northwest Europe: Proceedings of the 5th Conference,* 421-431. doi: 10.1144/0050421

Shannon, P. M., Jacob, A. W., O'Reilly, B. M., Hauserr, F., Readman, P. W., & Makris, J., (1999). Structural setting, geological development and basin modelling in the Rockall Trough. *Petroleum Geology of Northwest Europe: Proceedings of the 5th Conference,* 421-431. doi: 10.1144/0050421

Shannon, P. M., Mcdonnell, A., & Bailey, W. R., (2006). The evolution of the Porcupine and Rockall basins, offshore Ireland: the geological template for carbonate mound development. International Journal of Earth Sciences, 96(1), 21-35. doi: 10.1007/s00531 006-0081-y

Shannon, P. M., Moore, J. G., Jacob, A. W. B., & Makris, J., (1993). Cretaceous and Tertiary basin development west of Ireland. In J. R. Parker (Ed.), Petroleum geology of northwest Europe: proceedings of the fourth conference (pp. 1057–1066). The Geological Society of London.

Sibuet, J.C., (1992). New constraints on the formation of the nonvolcanic continental Galicia Flemish Cap conjugate margins. Journal of Geological Society of London 149, 829 840. doi: 10.1007/978-1-4684-6500-6_1

Sibuet, J.-C., Srivastava, S.P., Enachescu, M.E. & Karner, G.D., (2007). Early Cretaceous motion of Flemish Cap with respect to North America: implications on the formation of Orphan Basin and SE Flemish Cap–Galicia Bank conjugate margins, in Imaging, Mapping and Modelling Continental Lithosphere Extension and Breakup, Vol. 282, pp. 63–76, eds Karner, G.D., Manatschal, G. & Pinheiro, L.M., Geological Society, Special Publications. doi: 10.1144/sp282.4

Skogseid, J., (2010). The Orphan Basin - A Key to Understanding the Kinematic Linkage between North and NE Atlantic Mesozoic Rifting, Vol. 2, pp. 13–23, Statoil ASA.

Smythe, D. K., (1989). Rockall Trough—Cretaceous or Late Palaeozoic? Scottish Journal of Geology, 25, 5 43. doi: 10.1144/sjg25010005

Spiegelman, M. & J. R. Reynolds., (1999) Combined dynamic and geochemical evidence for convergent melt flow beneath the East pacific Rise. *Nature* 402:282-285.

Srivastava, S.P., Roest, W.R., Kovacs, L.C., Oakey, G., Lévesque, S., Verhoef, J. & Macnab, R., (1990). Motion of Iberia since the Late Jurassic: results from detailed aeromagnetic measurements in the Newfoundland Basin. Tectonophysics, 184, 229–260. doi: 10.1016/0040-1951(90)90442-b

Srivastava, S.P. & Verhoef, J., (1992). Evolution of Mesozoic sedimentary basins around the North Central Atlantic: a preliminary plate kinematic solution, *Geological Society, London, Special Publications*, 62(1), 397– 420. doi: 10.1144/gsl.sp.1992.062.01.30

Srivastava, S., Verhoef, J., & Macnab, R., (1988). Results from a detailed aeromagnetic survey across the northeast Newfoundland margin, Part II: Early opening of the North Atlantic between the British Isles and Newfoundland. Marine and Petroleum Geology, 5(4), 324 337. doi: 10.1016/0264-8172(89)90079-2

Stoker, M. S., van Weering, T. C. E., & Svaerdborg, T. (2001). A Mid- to Late Cenozoic tectonostratigraphic framework for the Rockall Trough. In P. M. Shannon, P. D. W. Haughton, & D. V. Corcoran, The Petroleum Exploration of Ireland's Offshore Basins. The Geological Society of London, Special Publication, 188, 411–438. doi: 10.1144/gsl.sp.2001.188.01.26

Tate, M. P., Dodd, C. D., & Grant, N. T., (1997). The Northeast Rockall Basin and its significance in the evolution of the Rockall-Faeroes/East Greenland rift system. Petroleum Geology of Northwest Europe: Proceedings of the 5th Conference, 391-406. doi: 10.1144/0050391

Tearpock, D. J., & Bischke, R. E. (2010). Applied subsurface geological mapping: with structural methods. Upper Saddle River (N.J.): Prentice Hall.

Tucholke, B., Austin, J. & Uchupi, E., (1989). Crustal structure and riftdrift evolution of the Newfoundland basin, in Extensional Tectonics and Stratigraphy of the North Atlantic Margins, Vol. 46, Chap. 16, pp. 247–263.

Vogt, U., Makris, J., O'reilly, B.M., Hauser, F., Readman, P.W., Jacob, A.W.B. & Shannon, P.M., (1998). The Hatton basin and continental margin: crustal structure from wide angle seismic and gravity data. Journal of Geophysical Research, 103, 12545–12566. doi: 10.1029/98jb00604

Watremez, L., Lau, K.W.H., Nedimovıc, M.R. & Louden, K.E., (2015). Traveltime tomography of a dense wide-angle profile across Orphan Basin, Geophysics, 80(3), B69–B82. doi: 10.1190/geo2014-0377.1

Watts, A. B. (2001). Isostasy and flexure of the lithosphere. Cambridge: Cambridge University Press.

Welford, J. K., Shannon, P. M., O'reilly, B. M., & Hall, J., (2010). Lithospheric density variations and Moho structure of the Irish Atlantic continental margin from constrained 3-D gravity inversion. Geophysical Journal International, 183(1), 79-95. doi: 10.1111/j.1365-246x.2010.04735.x

Welford, J. K., Shannon, P. M., O'reilly, B. M., & Hall, J., (2012). Comparison of lithosphere structure across the Orphan Basin-Flemish Cap and Irish Atlantic conjugate continental

margins from constrained 3D gravity inversions. *Journal of the Geological Society, 169*(4), 405-420. doi: 10.1144/0016-76492011-114

Whittaker, R. C., K. Štolfová, and P. M. Shannon, (2012). A regional stratigraphic and structural interpretation of the Newfoundland and Ireland conjugate margins, in Third Central and North Atlantic Conjugate Margins Conference (Abstracts), pp. 195–196, PIPCo RSG Ltd., Dublin, Ireland.

Williams, H., (1984). Miogeoclines and suspect terranes of the Caledonian-Appalachian orogen: tectonic patterns in the North Atlantic region, Can. J. Earth Sci., 21(887–901). doi: 10.1139/e84-095

Williams, H., (1995). Geology of the Appalachian-Caledonian orogen in Canada and Greenland, Geological Survey of Canada, Geology of Canada, no. 6. doi: 10.4095/205242

Appendix A

| Rock Properties table | Porosity | Depth Coefficient ($Km^{-1}$) | Compaction Curve | K (Hz) | Poisson Ratio |
|---|---|---|---|---|---|
| Water Column | 1.0 | 0.55 | Sclater-Christie | 0.5 | 0.25 |
| Cenozoic | 0.37 | 0.55 | Sclater-Christie | 0.5 | 0.25 |
| Upper Cretaceous | 0.2 | 0.55 | Sclater-Christie | 0.5 | 0.25 |
| Lower Cretaceous | 0.37 | 0.55 | Sclater-Christie | 0.5 | 0.25 |
| Jurassic | 0.37 | 0.55 | Sclater-Christie | 0.5 | 0.25 |
| Basement | 0.1 | 0.55 | Sclater-Christie | 0.5 | 0.25 |

*Table 1: Rock properties and stratigraphy of the Rockall Basin. Parameters used in the reconstruction process in Move©.*

| Rock Properties table | Porosity | Depth Coefficient ($Km^{-1}$) | Compaction Curve | K (Hz) | Poisson Ratio |
|---|---|---|---|---|---|
| Water Column | 1.0 | 0.55 | Sclater-Christie | 0.5 | 0.25 |
| Cenozoic | 0.37 | 0.55 | Sclater-Christie | 0.5 | 0.25 |
| Upper Cretaceous | 0.3 | 0.55 | Sclater-Christie | 0.5 | 0.25 |
| Lower Cretaceous | 0.37 | 0.55 | Sclater-Christie | 0.5 | 0.25 |
| Jurassic | 0.30 | 0.55 | Sclater-Christie | 0.5 | 0.25 |
| Basement | 0.1 | 0.55 | Sclater-Christie | 0.5 | 0.25 |

*Table 2: Rock properties and stratigraphy of the Orphan Basin. Parameters used in the reconstruction process in Move©.*

| Other Parameters Used in 2D Thermal Subsidence for both the Rockall and the Orphan Basin | |
|---|---|
| Initial Crustal Thickness | 30 km |
| Initial Lithosphere Thickness | 125 km |
| Uniform Beta Value | 2.0 |
| Mantle Density | 3340 $kg/m^3$ |

*Table 3: Other parameters used in the 2D Thermal Subsidence calculations in Move© for both the Rockall Basin and the Orphan Basin*